Search for Heavy Boson Resonances in Final States with a W or Z Boson and a Photon Using 139 fb^{-1} of Proton-Proton Collision Data at $\sqrt{s} = 13$ TeV Collected with the ATLAS Detector

Nov. 12, 2020

Minyu Feng
Duke University

Theory Motivation: Standard Model

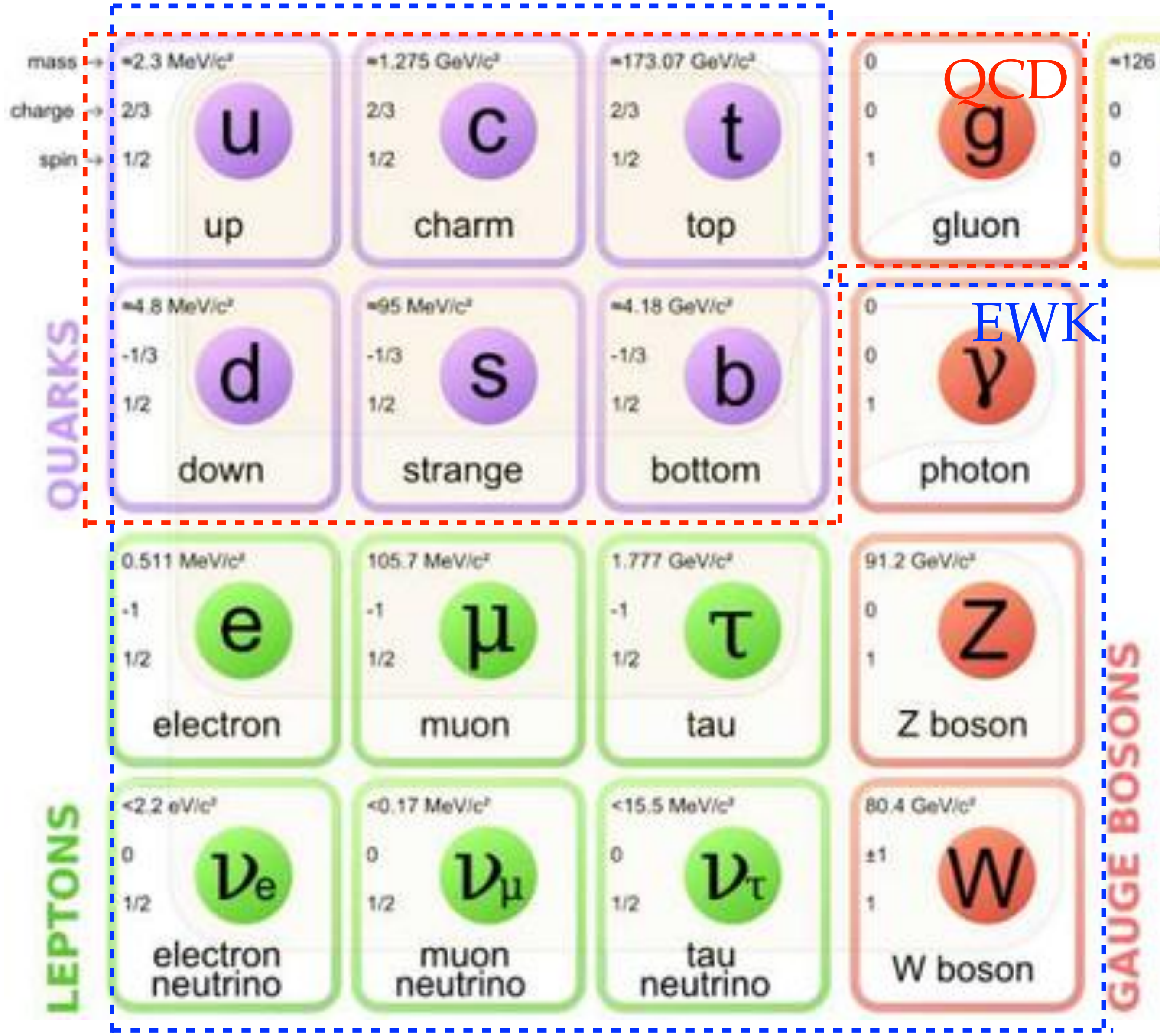

- Standard Model unified all particles and interactions by a symmetry of:

$$SU(3)_C \times \underbrace{SU(2)_L \times U(1)_Y}$$

$SU(3)_C$ → QCD

$SU(2)_L \times U(1)_Y$ → EWK

Theory Motivation: Measurements

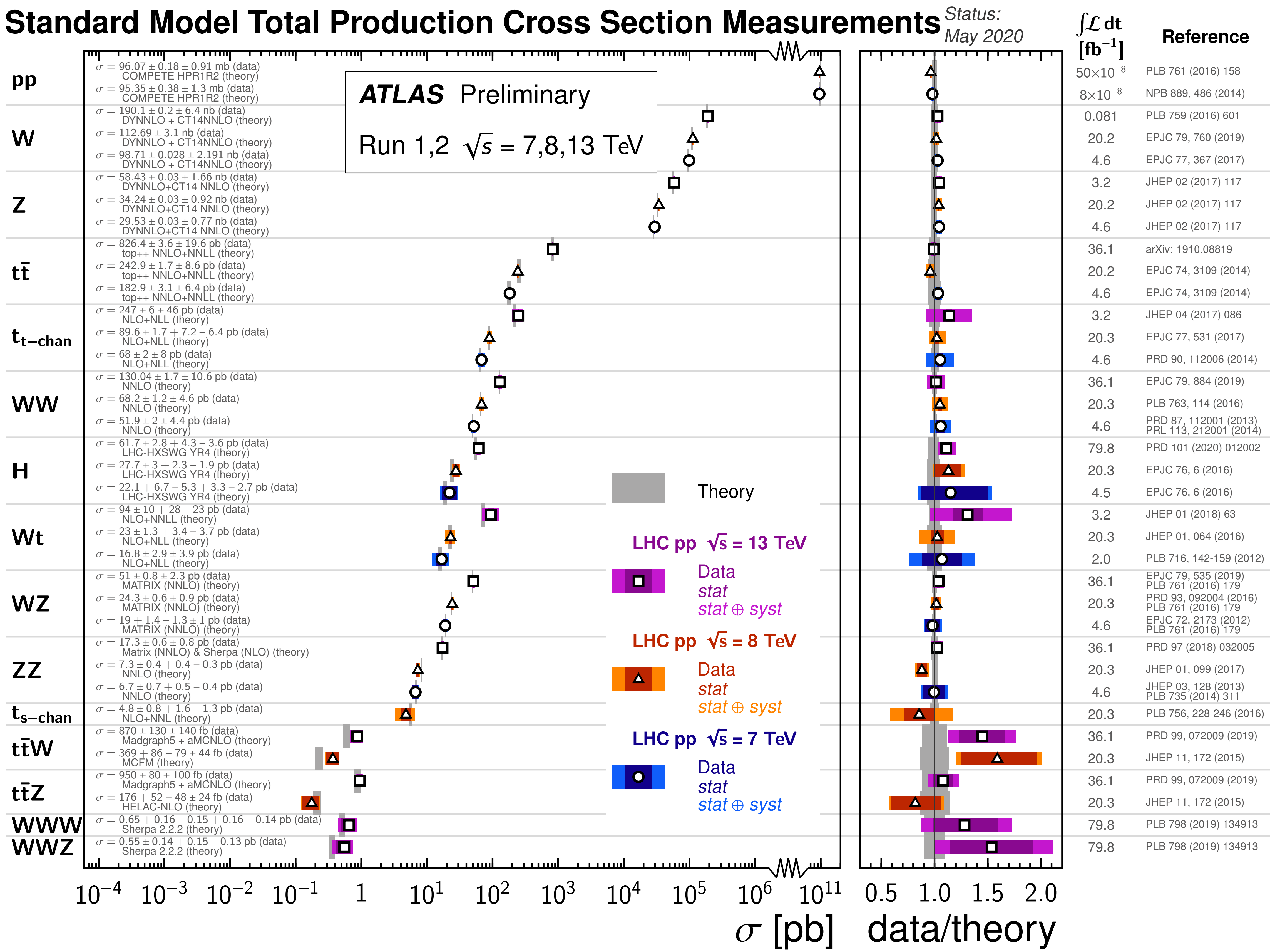

Theory Motivation: Beyond the Standard Model

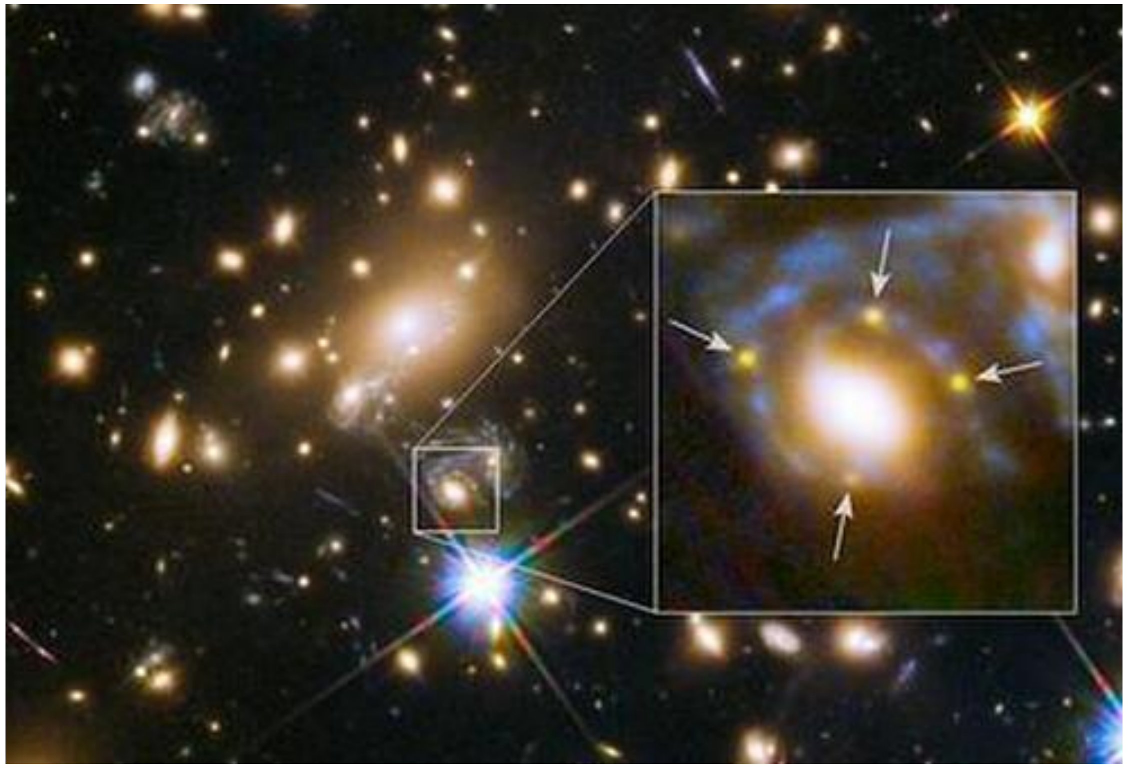

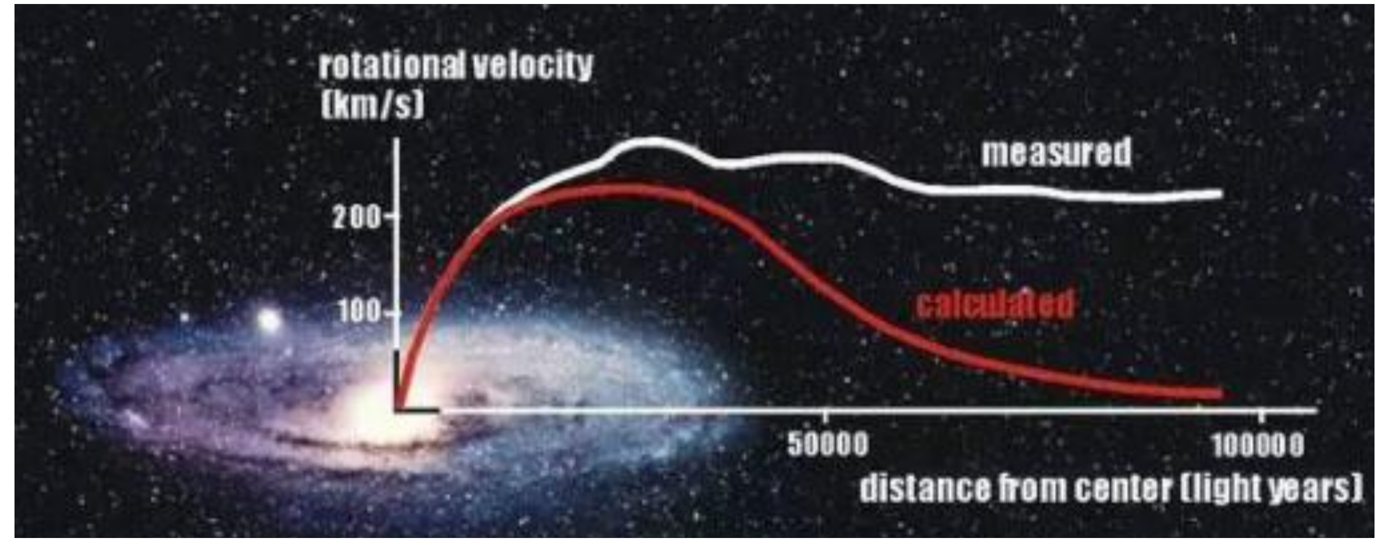

- More and more evidences implying new physics beyond the SM:
  - Gravity
  - Dark matter
  - Neutrino oscillation
- Electroweak sector could be the connection between SM and BSM
- Many theories provide mechanisms extending SM from electroweak sector. Some of them are used as our benchmark models for searching new heavy resonances.

BSM Model	Boson Spin	Process
Singlet Scalar	0	$gg \to X \to \gamma Z(\to q\bar{q})$
Heavy Vector Triplet	1	$qq' \to X \to \gamma W(\to qq')$
Deconstruction of Extra Dimensions	2	$gg \to X \to \gamma Z(\to q\bar{q})$
		$q\bar{q} \to X \to \gamma Z(\to q\bar{q})$

LHC and ALTAS: LHC Overview

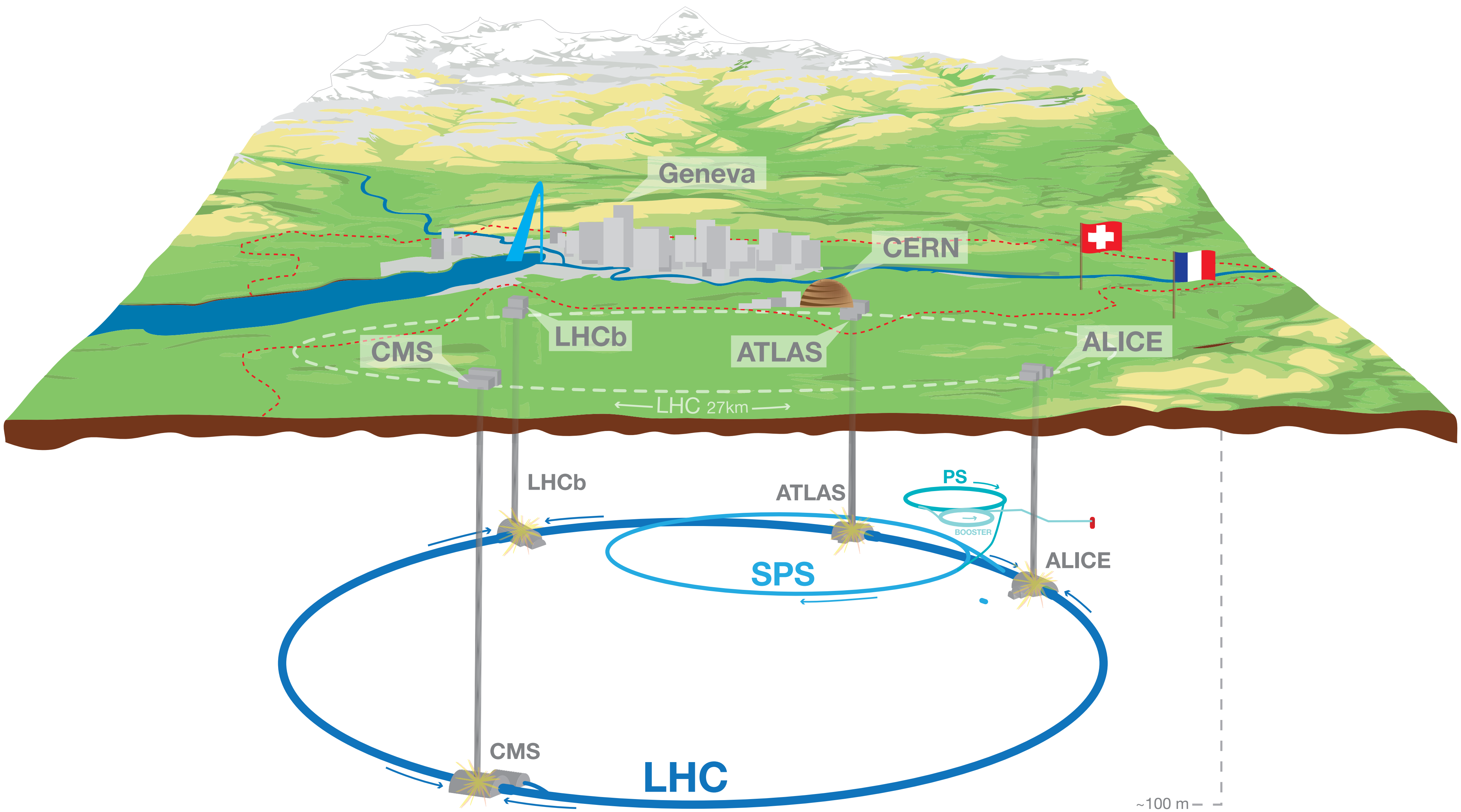

- LHC boost protons to 6.5 TeV
- Protons are grouped in bunches (~1.1 x 10^11 each), separated by 25 ns
- The collision rate is ~40 MHz

LHC and ALTAS: Luminosity

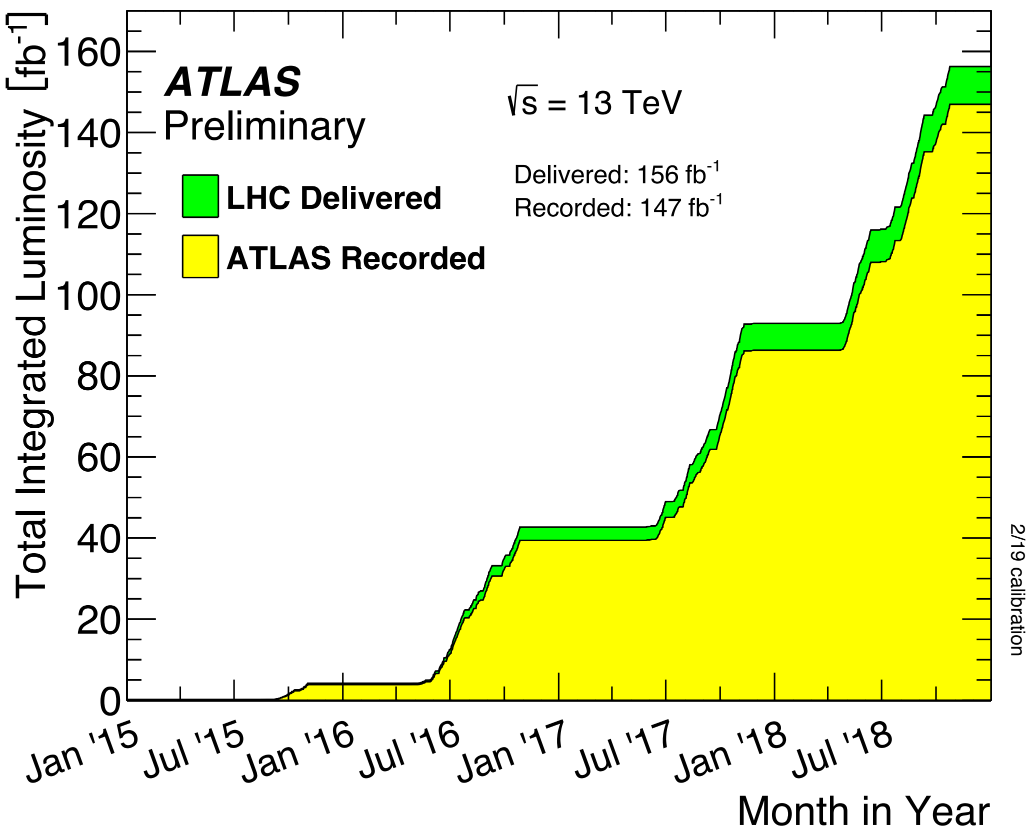

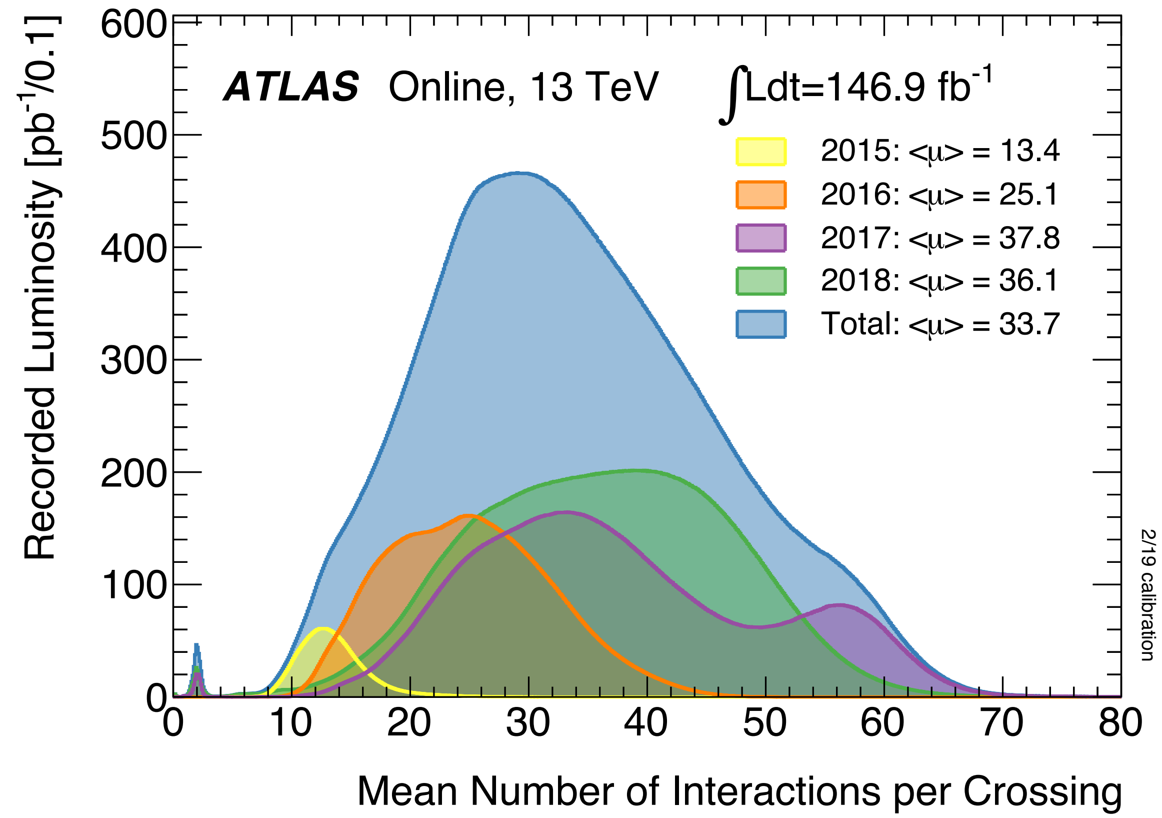

- LHC has delivered 156 fb^{-1} data
- ATLAS has recorded 147 fb^{-1}
- 139 fb^{-1} is regarded good for physics usage

LHC and ALTAS: ATLAS Overview

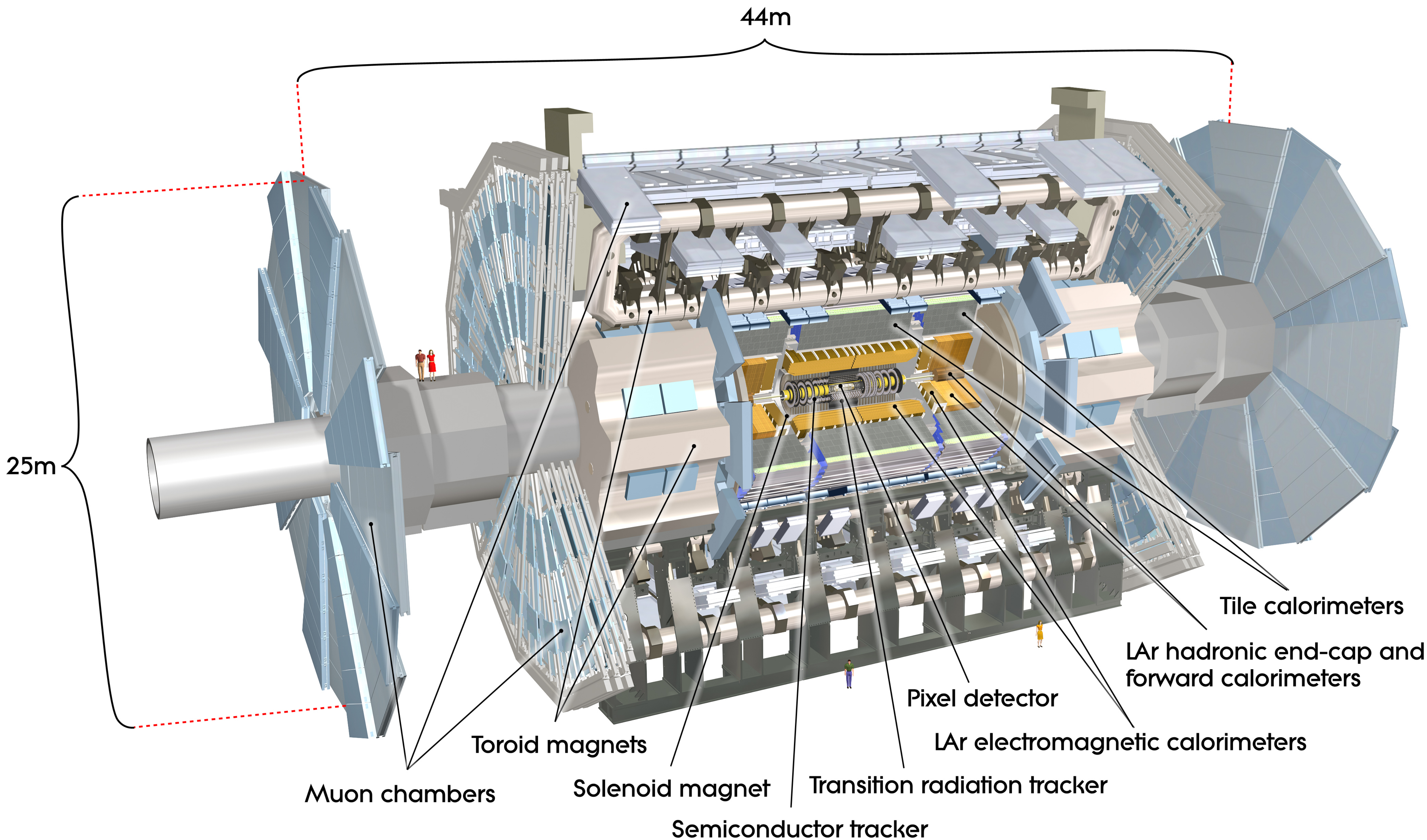

LHC and ALTAS: Detecting Particles

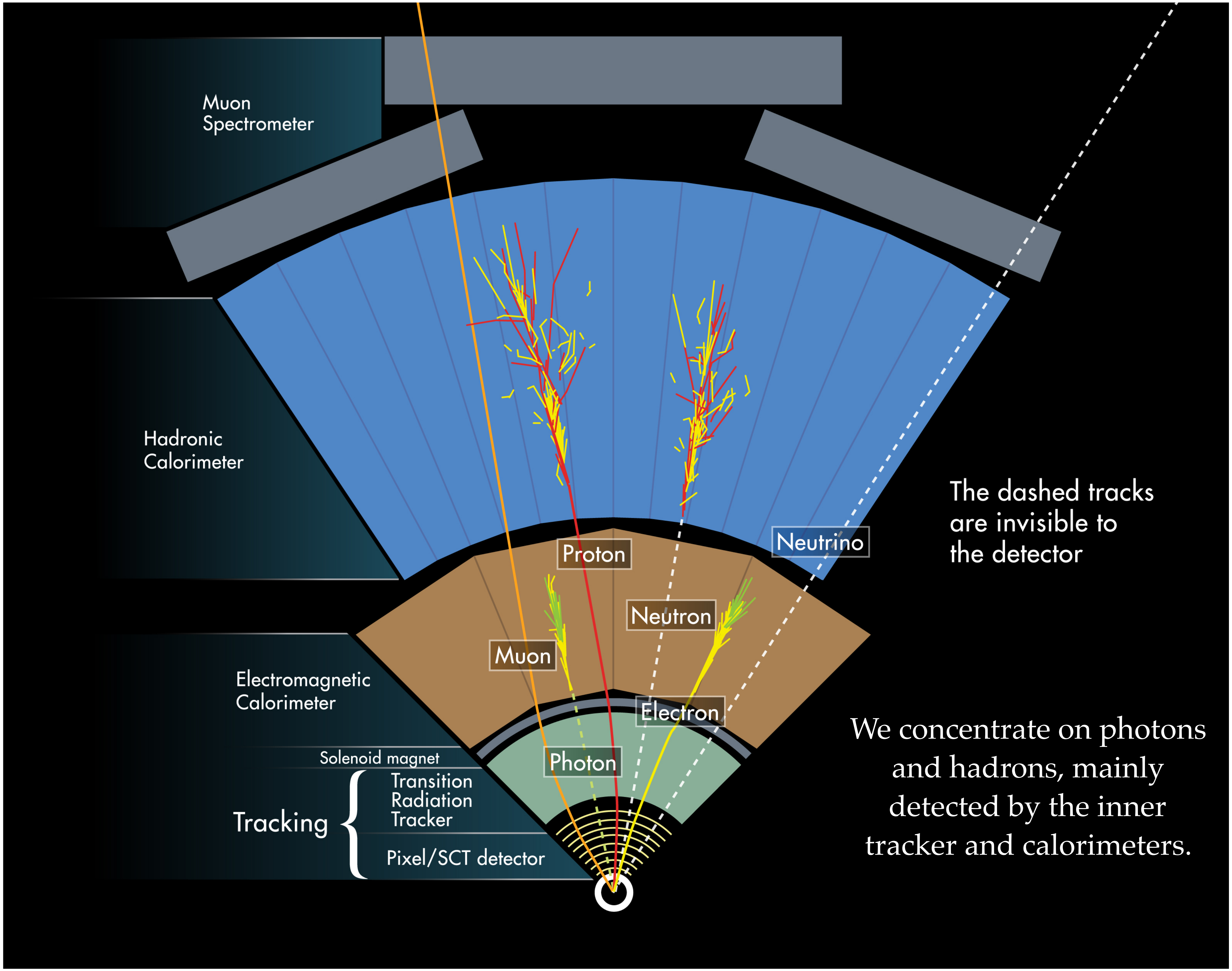

We concentrate on photons and hadrons, mainly detected by the inner tracker and calorimeters.

LHC and ALTAS: Inner Detector

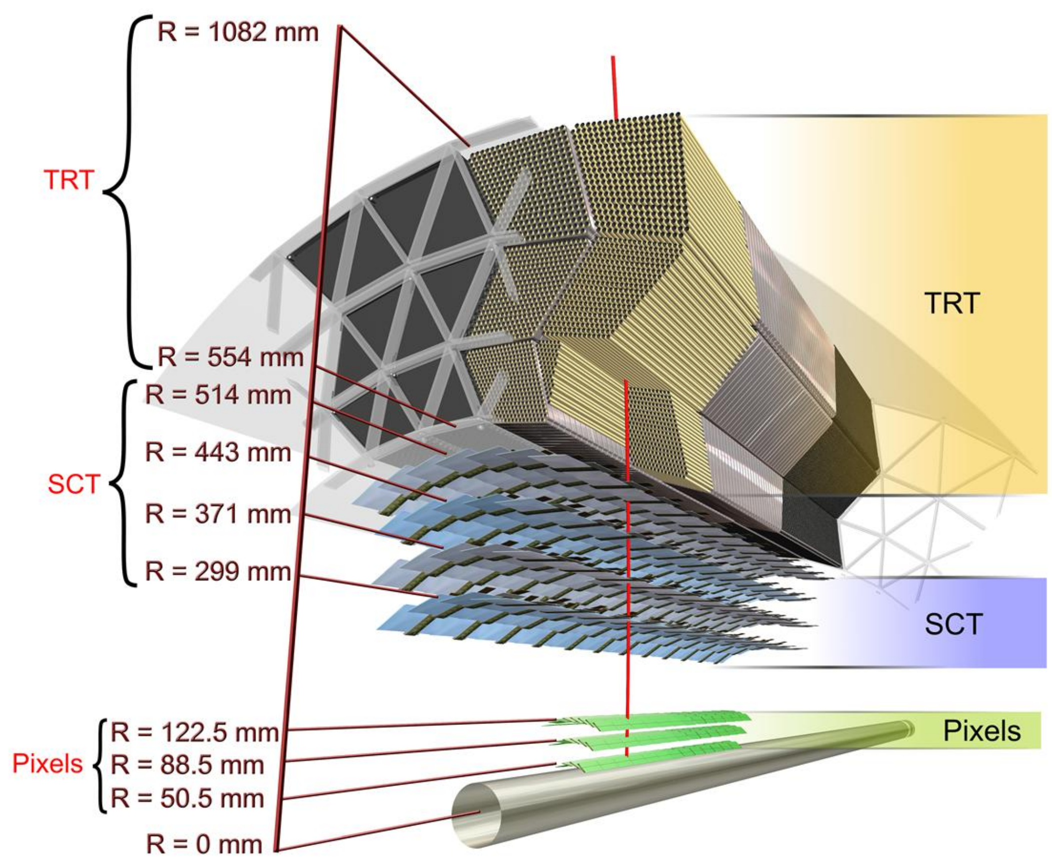

- Inner detector measures the path of charged particles.
- TRT helps discriminating electrons and pions.
- An insertable B-layer is added since 2014 to improve tracking and b-tagging performance.

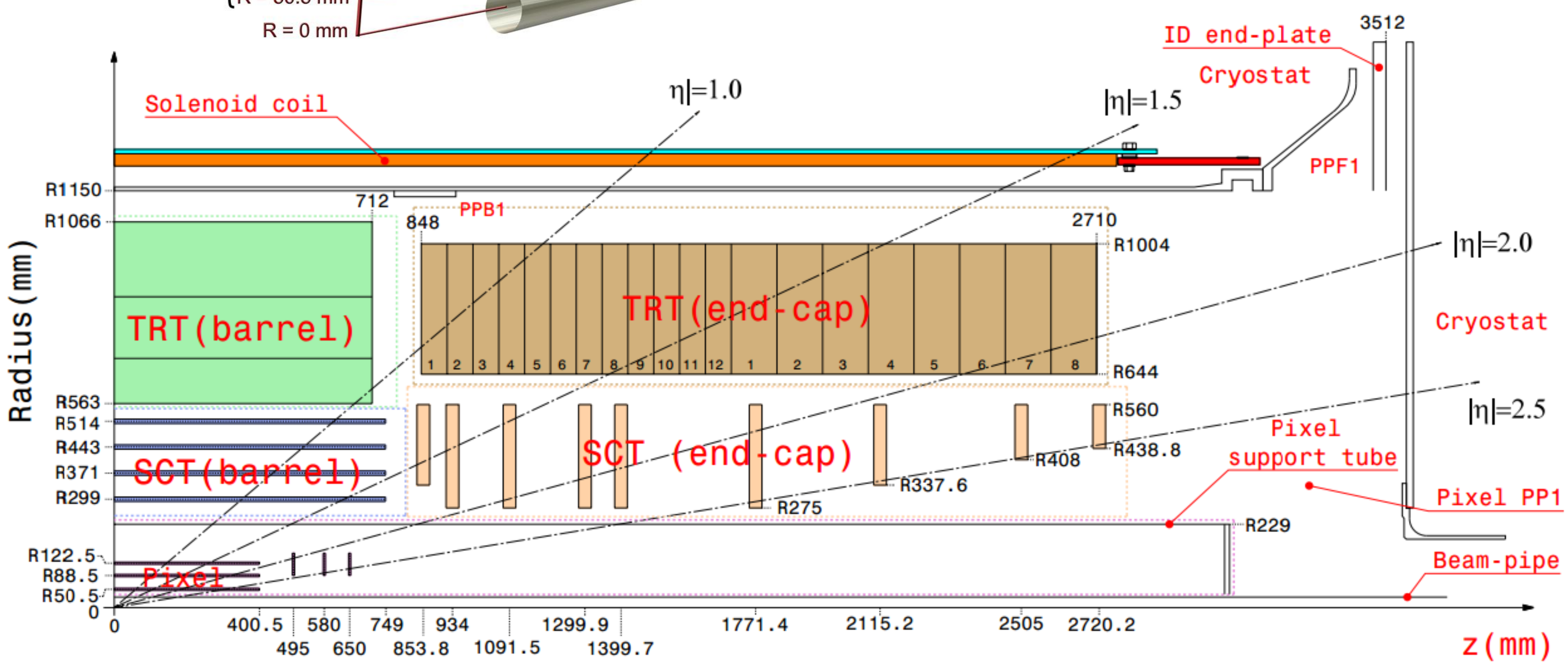

LHC and ALTAS: Calorimeters

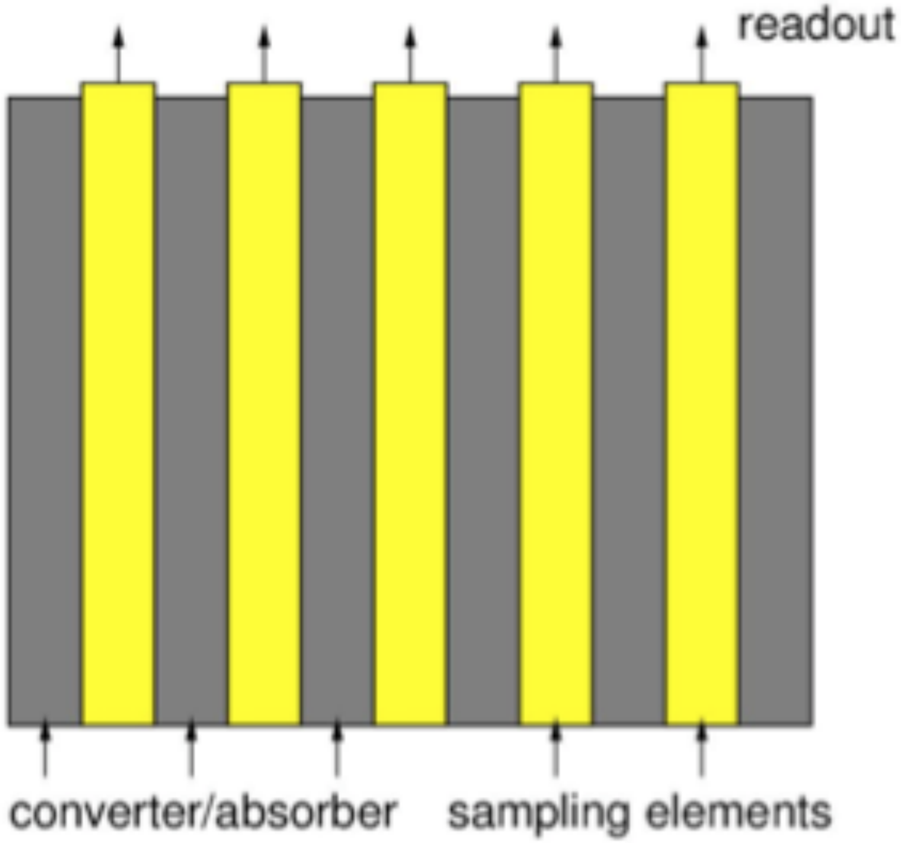

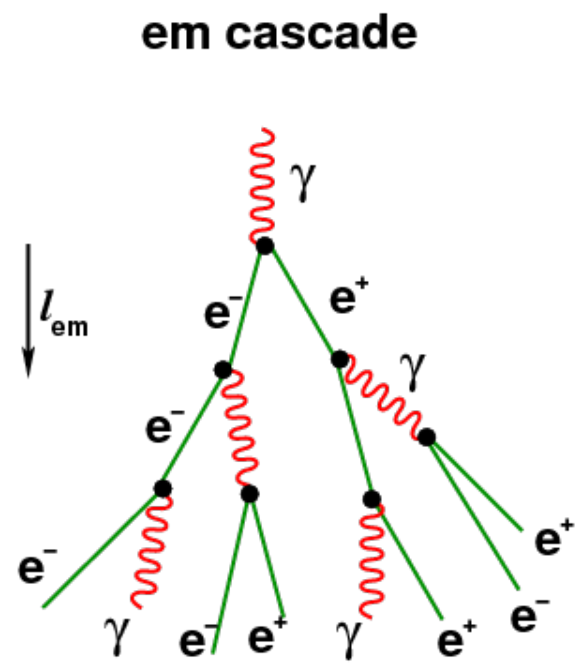

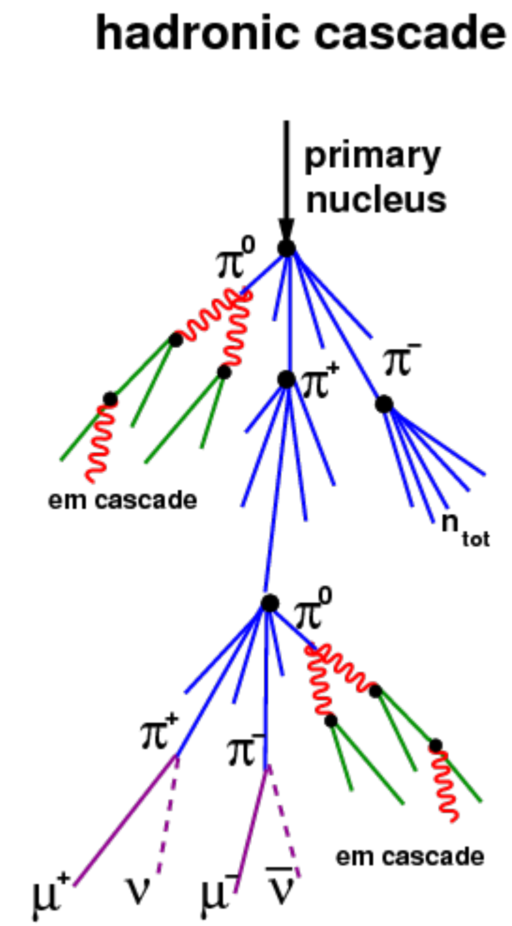

- Calorimeters measure particle energy by absorbing it and producing corresponding electronic signals.
- Usually built by alternating layers of absorber and sampling elements
- EM cascade and hadronic cascade have different features

LHC and ALTAS: Calorimeters

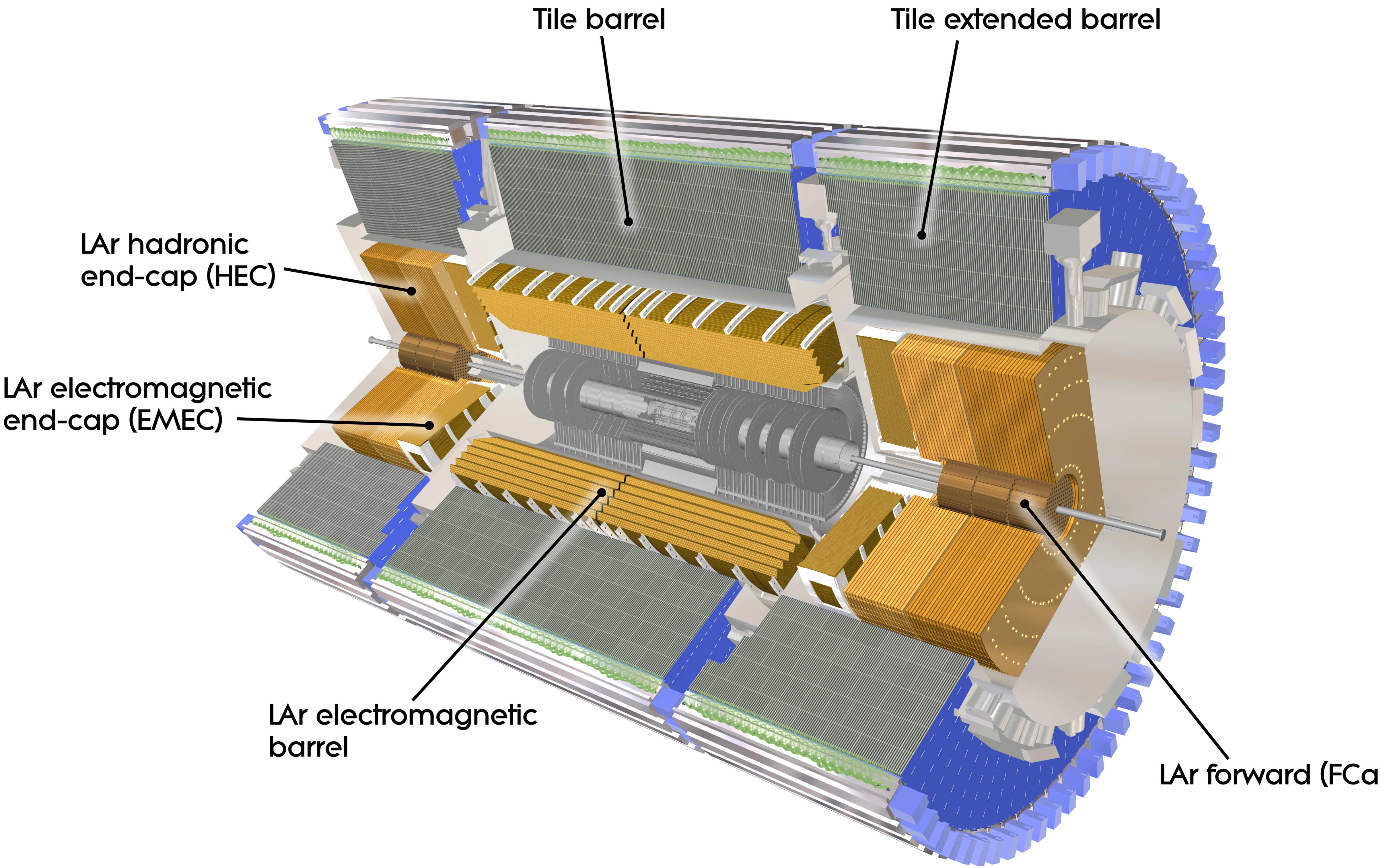

LHC and ALTAS: EM Calorimeter

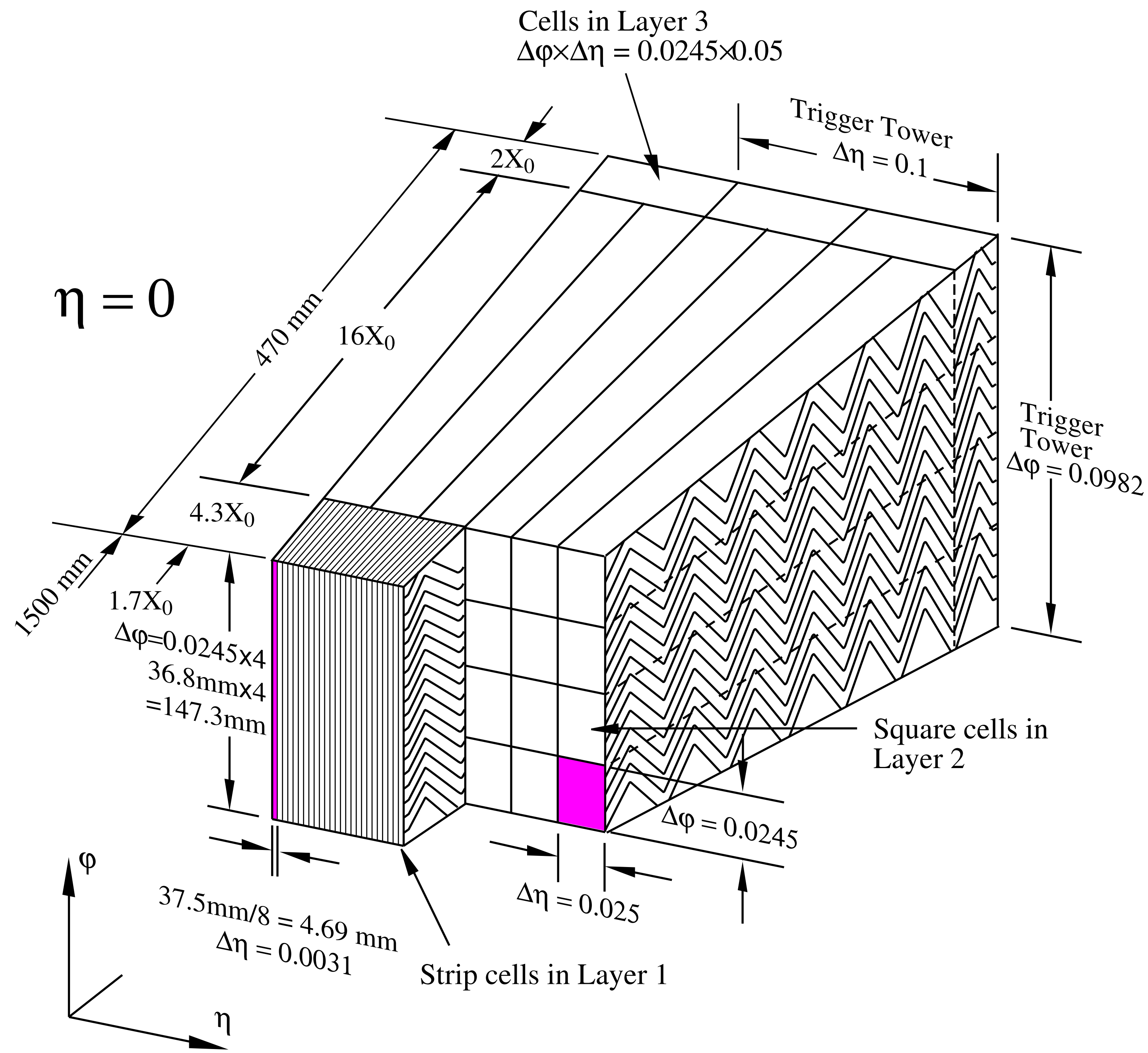

$$\frac{\sigma(E)}{E} = \frac{10\%}{\sqrt{E(\text{ GeV})}} \oplus 0.17\%$$

LHC and ALTAS: Hadronic Calorimeter

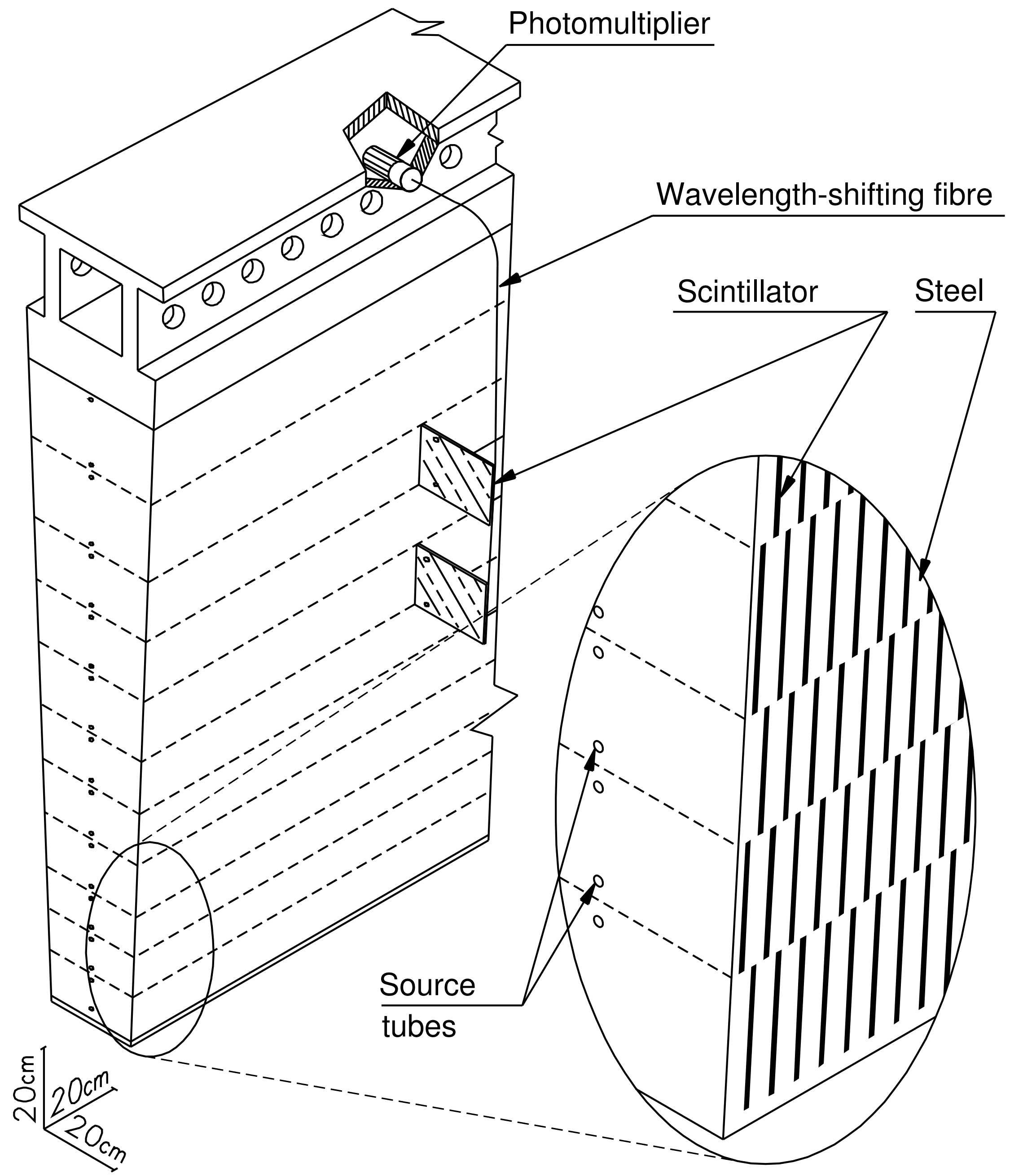

$$\frac{\sigma(E)}{E} = \frac{56.4\%}{\sqrt{E(\text{ GeV})}} \oplus 5.5\%$$

LHC and ALTAS: Triggers

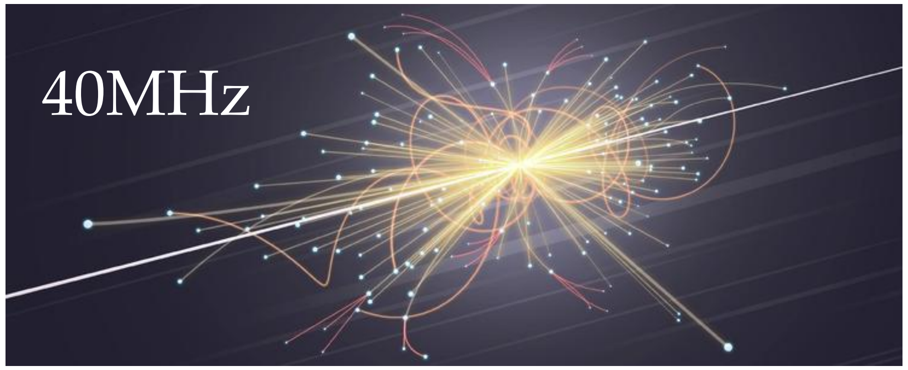

With 1-2 MB for each event, the data need to be stored in a rate of 40-80 TB/s.

Level-1 Trigger

Hardware based trigger. No complicated algorithms. (Need to make decision in 2.5 μs.)
Look for events with interesting features like high pT particles or large MET…

~100kHz

High Level Trigger

Mostly software based triggers. The average event processing time for HLT is about 40 ms.
Complex algorithms like particle identifications can be applied with much longer processing time.

Events reconstructed and stored at ~1kHz

Performance: Physics Objects of Interests

BSM Model	Boson Spin	Process
Singlet Scalar	0	$gg \to X \to \gamma Z(\to q\bar{q})$
Heavy Vector Triplet	1	$qq' \to X \to \gamma W(\to qq')$
Deconstruction of Extra Dimensions	2	$gg \to X \to \gamma Z(\to q\bar{q})$
		$q\bar{q} \to X \to \gamma Z(\to q\bar{q})$

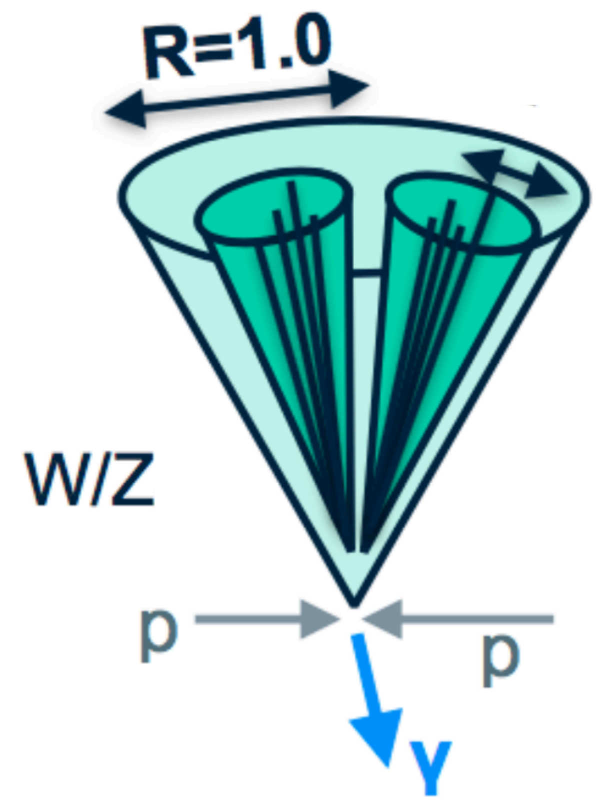

- **Photon** with high energy and passing the identification
- **W/Z boson** with high energy, and decaying hadronically

Performance: Photon Measurement

- Inner tracker information is used for identification of particles
- Calorimeter information is used to determine the energy of photon
- An algorithm called "ringer" is used to improve the identification and reconstruction performance
- The trigger used in this search (HLT_g140_loose) is almost 100% efficient, and the turn on is much below our selection cut.

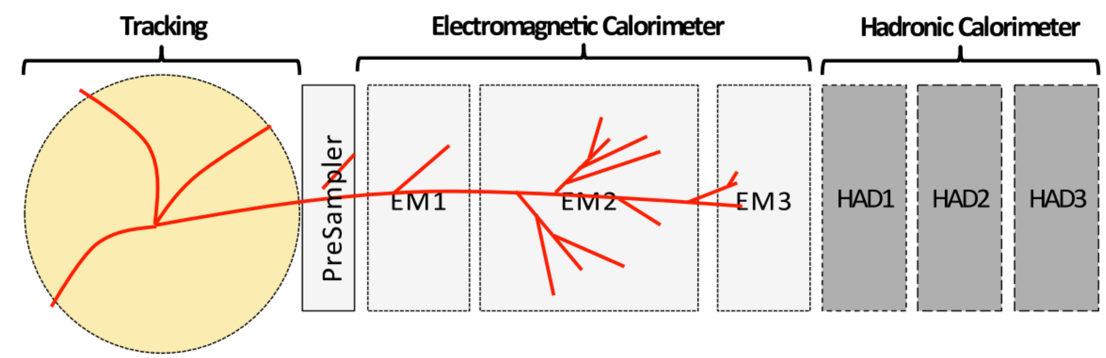

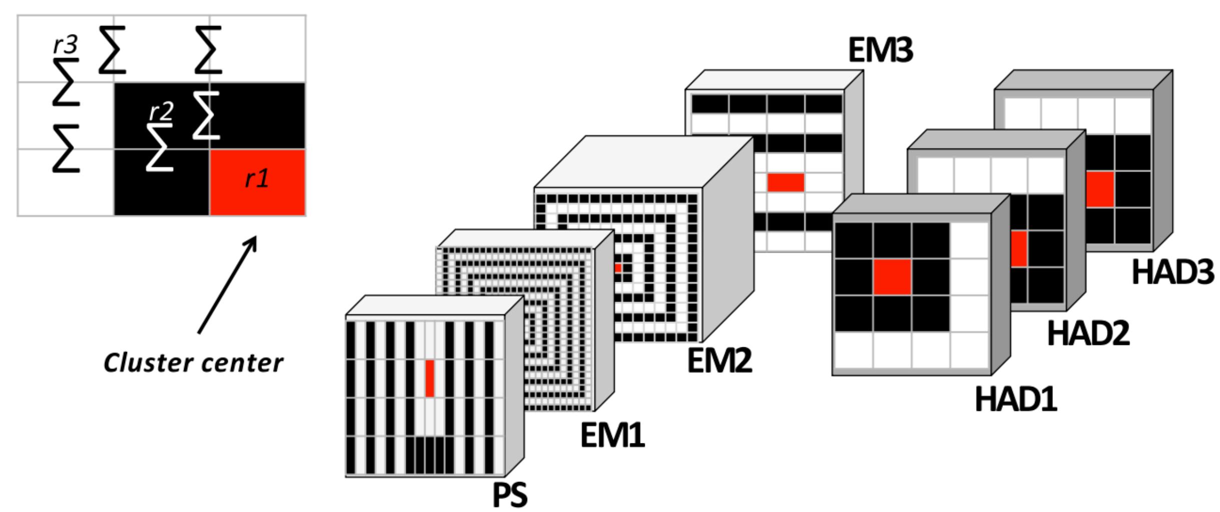

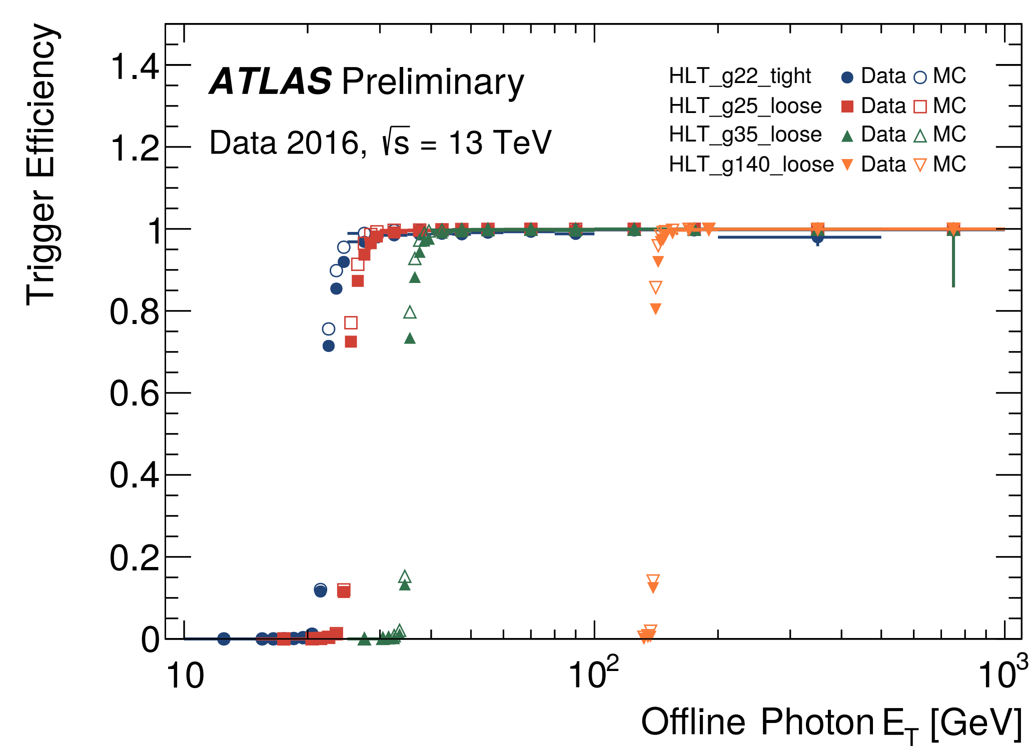

Performance: Boosted Jet Reconstruction

The clustering algorithm is conducted by repetitively grouping the two closest cells into a cluster, with the distance d between i-th and j-th cell defined as:

$$d_{ij} = min(k_{ti}^{2p}, k_{tj}^{2p}) \frac{\Delta R_{ij}^2}{R_{jet}^2}$$

$$d_{iB} = k_{ti}^{2p}$$

p = -1 is taken for the anti-kt algorithm

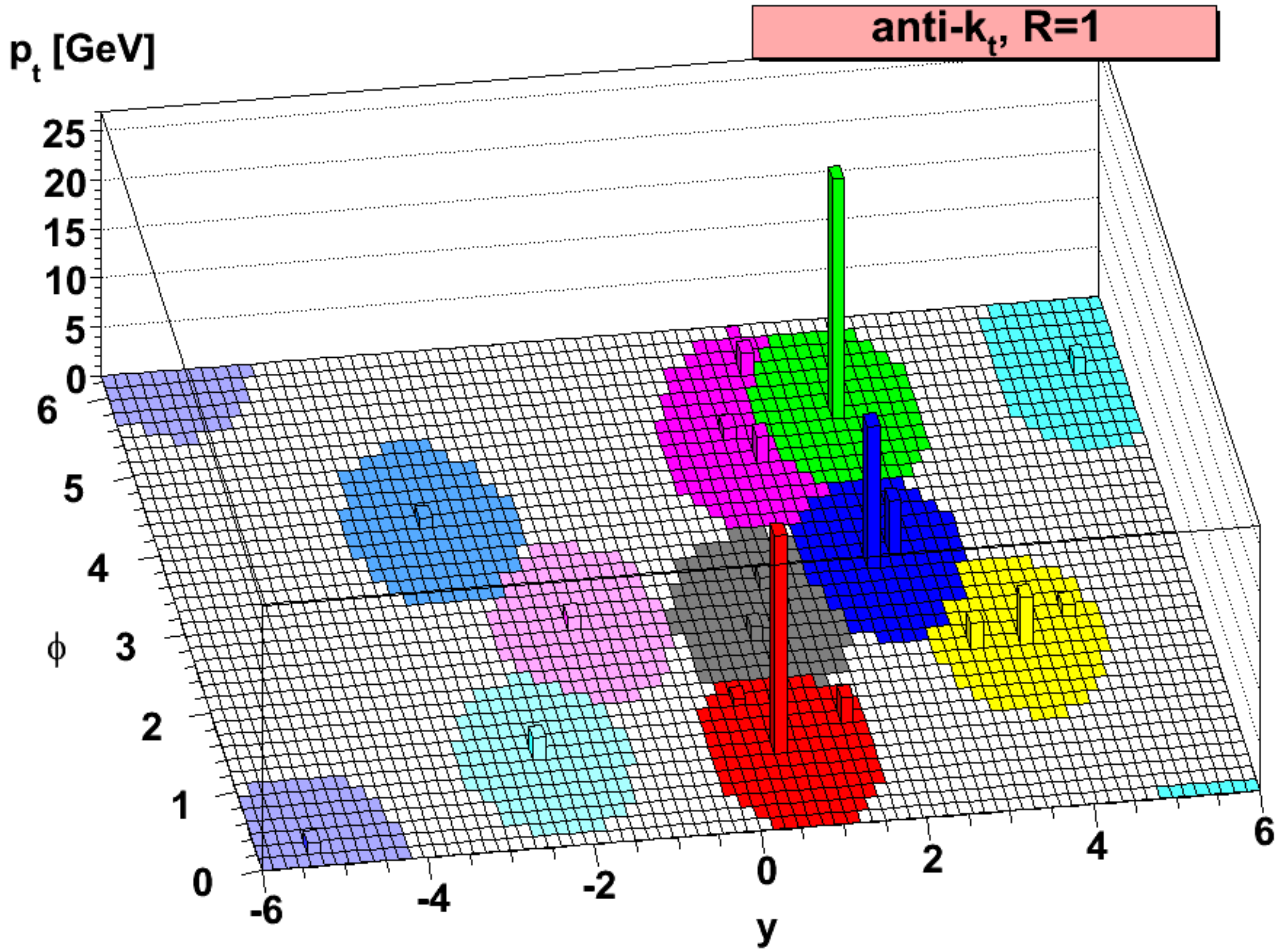

Performance: Identification of W/Z jets

The high level variable D2 used for boson tagging is defined as:

$$\epsilon_2^{(\alpha)} = \frac{1}{E_J^2} \sum_{i<j}^{N} E_i E_j \left(\frac{2p_i \cdot p_j}{E_i E_j}\right)^{\alpha/2}$$

$$\epsilon_3^{(\alpha)} = \frac{1}{E_J^3} \sum_{i<j<k}^{N} E_i E_j E_k \left(\frac{2p_i \cdot p_j}{E_i E_j} \frac{2p_i \cdot p_k}{E_i E_k} \frac{2p_j \cdot p_k}{E_j E_k}\right)^{\alpha/2}$$

$$D_2^{(\alpha)} = \frac{e_3^{(\alpha)}}{(e_2^{(\alpha)})^3}$$

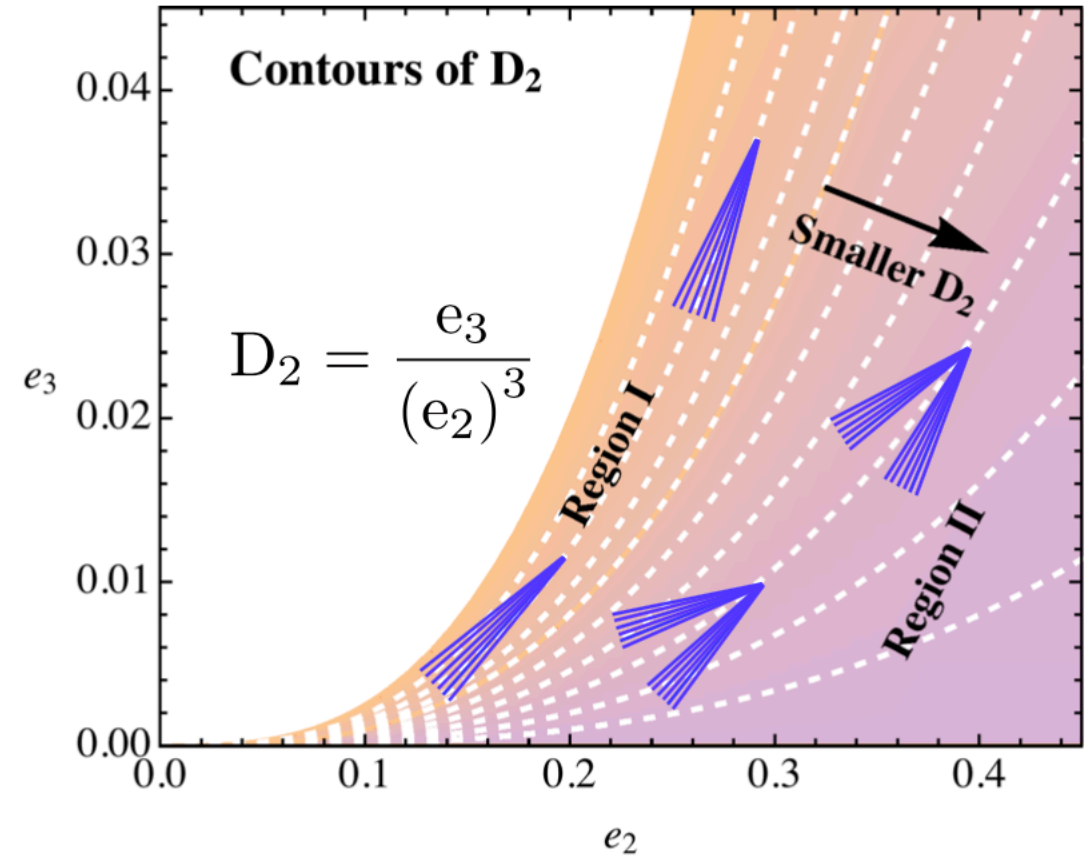

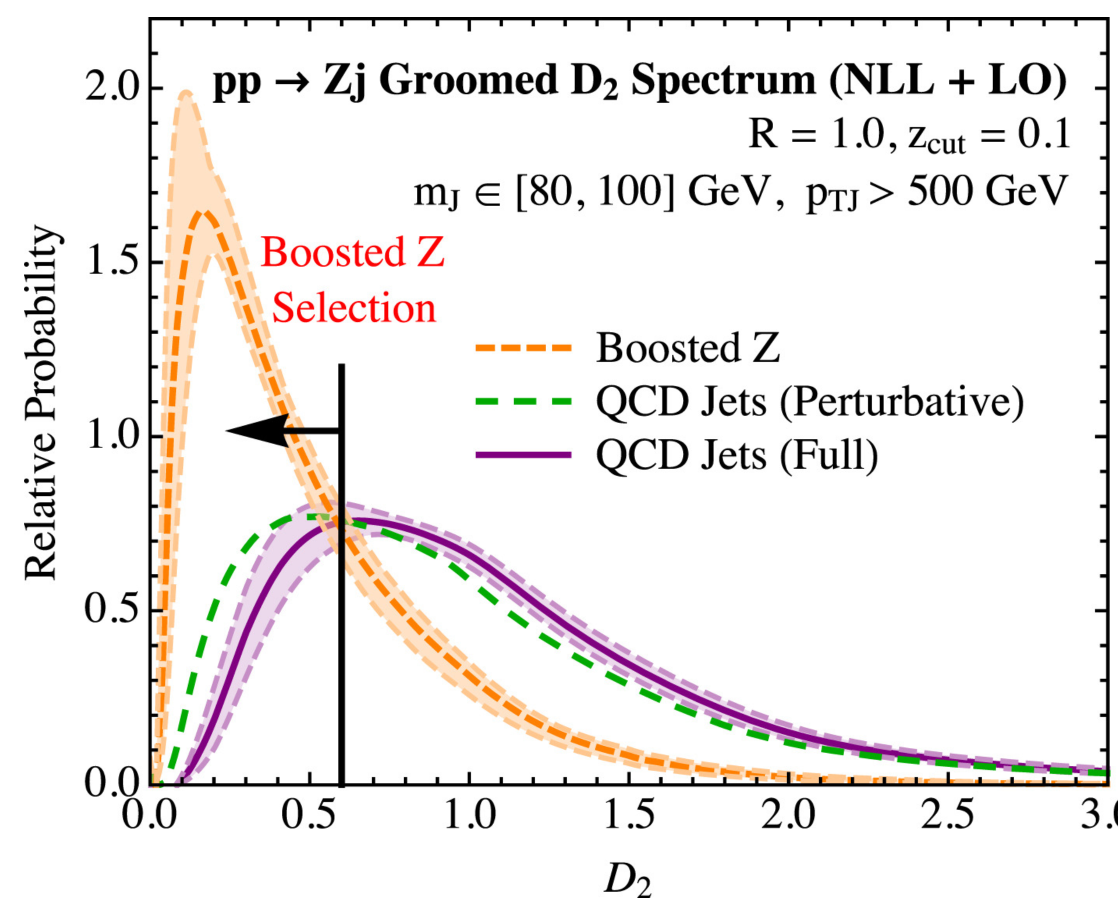

Performance: Identification of W/Z jets

The D2 variable and the mass of jet are combined to identify jets from boosted bosons.

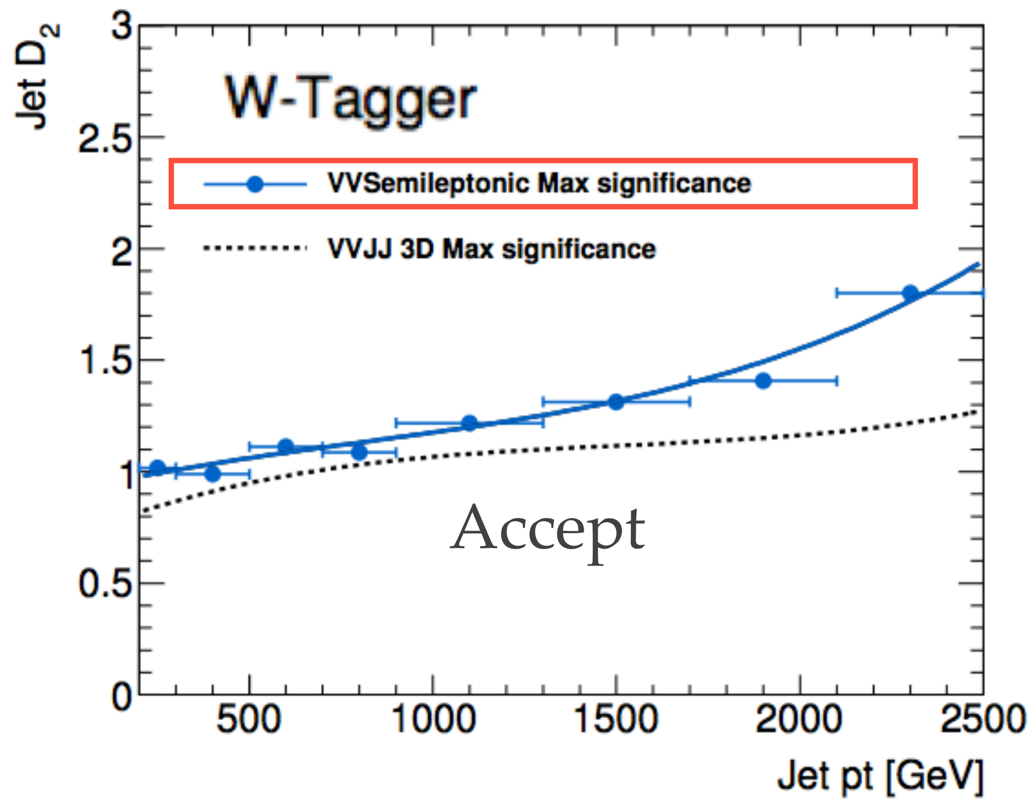

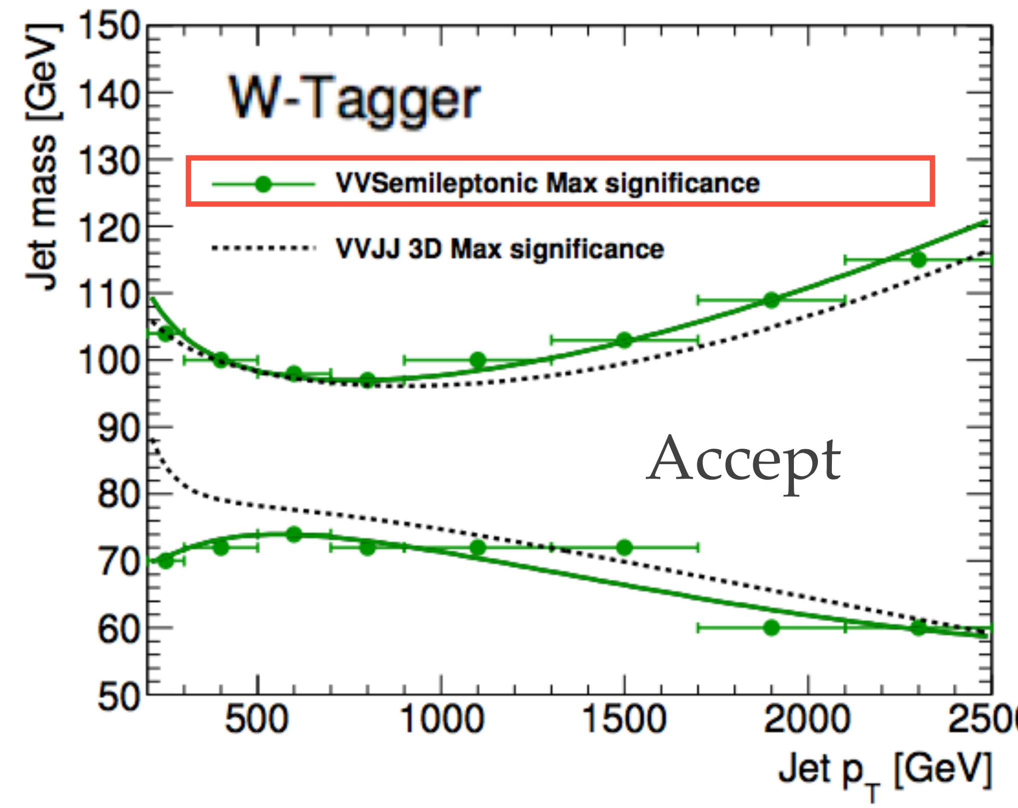

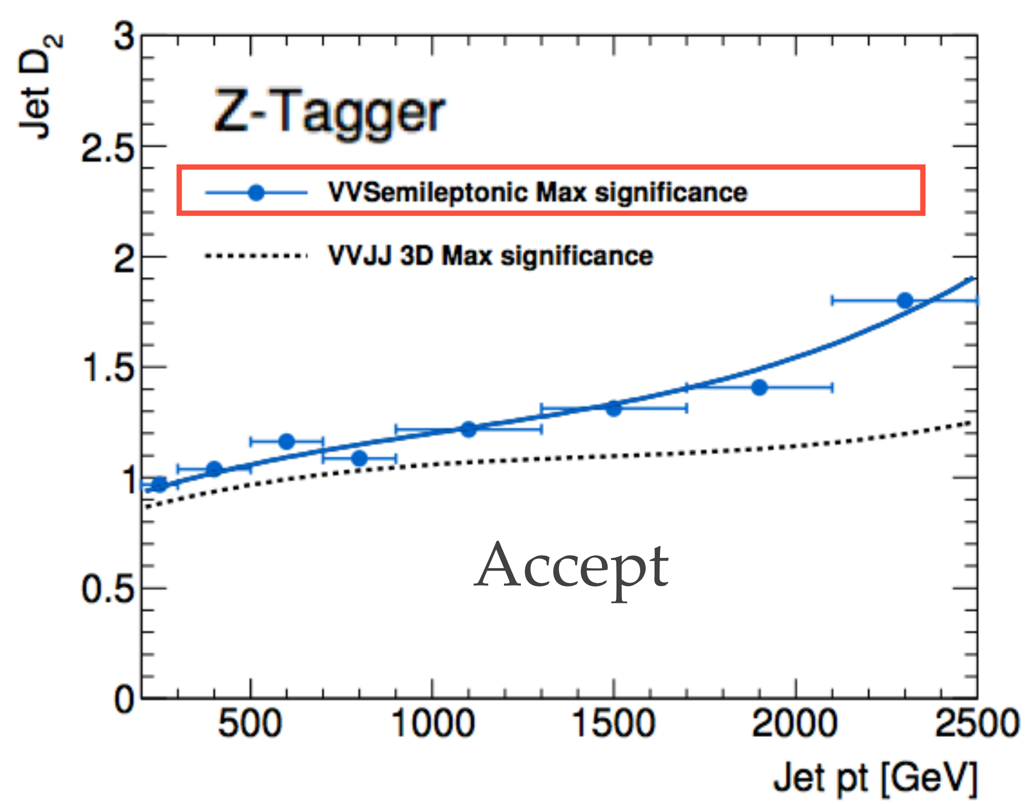

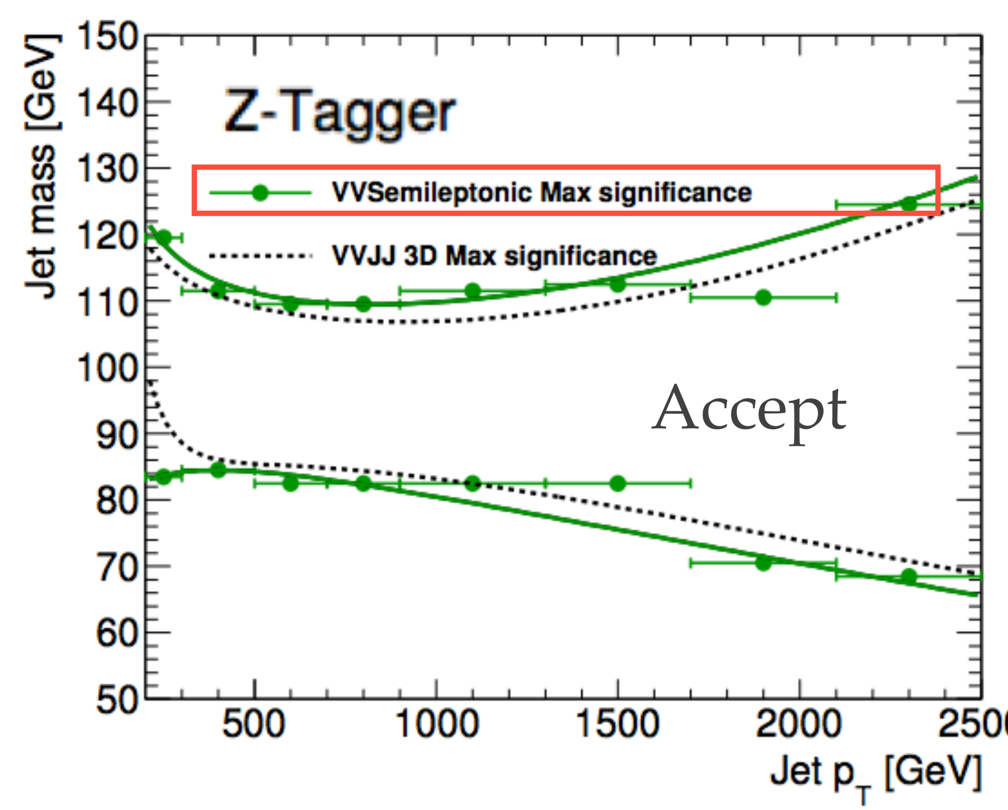

Performance: Identification of b-hadron jets

A boosted decision tree (BDT) is trained to optimize the identification of b-hadron jets, with inputs from multiple algorithms.

This BDT has different working points with different efficiencies. The most loose one with 60% efficiency is used in this search.

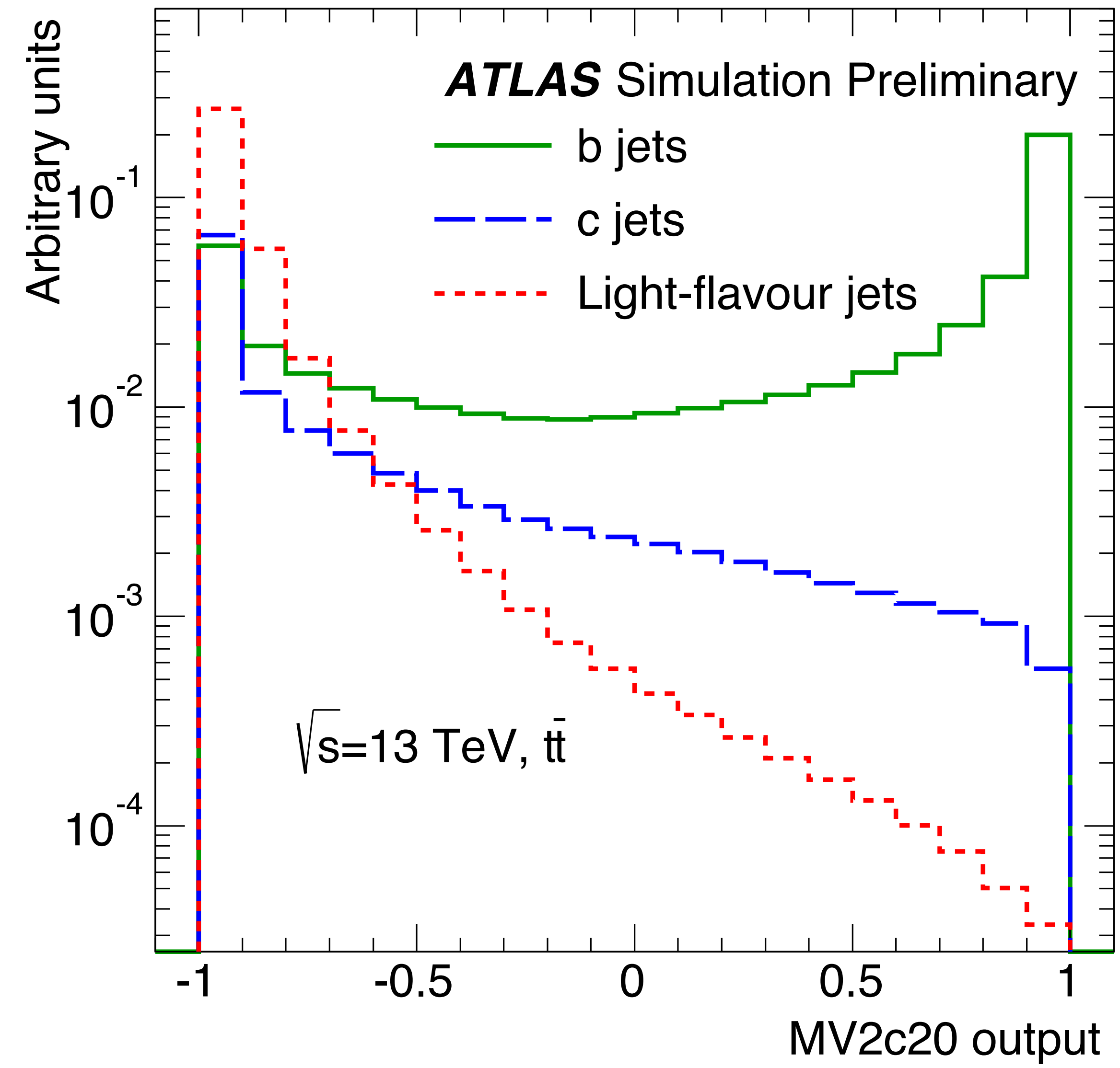

Efficiency	Cut Value	c-jet Rejection	τ-jet Rejection	Light-jet Rejection
60%	0.4496	21	93	1900
70%	-0.0436	8.1	26	449
77%	-0.4434	4.5	10	140
85%	-0.7887	2.6	3.8	28

Analysis: Previous results

Search for a heavy resonance decay to a photon and a W/Z boson with the W/Z boson decaying hadronically

Similar search was done with 36.1 fb^{-1}

Improvements:

- Increase total luminosity to 139 fb^{-1}
- Better W/Z boson tagger and b-tagger
- Re-optimized selections

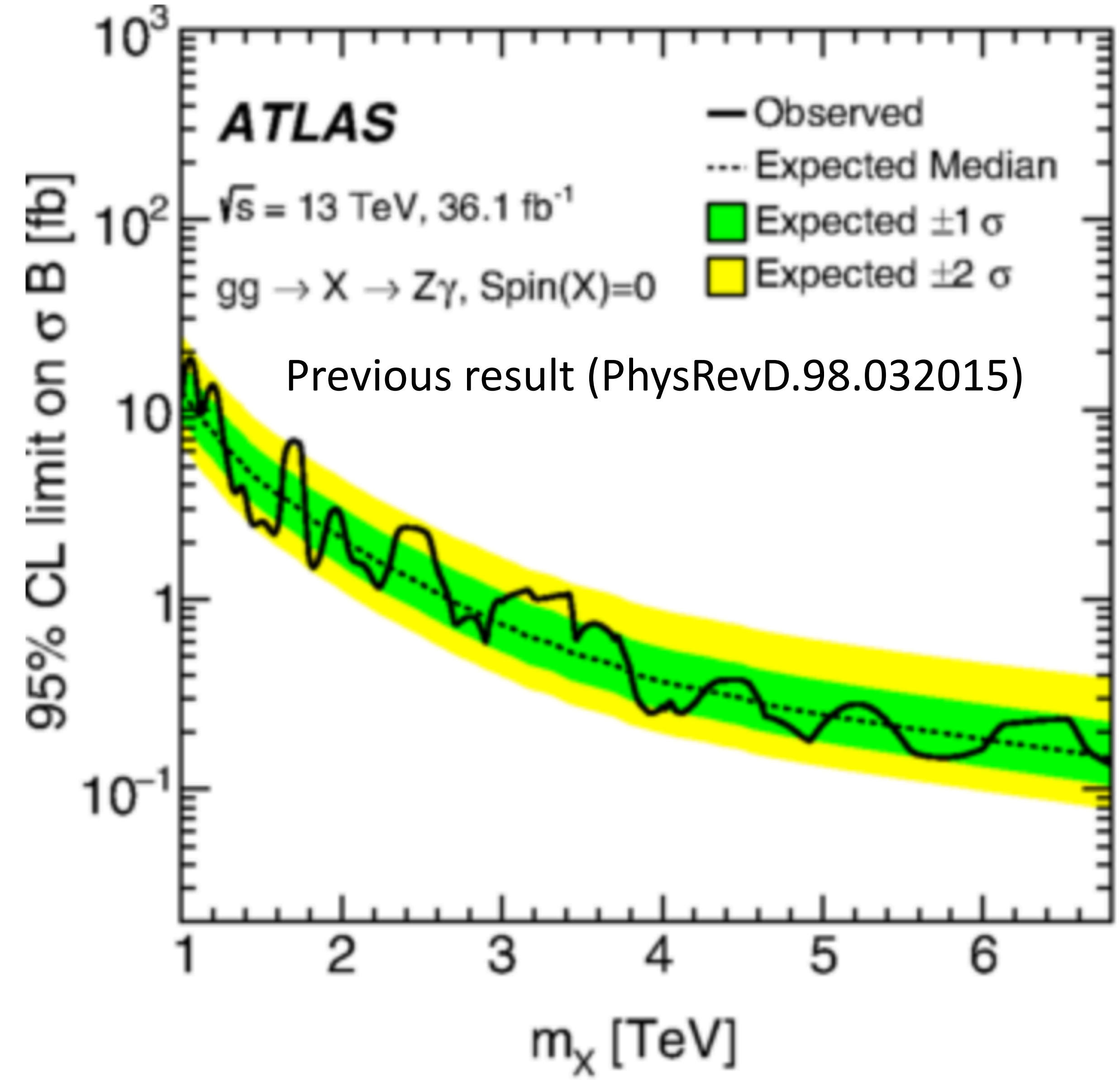

Previous result (PhysRevD.98.032015)

Analysis: MC Samples

MC Sample	Process	Generator	Boson spin	W/Z Boson Polarization
$Z\gamma$ Spin 0	$gg \to X \to \gamma Z(\to q\bar{q})$	Powheg+Pythia8	0	Transverse
$W\gamma$ Spin 1	$q\bar{q}' \to X^{\pm} \to \gamma W^{\pm}(\to q\bar{q}')$	MadGraph + Pythia8	1	Longitudinal
qq$Z\gamma$ Spin 2	$q\bar{q} \to X \to \gamma Z(\to q\bar{q})$		2	Transverse
gg$Z\gamma$ Spin 2	$gg \to X \to \gamma Z(\to q\bar{q})$		2	Transverse
SM γ+Jet (Background)		Sherpa NLO	-	-

Analysis: Event Selection

Baseline Selection:

Trigger: HLT_g140_loose

Preselection: GRL + LooseBadJet cut on Resolved jets

TightPhoton with TightIsolation $P_T(\gamma) > 200$ GeV and $|\eta(\gamma)| < 1.37$

AntiKt10 TCC fatjet not overlap with photon

$P_T(\text{jet}) > 200$ GeV and $|\eta(\text{jet})| < 2.0$

An additional photon/jet pT cut is applied after categorization

Analysis: Categorization

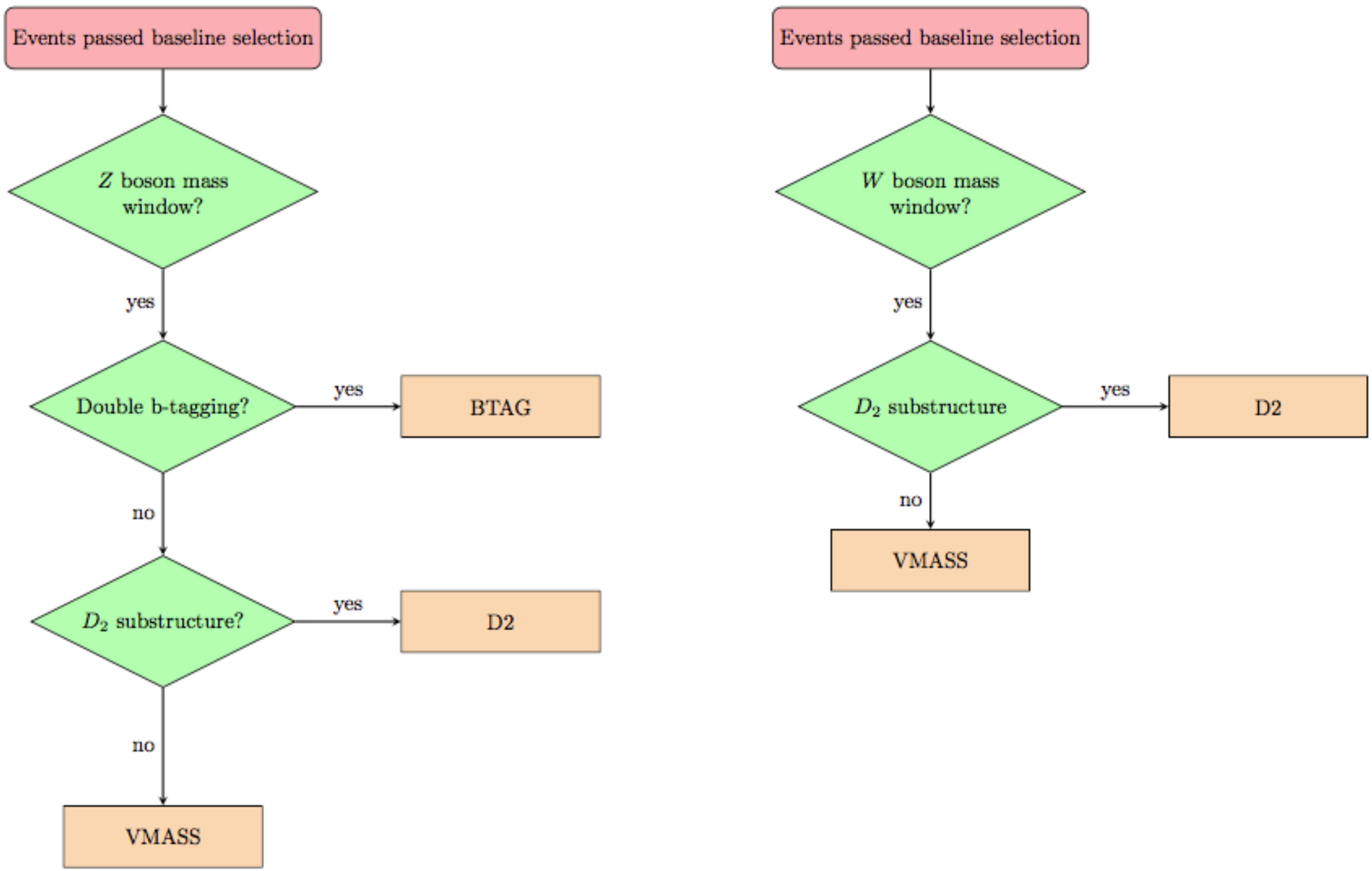

Analysis: Further Optimization

P_T cut is optimized in D2 and Vmass categories

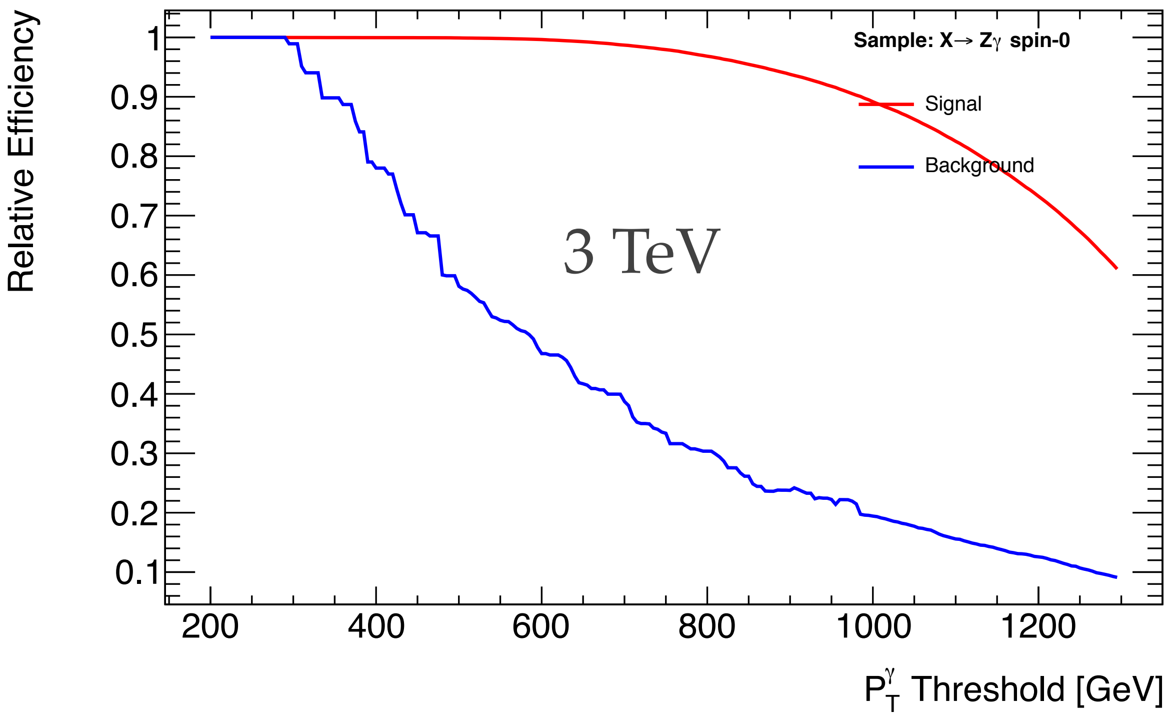

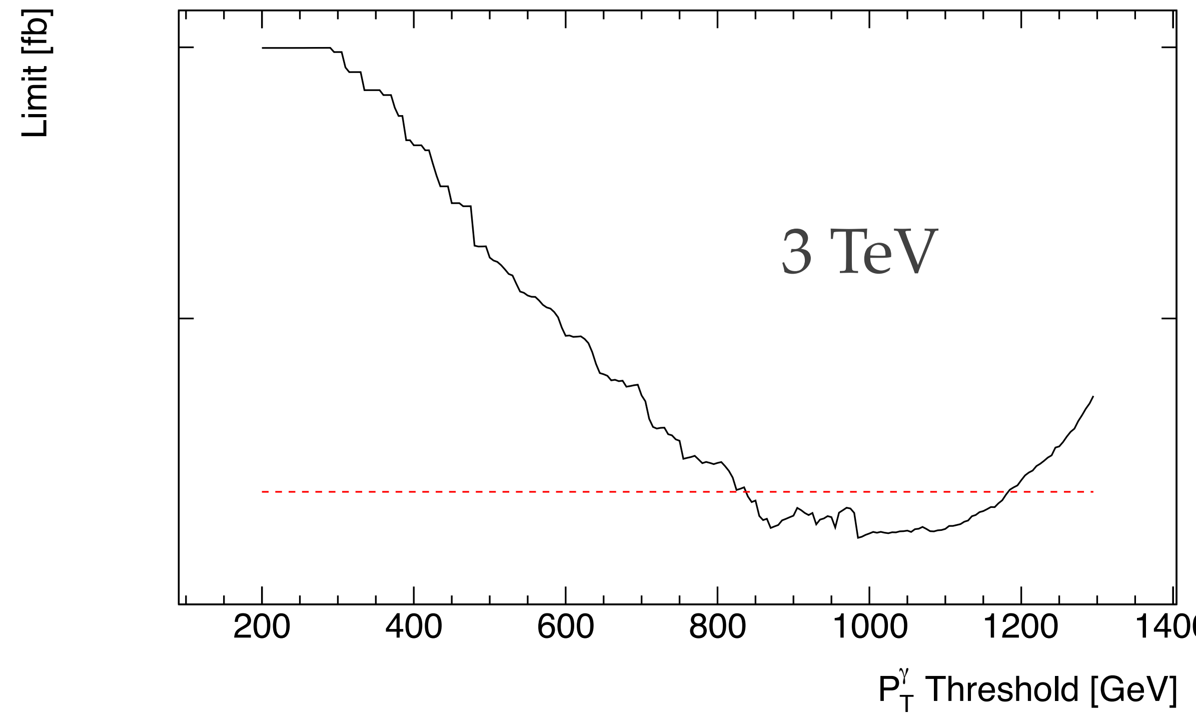

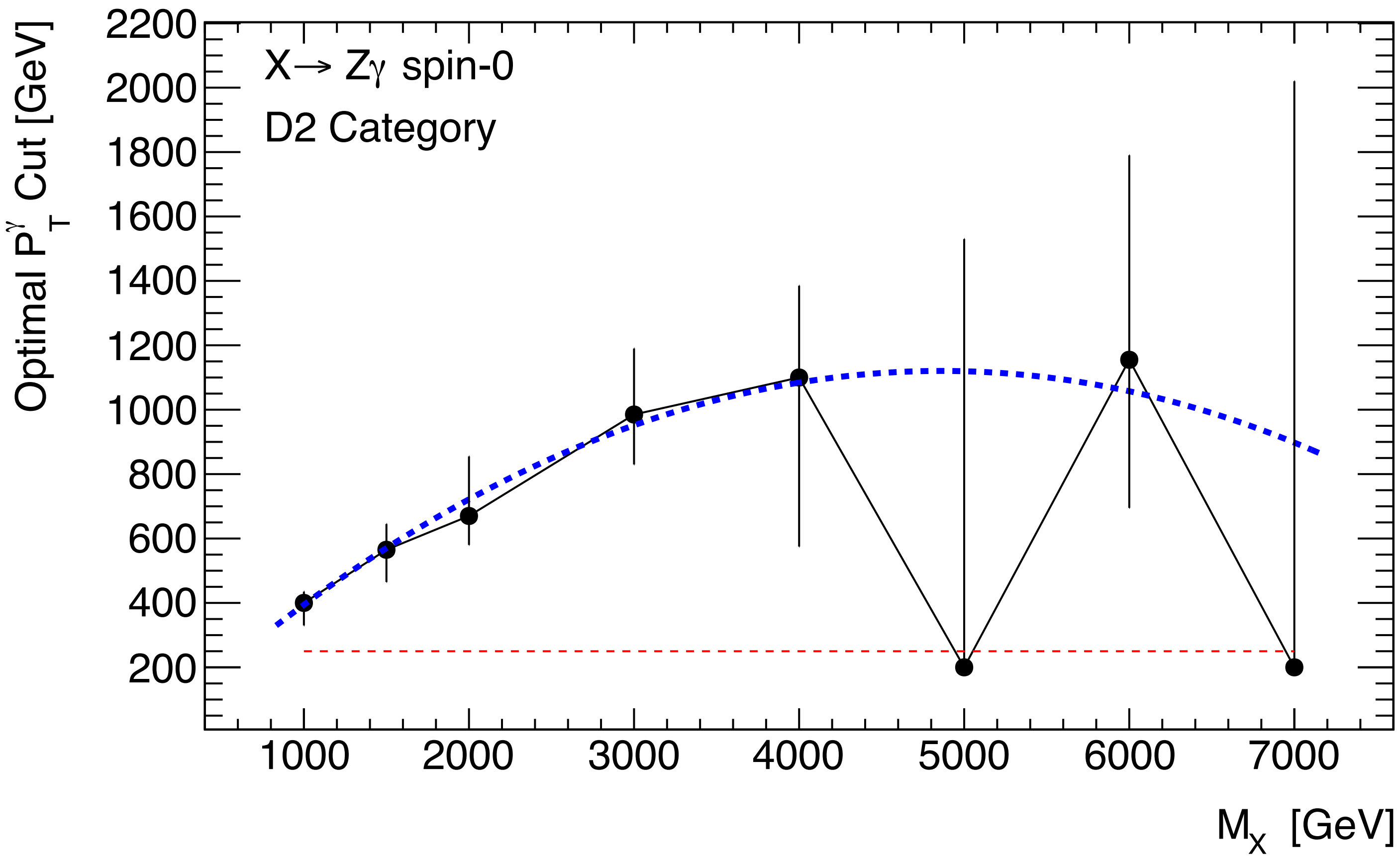

- The motivation of this cut is on the difference of pT distribution between signal and bkg
- For each category and mass point, scan through all possible pT cuts with 5 GeV step
- The optimal cut is taken based on the statistical only limit (asymptotic calculation)
- The error on each point in right bottom plot is set by the cut value window with less than 1.05 optimal limit
- A parabola is fitted for cut values, and after the maximum of parabola, cut value become constant

Analysis: Signal Efficiency

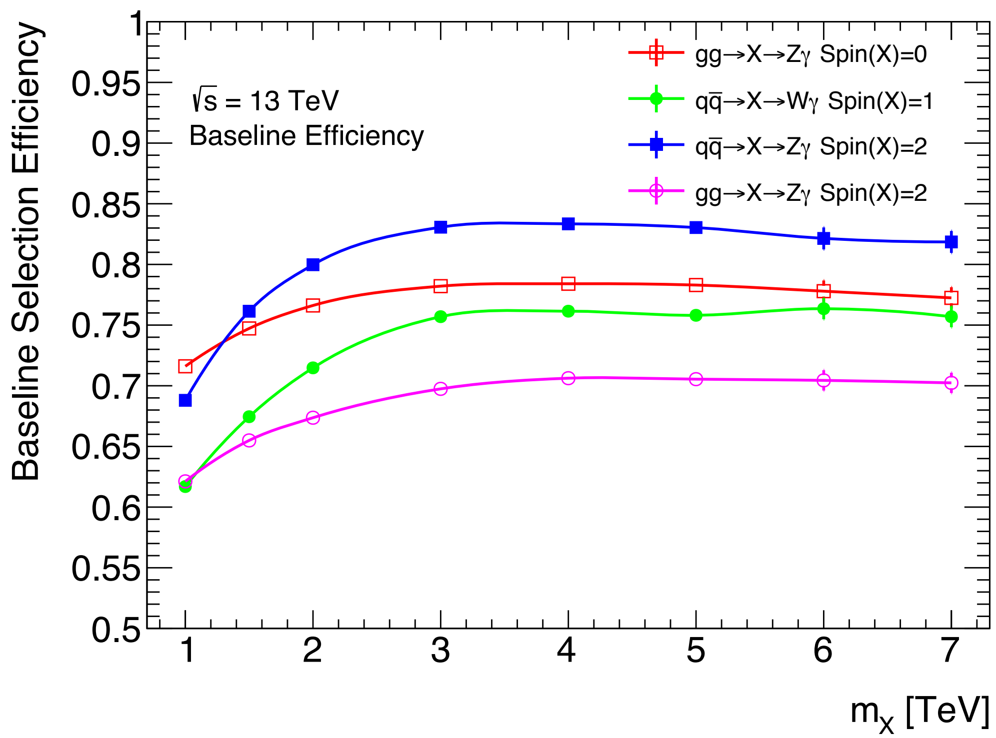

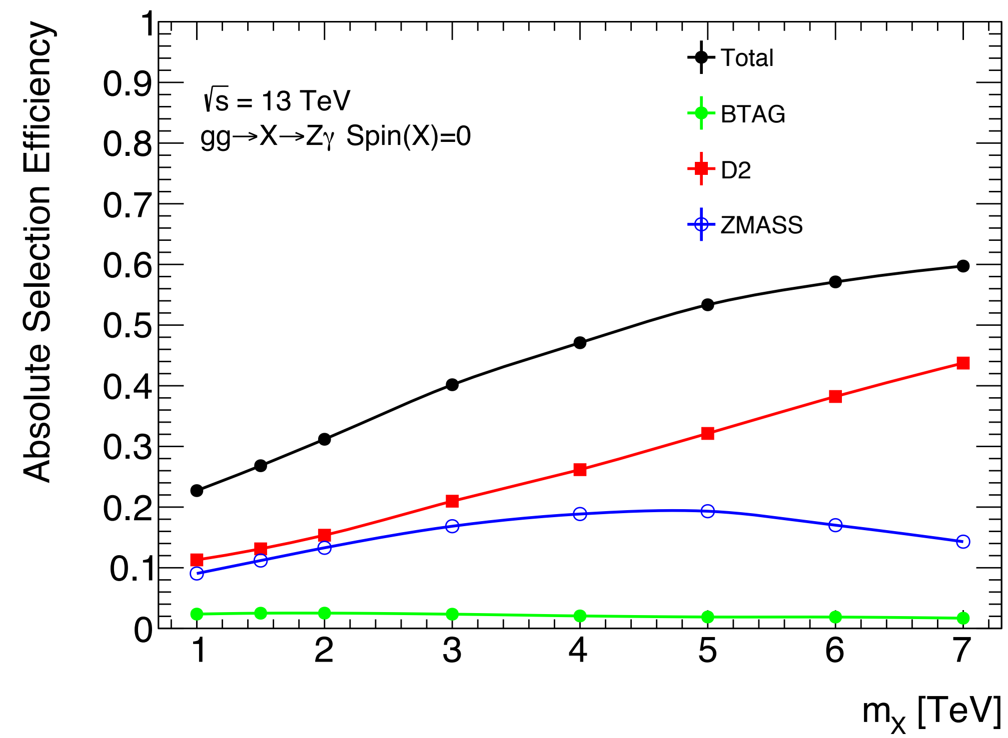

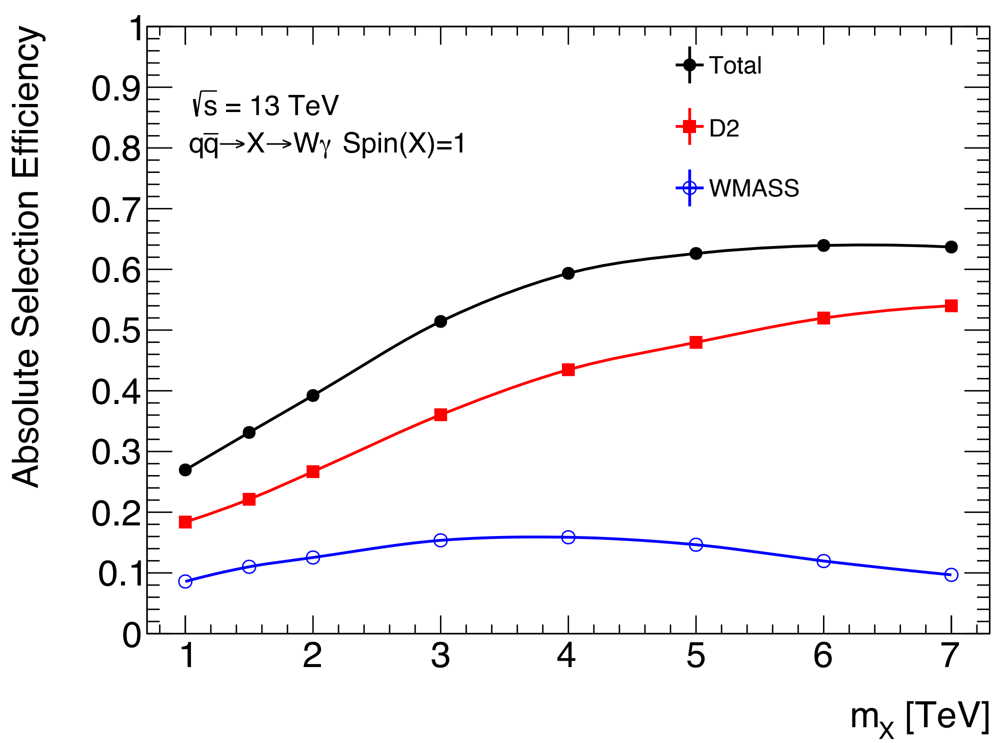

The signal categorization efficiency here is after applying the optimized P_T cut

Due to the boson polarization, the boson tagging on W boson is more efficient than Z boson

Variable-radius jet b-tagging making b-tag efficiency smooth after 3 TeV

The total number excluded the events filtered by the additional pT cut on non-btag categories

Analysis: Signal Modelling

$$DSCB(m; N, \mu, \sigma, \alpha_1, n_1, \alpha_2, n_2) =$$

$$N \cdot \begin{cases} \left(\frac{n_1}{|\alpha_1|}\right)^{n_1} \exp\left(-\frac{|\alpha_1|^2}{2}\right)\left(\frac{n_1}{|\alpha_1|} - |\alpha_1| - \frac{m-\mu}{\sigma}\right)^{-n_1} & \frac{m-\mu}{\sigma} \leq -\alpha_1 \\ \exp\left(-\frac{(m-\mu)^2}{2\sigma^2}\right) & -\alpha_1 < \frac{m-\mu}{\sigma} \leq \alpha_2 \\ \left(\frac{n_2}{|\alpha_2|}\right)^{n_2} \exp\left(-\frac{|\alpha_2|^2}{2}\right)\left(\frac{n_2}{|\alpha_2|} - |\alpha_2| + \frac{m-\mu}{\sigma}\right)^{-n_2} & \alpha_2 < \frac{m-\mu}{\sigma} \end{cases}$$

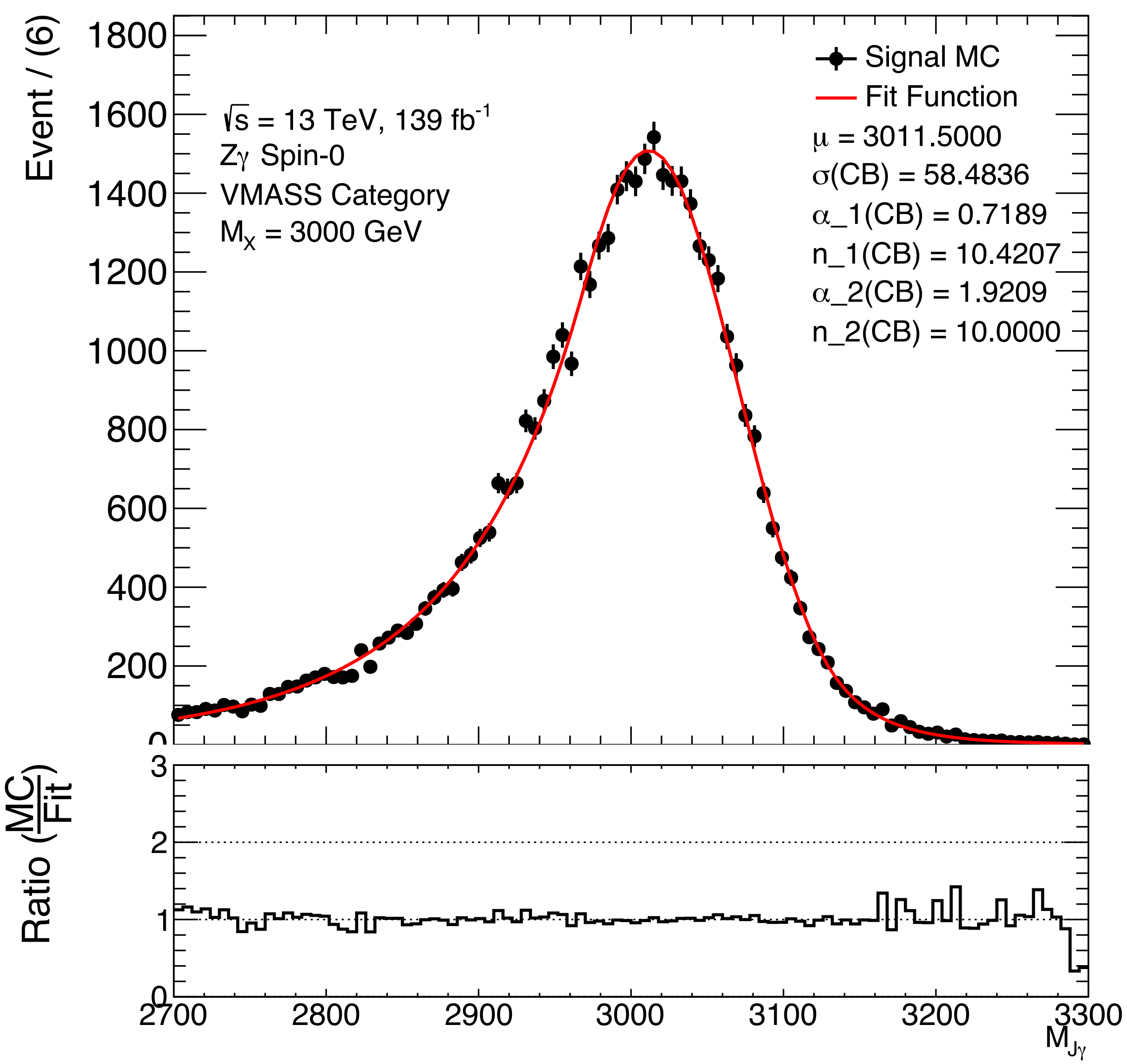

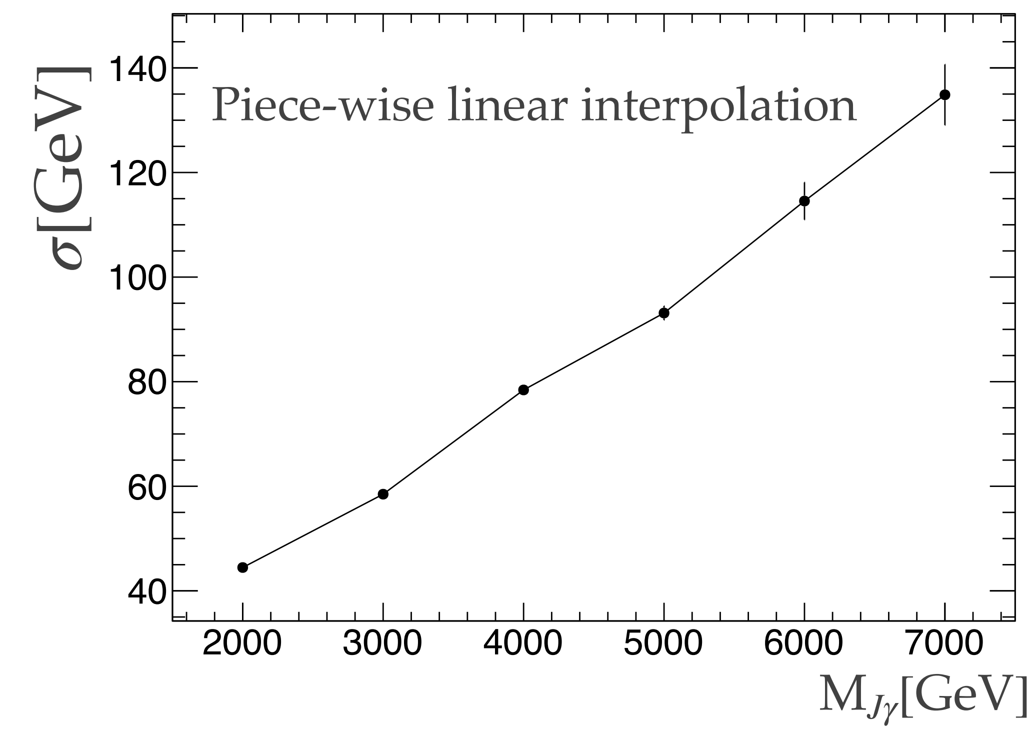

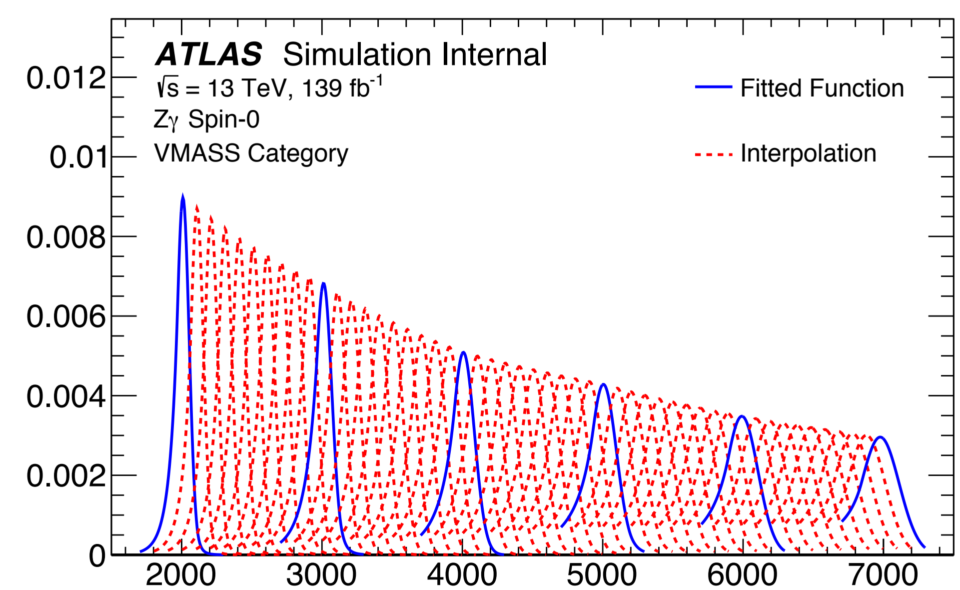

Analysis: Background Estimation

- The background estimation is data-driven, but the form of fit function is determined by spurious signal test on MC
- Test on the MC to determine number of parameters for di-jet function:

$$B(m_{\gamma J}; p_i) = (1-x)^{p_1} x^{p_2 + p_3 \log(x + p_4 \log^2(x) + p_5 \log^3(x))}$$

- Use the spurious signal test result to estimate background modeling uncertainty
- Cross checked with F-test to validate our function form choice

$Z\gamma$ Spin-0 Btag Category

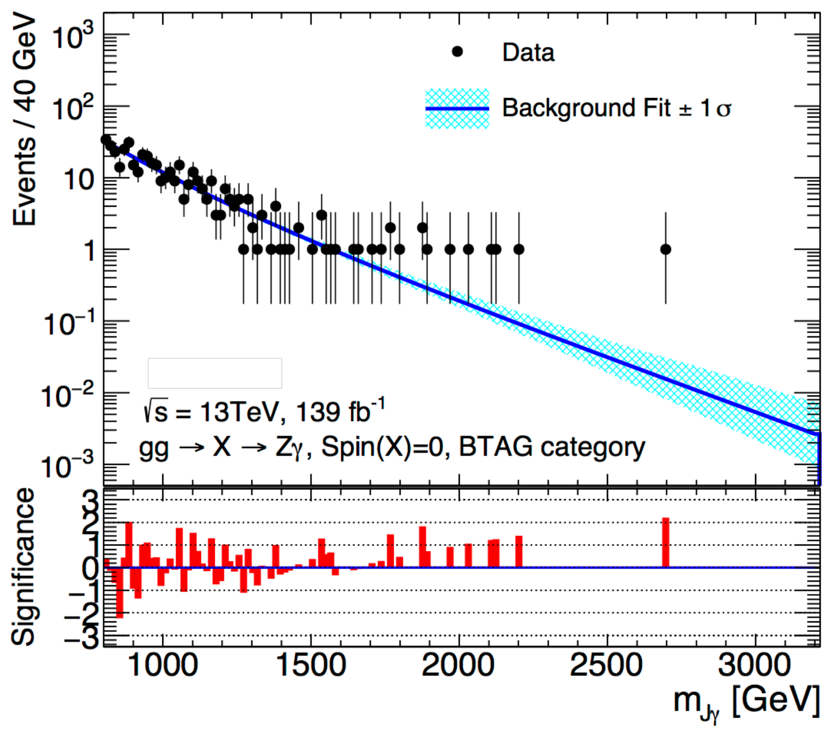

$Z\gamma$ Spin-0 D2 Category

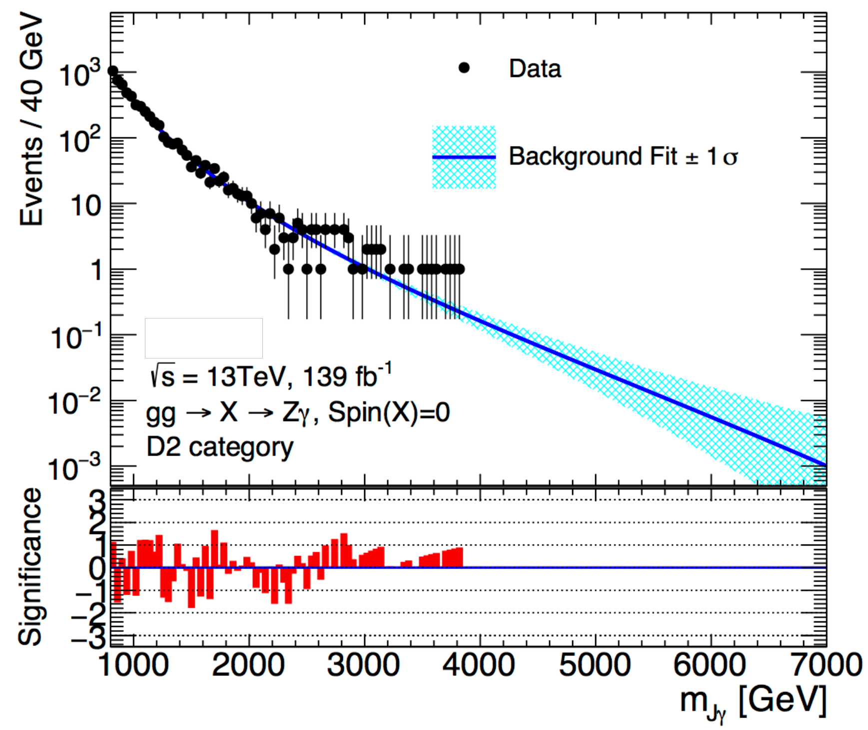

$Z\gamma$ Spin-0 Vmass Category

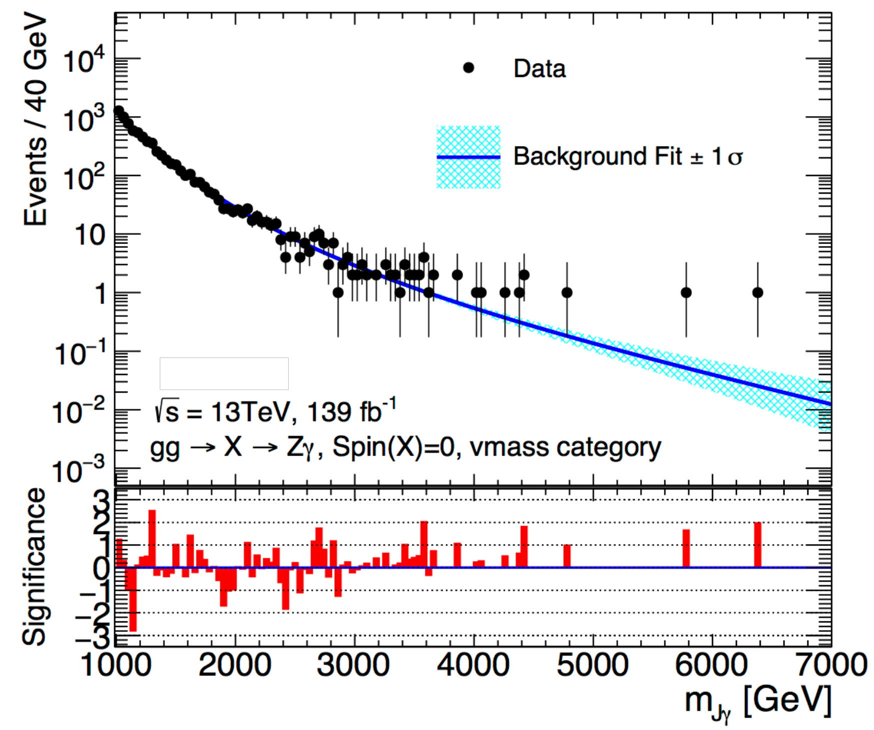

Analysis: Spurious Signal Test

- Fit the distribution with signal+background fit, the number of signal fitted is N_{SS}
- Estimate the statistical uncertainty assuming the distribution is background only, which is called δ_B. If the background is large enough, it will be about $\sqrt{N_B}$
- The ratio N_{SS}/δ_B is taken as the criteria of goodness of fit.
- If no significant improvement, use the lowest number of parameters

$Z\gamma$ Spin-0 Btag Category

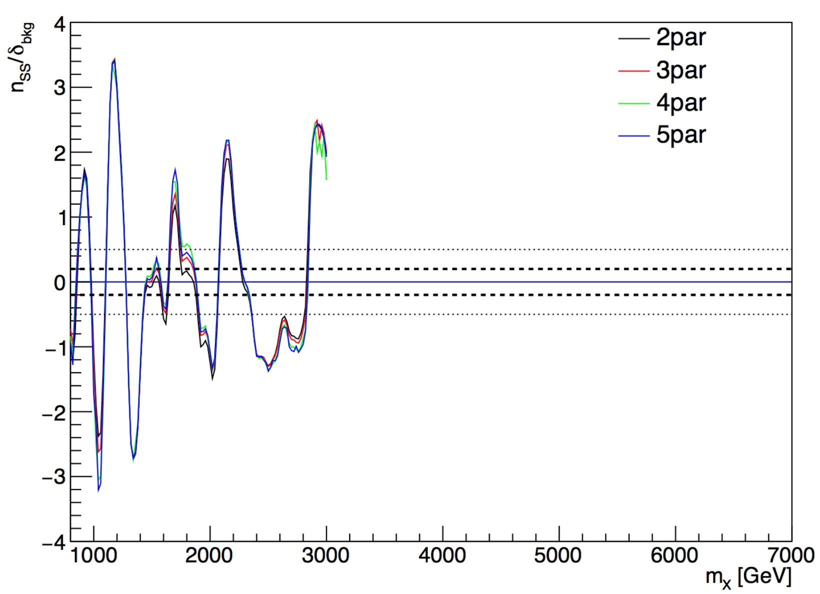

$Z\gamma$ Spin-0 D2 Category

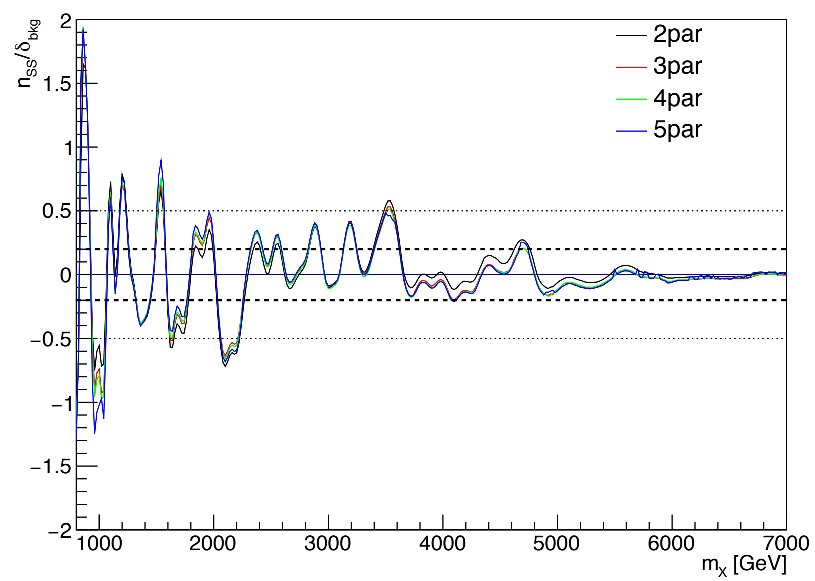

$Z\gamma$ Spin-0 Vmass Category

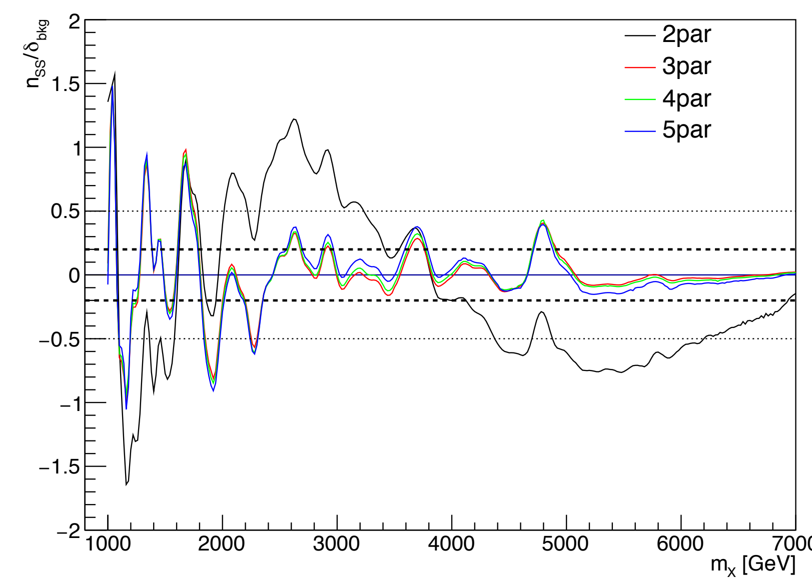

Parameter Number Choice

Channel	btag	d2	vmass
$gg \to X(spin=0) \to \gamma Z(\to q\bar{q})$	2	2	3
$qq \to X^{\pm}(spin=1) \to \gamma W^{\pm}(\to qq')$	-	2	3
$qq \to X(spin=2) \to \gamma Z(\to q\bar{q})$	2	3	3
$gg \to X(spin=2) \to \gamma Z(\to q\bar{q})$	2	2	3

Analysis: Systematical Uncertainties

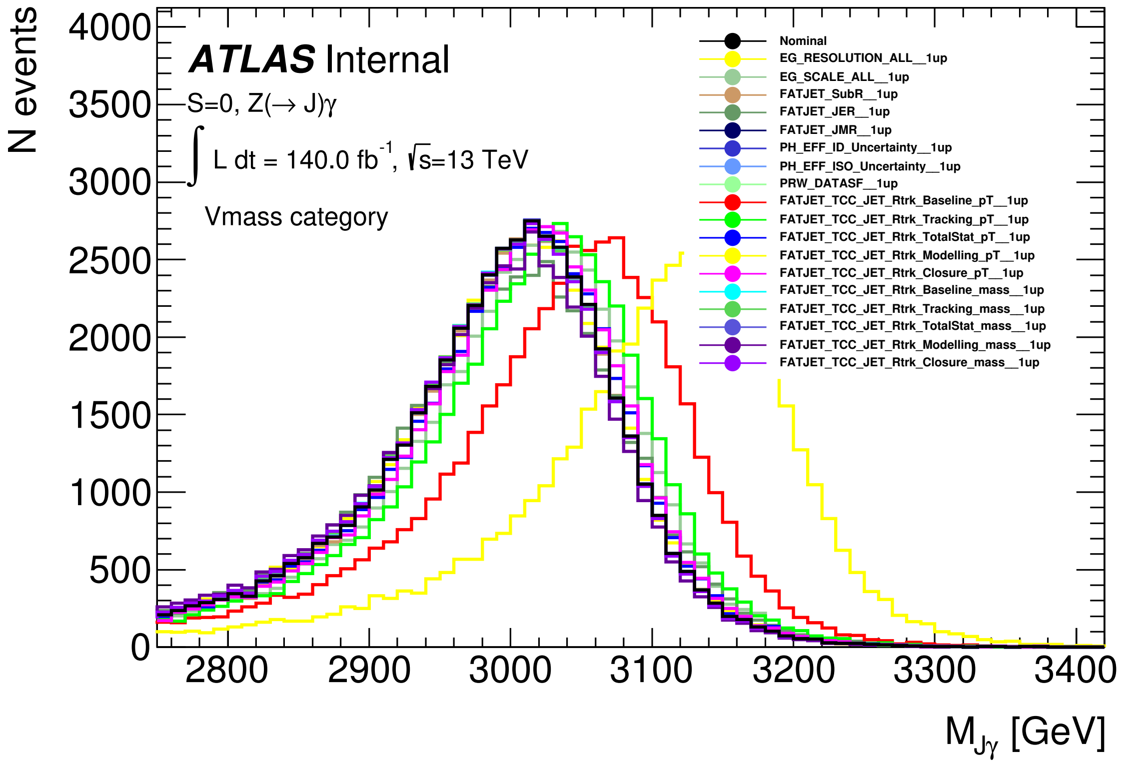

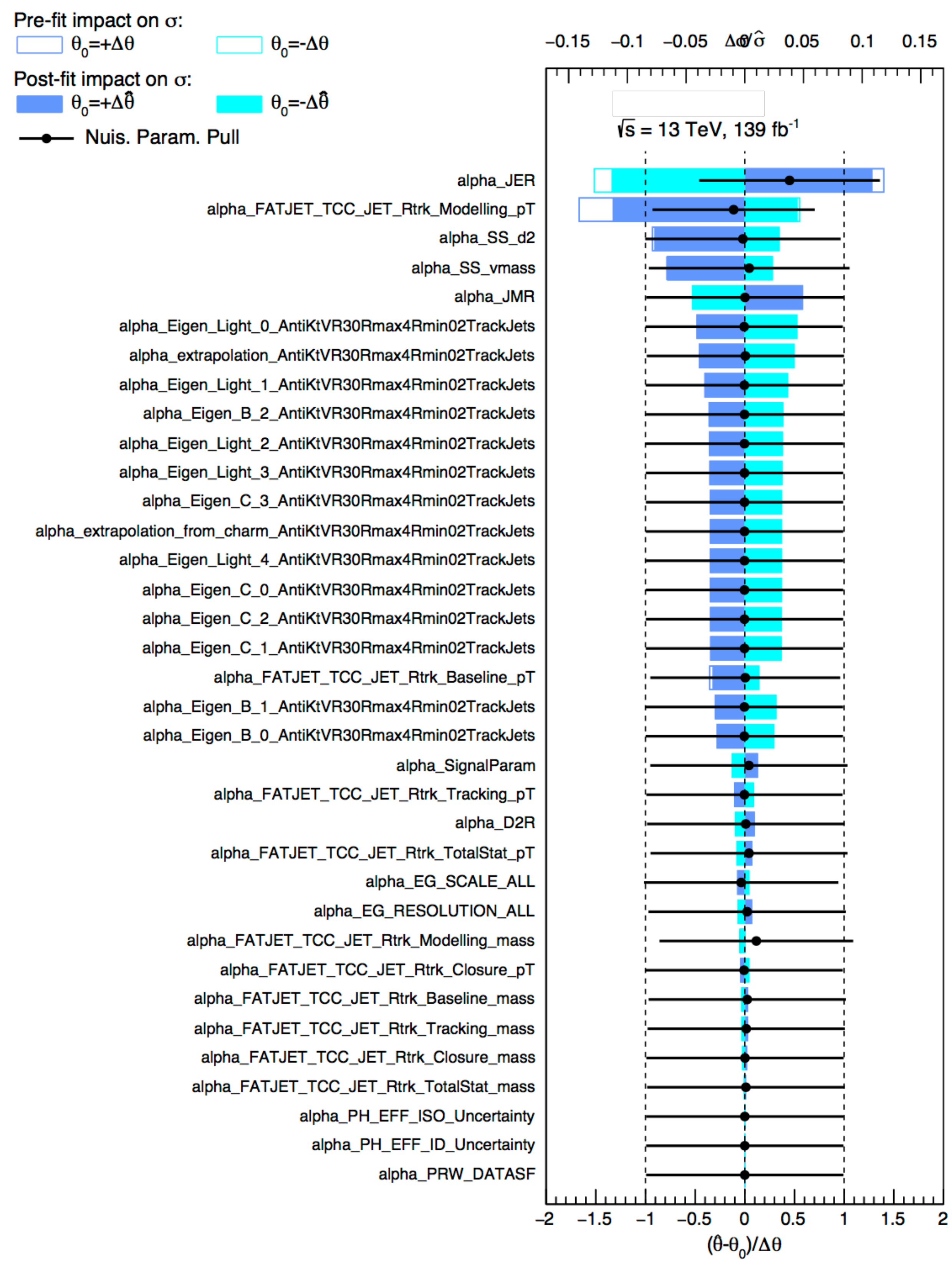

- Luminosity (~1.7%)
- **Photon energy**
  - Dominant at very high mass
- Photon identification and isolation
  - Negligible
- **Jet energy and mass**
  - Major contribution in full range
- Jet tagging
  - Negligible

Analysis: Statistical Implementation

Likelihood of events in each category

$$\mathcal{L}(\overrightarrow{m^{\text{obs}}_{\text{J}\gamma}}|\,\sigma,\vec{\theta},\theta^{\vec{\text{SS}}},\vec{N^{\text{b}}},\vec{p}) = \prod_{c\in\mathbb{C}}\Bigg\{\text{Pois}(N_c^{\text{obs}}|N_c^{\text{s}}(\sigma,\vec{\theta})+N_c^{SS}+N_c^{\text{b}})$$

Likelihood of signal and background distributions

$$\prod_{i=1}^{N_c^{\text{obs}}}\Bigg[\left(\frac{N_c^{\text{s}}(\sigma,\vec{\theta})+N_c^{SS}(\theta_c^{SS})}{N_c^{\text{s}}(\sigma,\vec{\theta})+N_c^{SS}(\theta_c^{SS})+N_c^{\text{b}}}\right)\mathcal{S}(m_{J\gamma}^{c,i,\text{obs}}|\,\vec{\theta})+$$

Fraction of signal and background

$$\left(\frac{N_c^{\text{b}}}{N_c^{\text{s}}(\sigma,\vec{\theta})+N_c^{SS}(\theta_c^{SS})+N_c^{\text{b}}}\right)\mathcal{B}(m_{J\gamma}^{c,i,\text{obs}}|\,\vec{p^c})\Bigg]\Bigg\}\times$$

$$\prod_{s\in\mathbb{S}}\mathcal{G}(0|\theta_s,1)\prod_{c\in\mathbb{C}}\mathcal{G}(0|\theta_c,1),$$

Constrains on nuisance parameters determined by systematical uncertainty

Analysis: Expected Limits

$$gg \rightarrow X \rightarrow \gamma Z(\rightarrow q\bar{q})$$

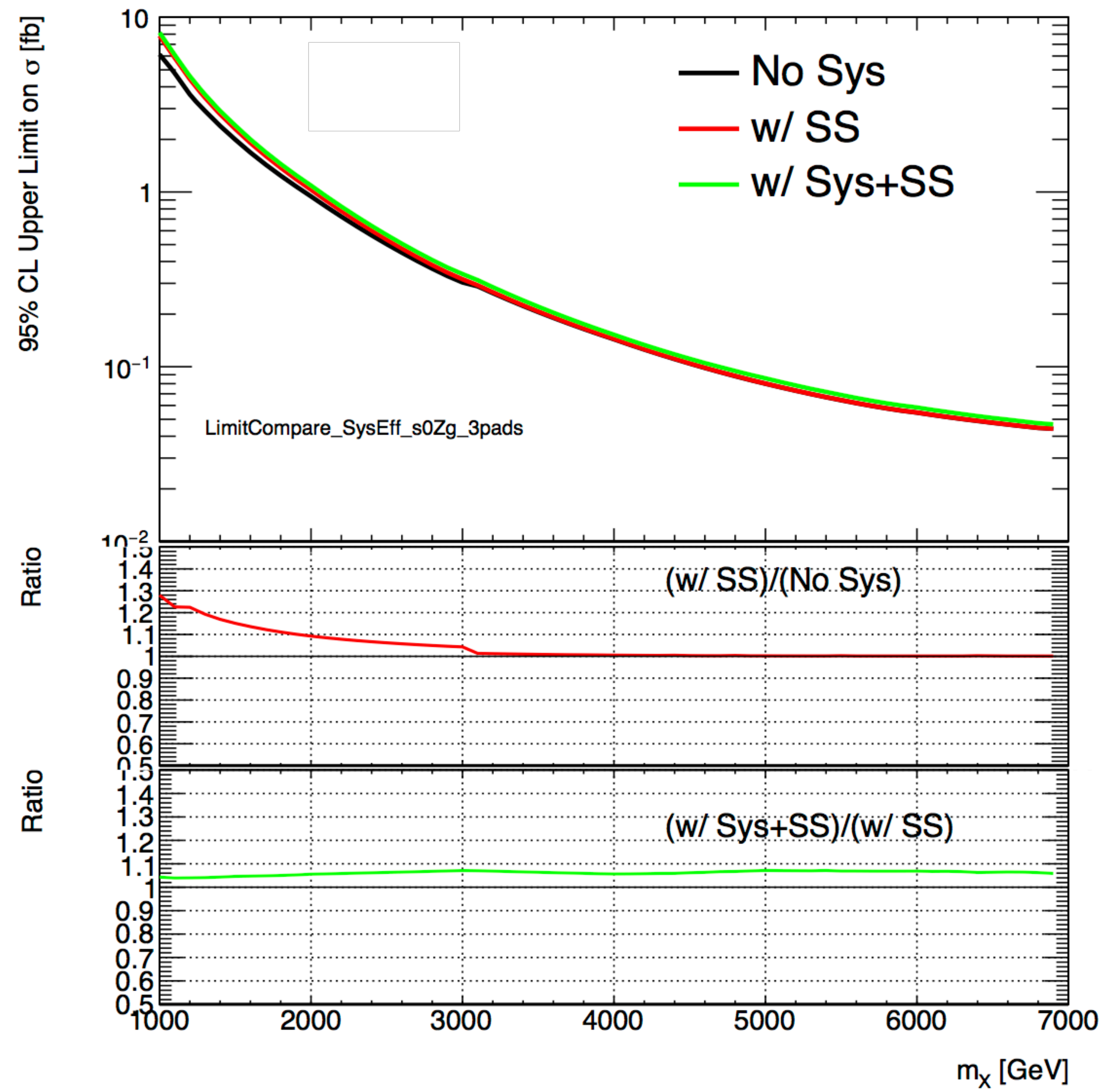

- Spurious signal contribution is only in low mass range
- Systematical uncertainty is below 10% in the full range
- The major limitation of this search is from the statistical uncertainty
- Similar results for other signal channels

Analysis: Observed Significance

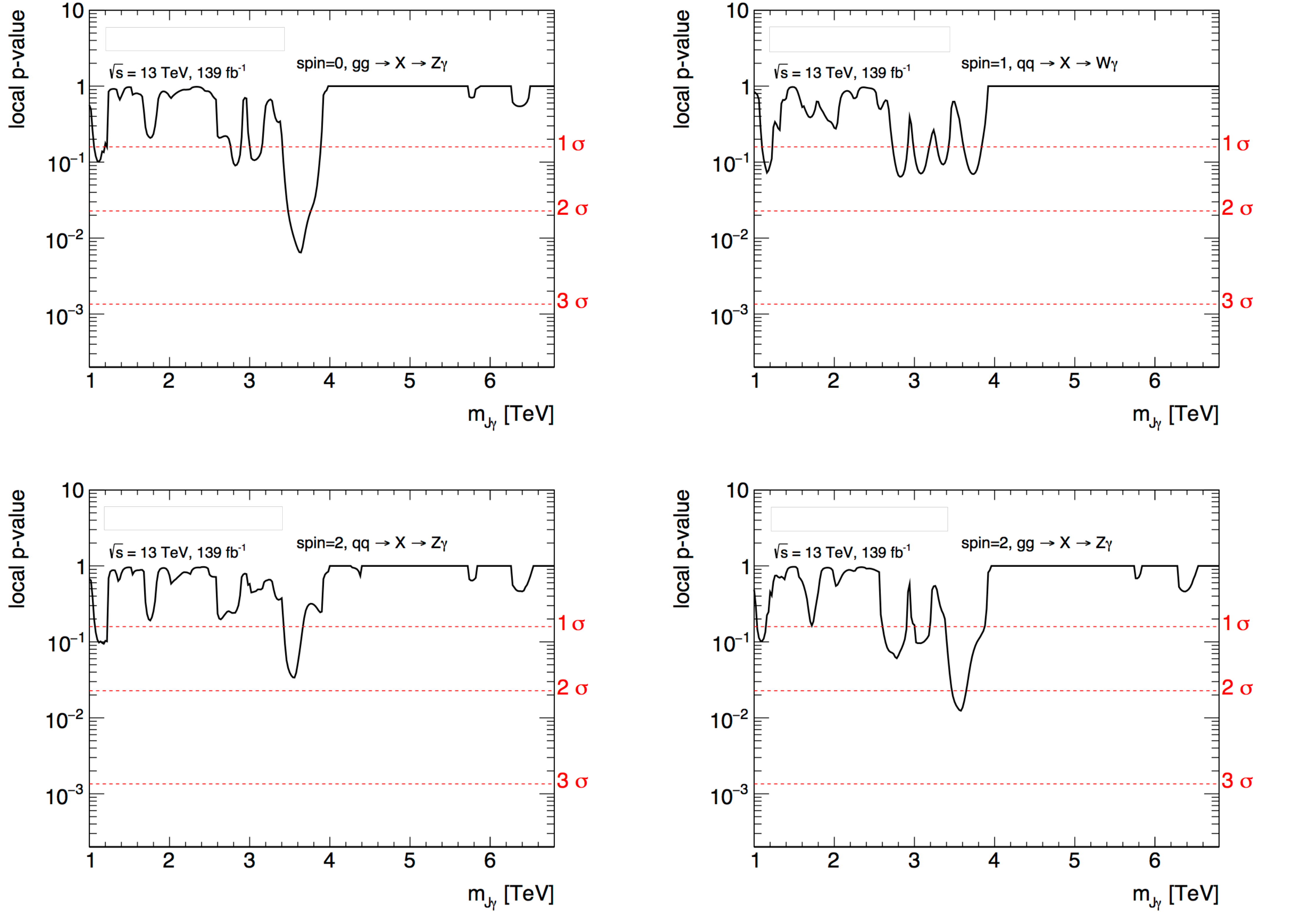

Analysis: Observed Limits

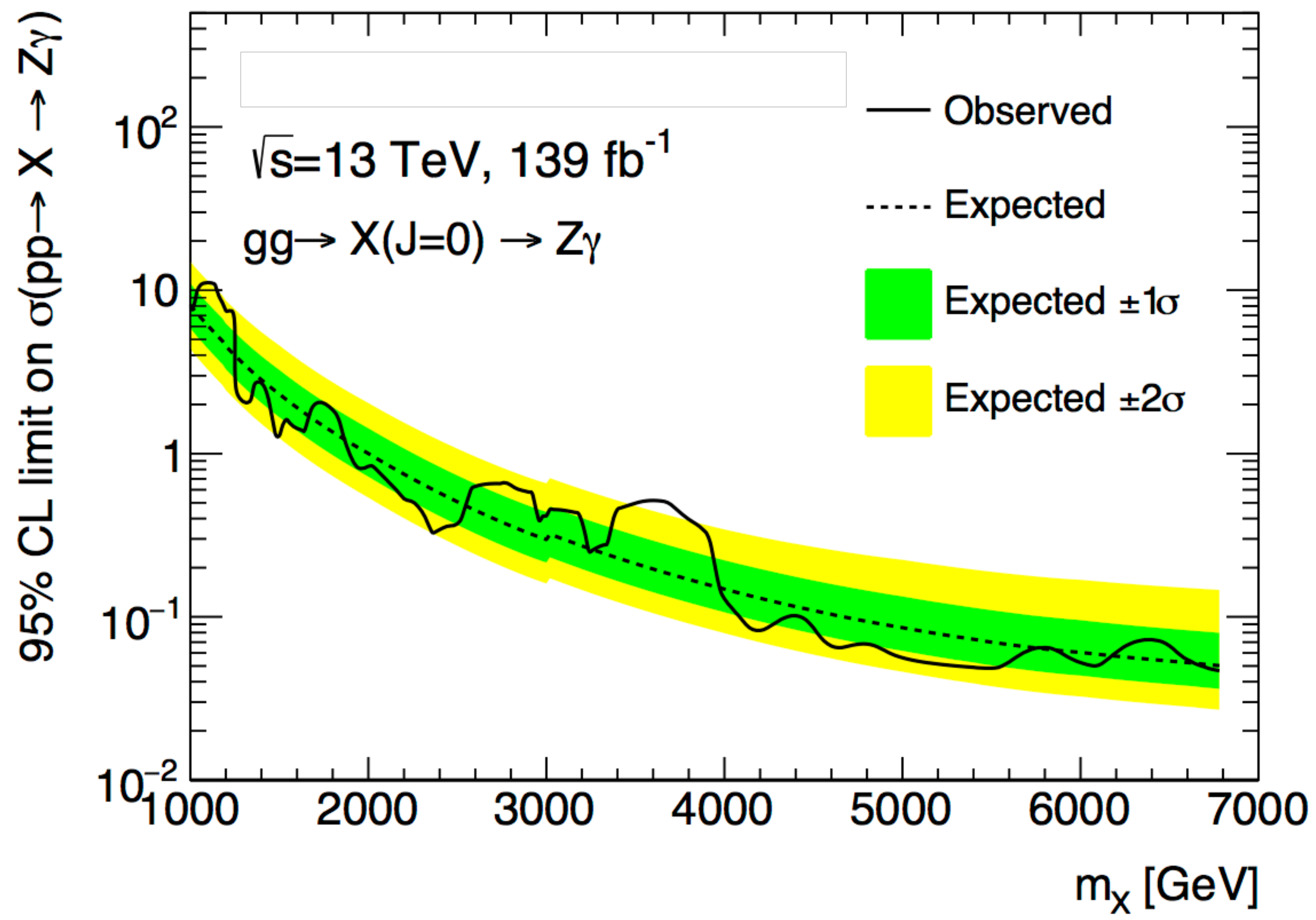

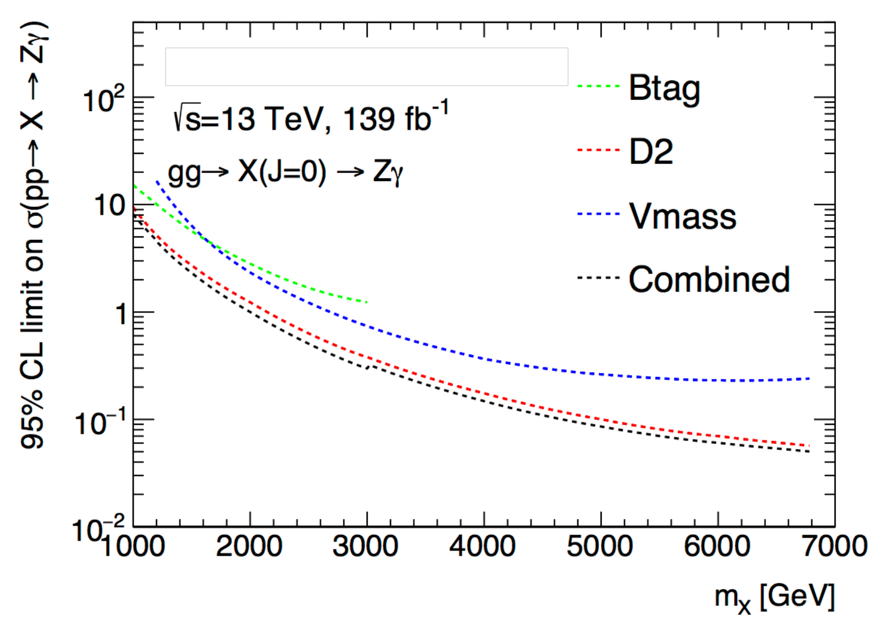

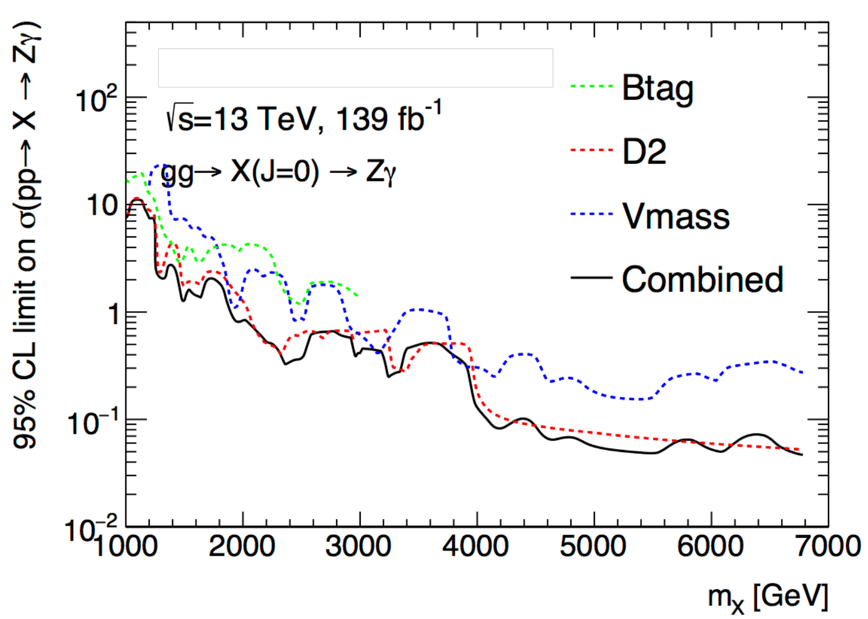

Analysis: Observed Limits

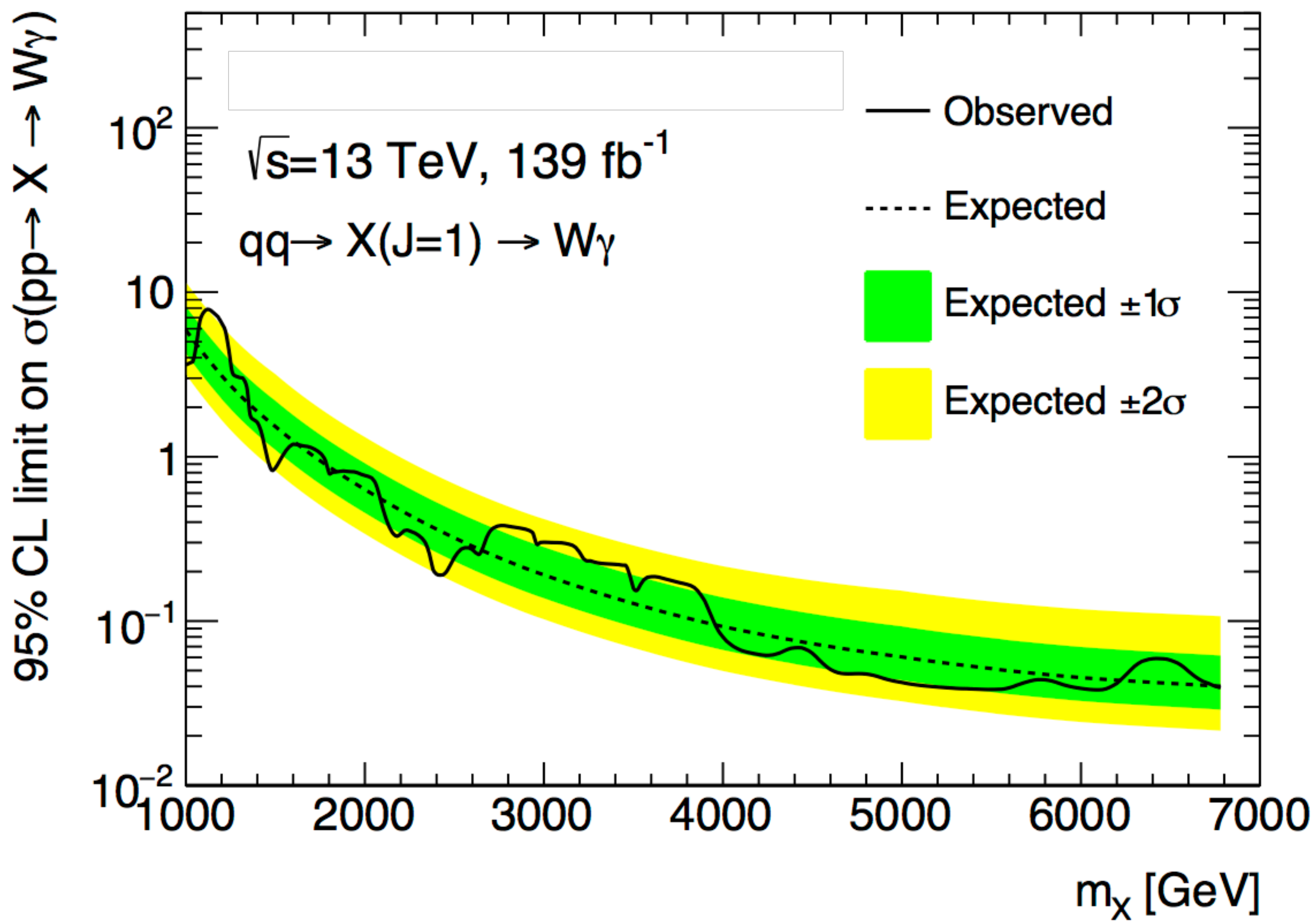

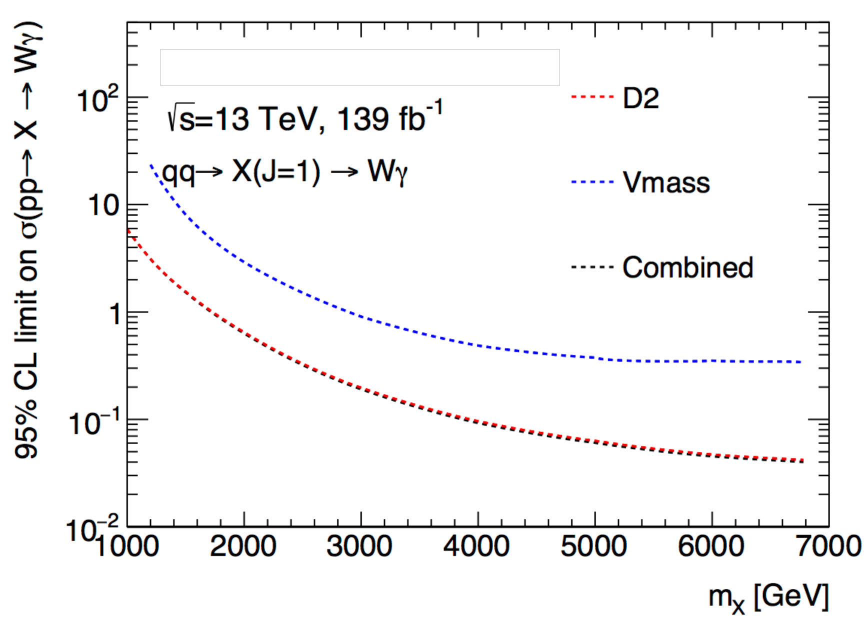

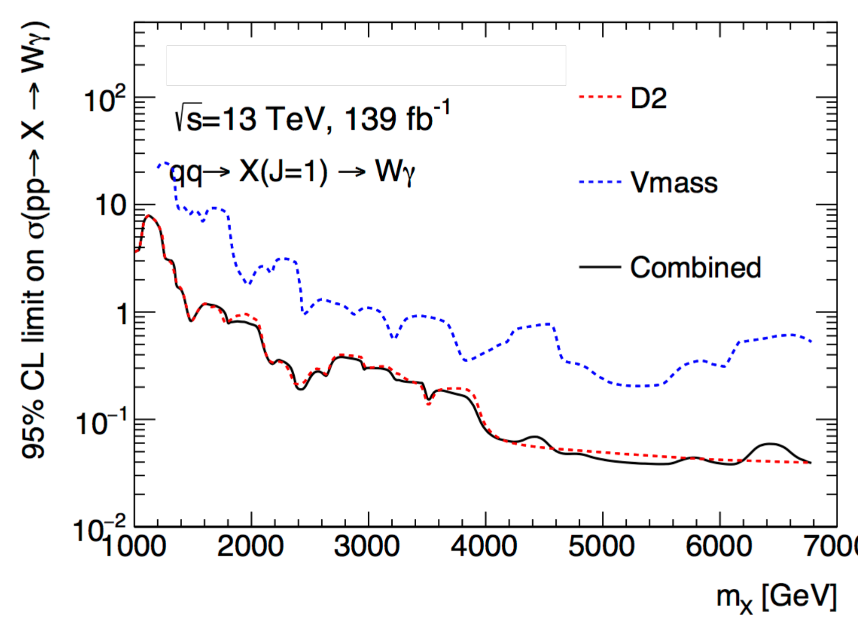

Analysis: Observed Limits

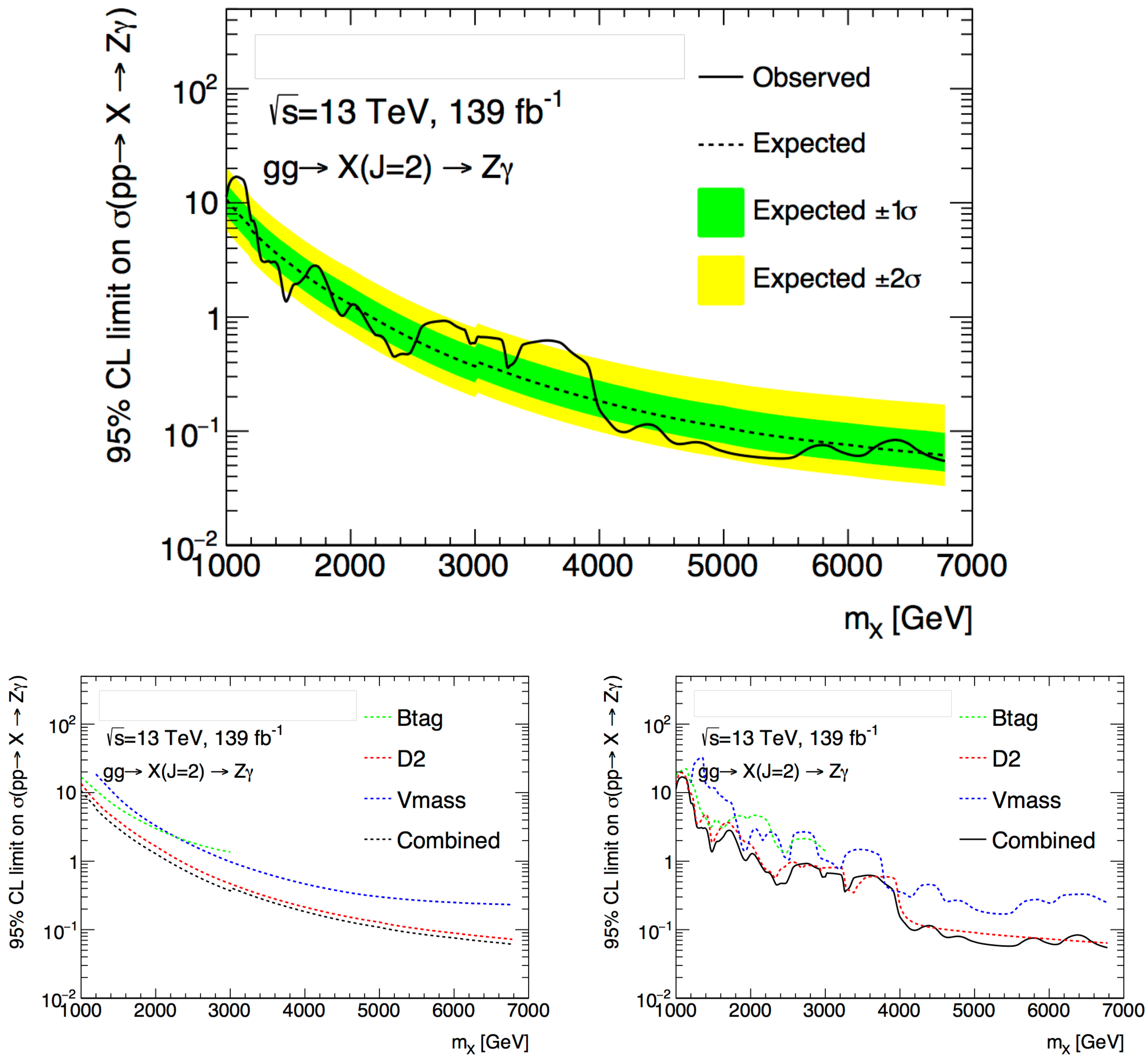

Analysis: Observed Limits

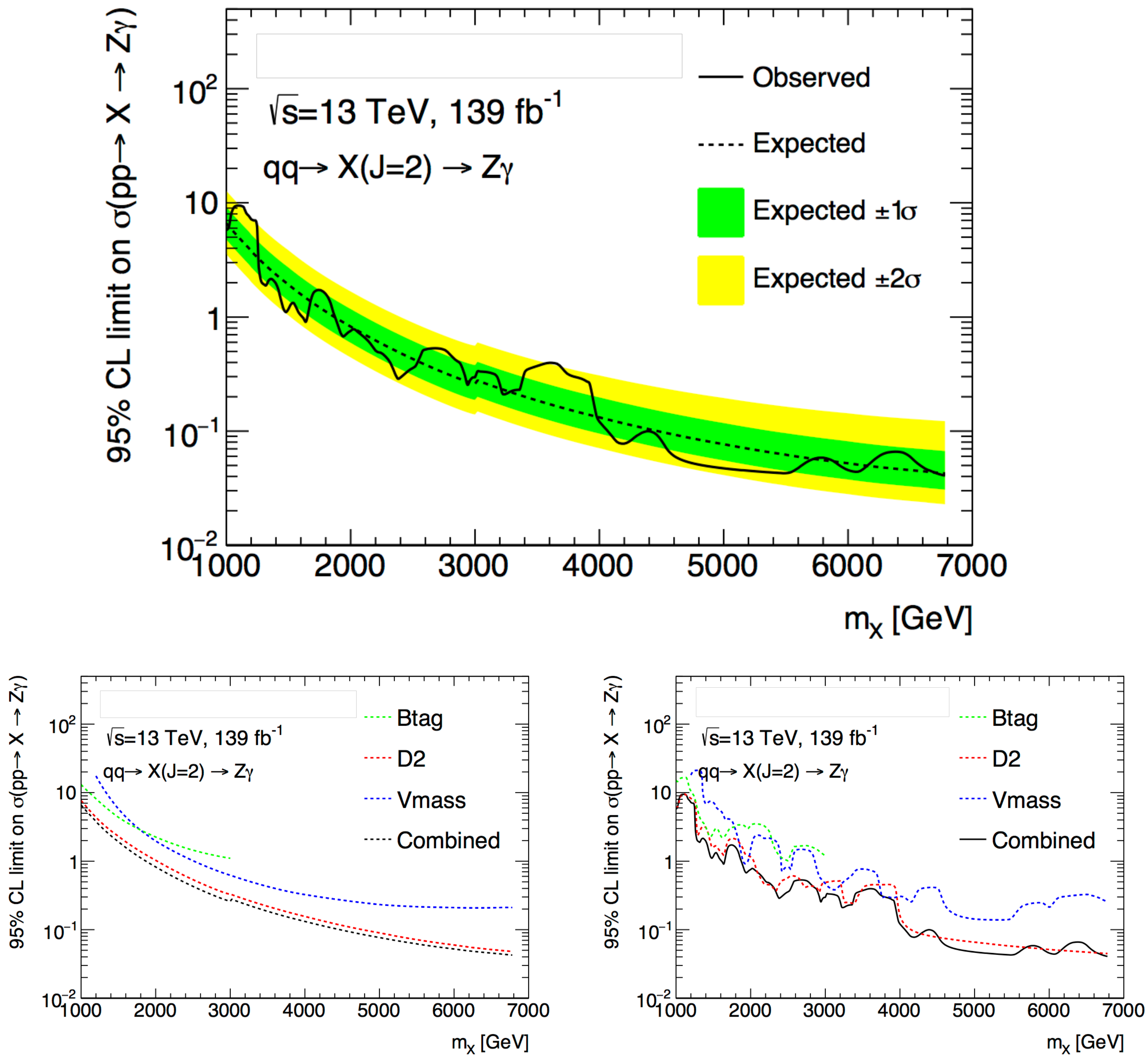

Backup

Significance and P-value

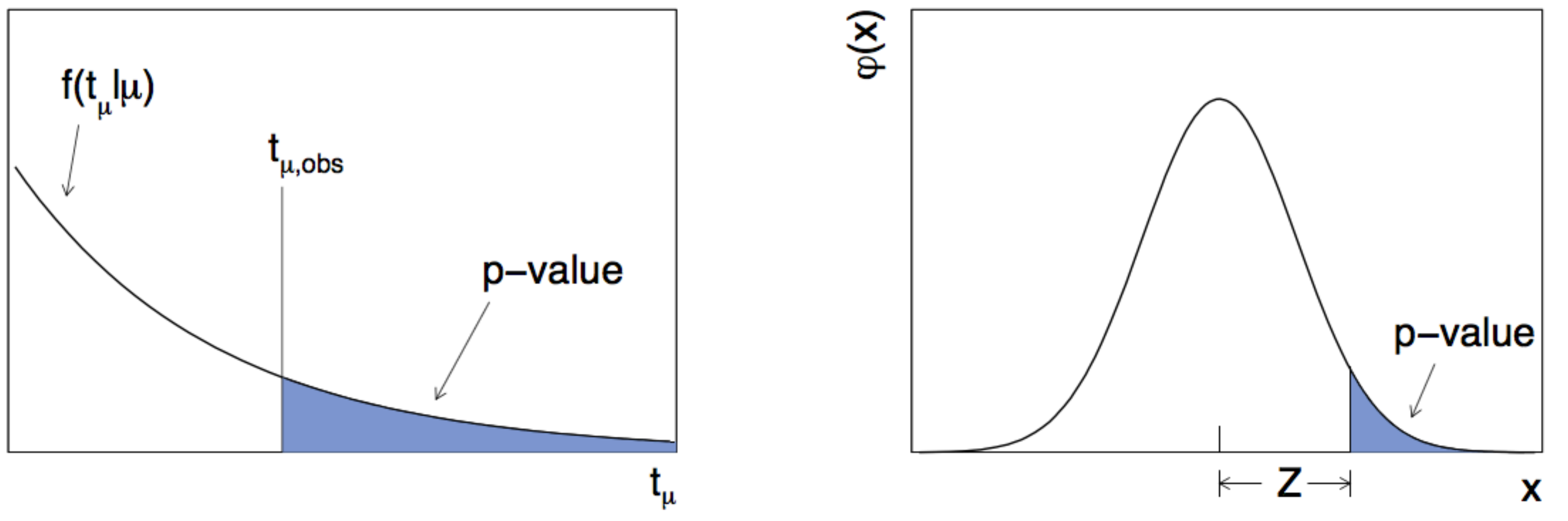

$$Z = \Phi^{-1}(1 - p)$$

Signal Categorization Efficiencies

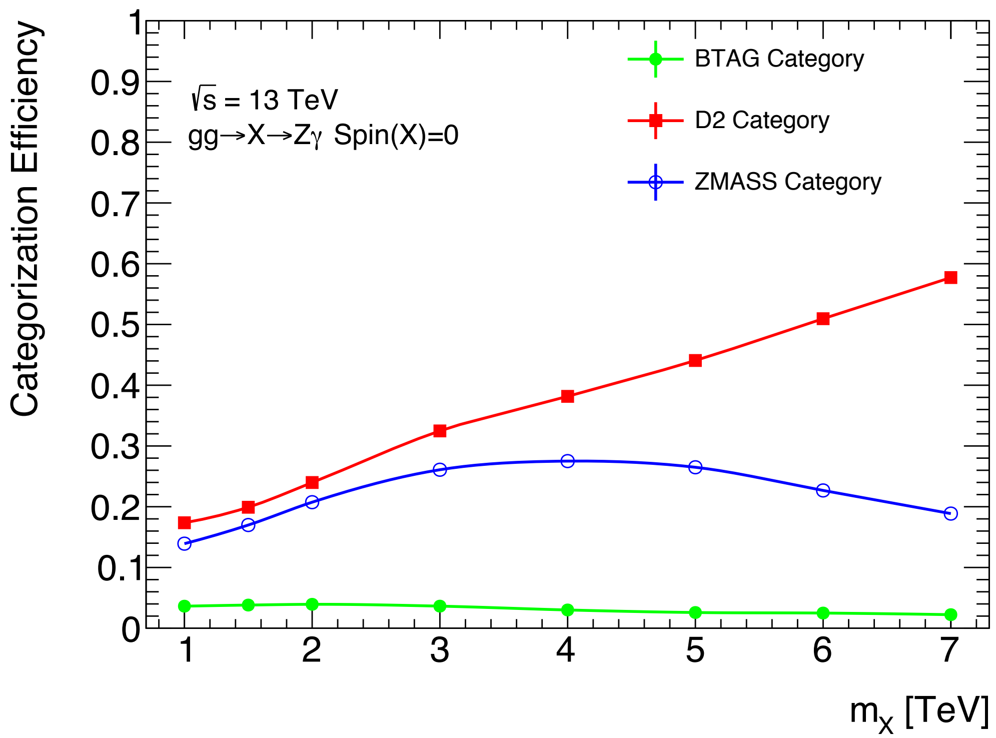

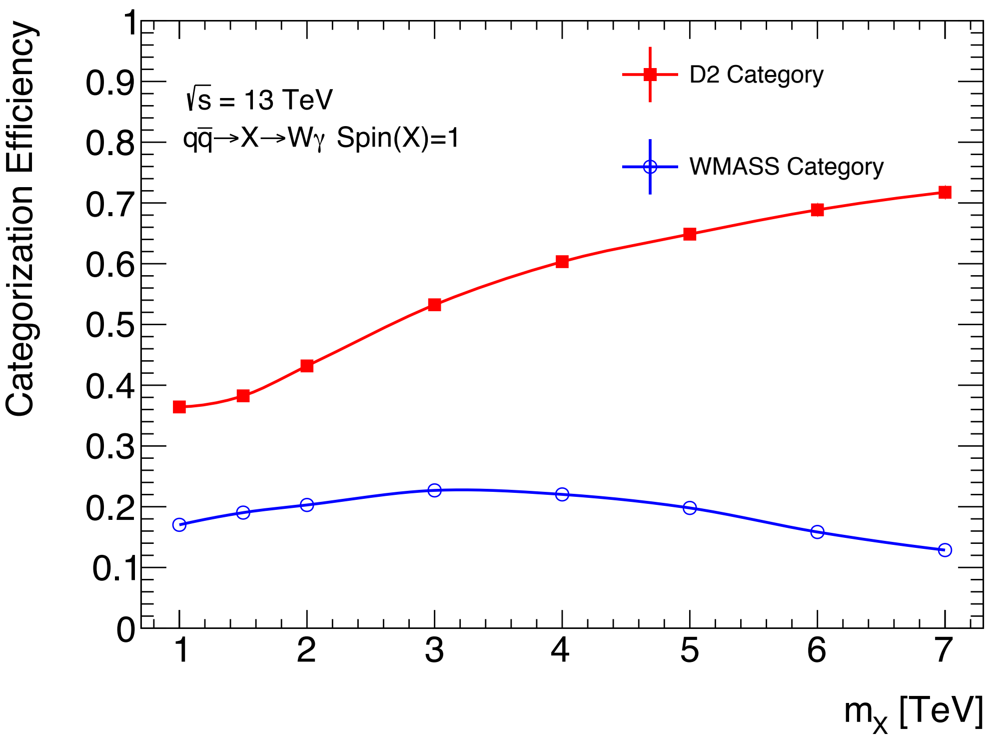

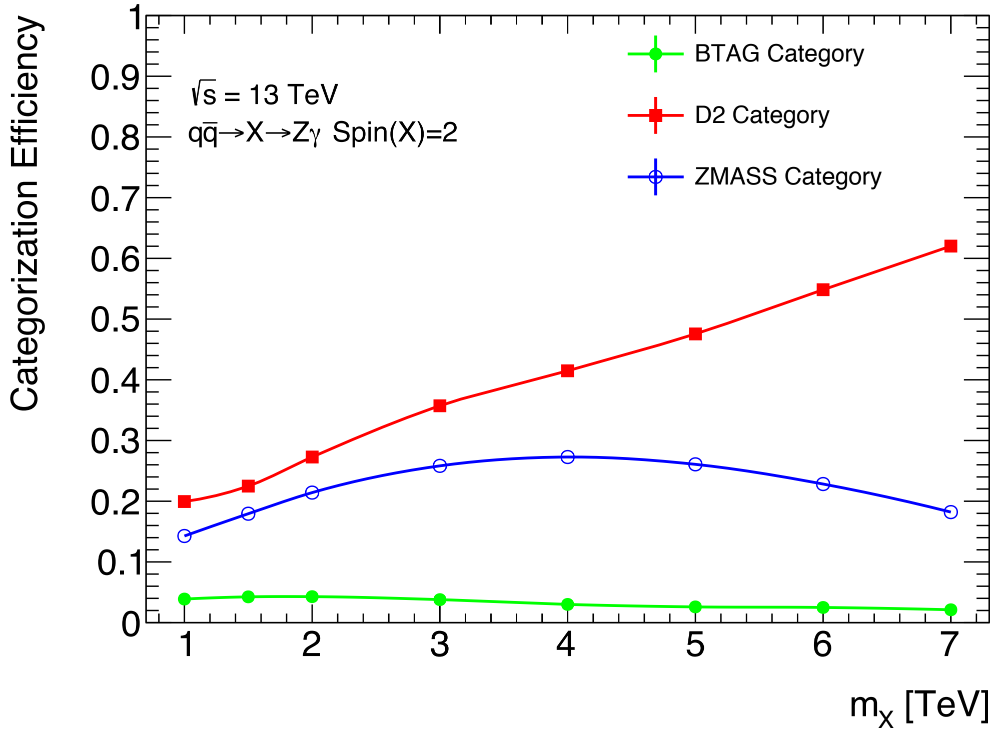

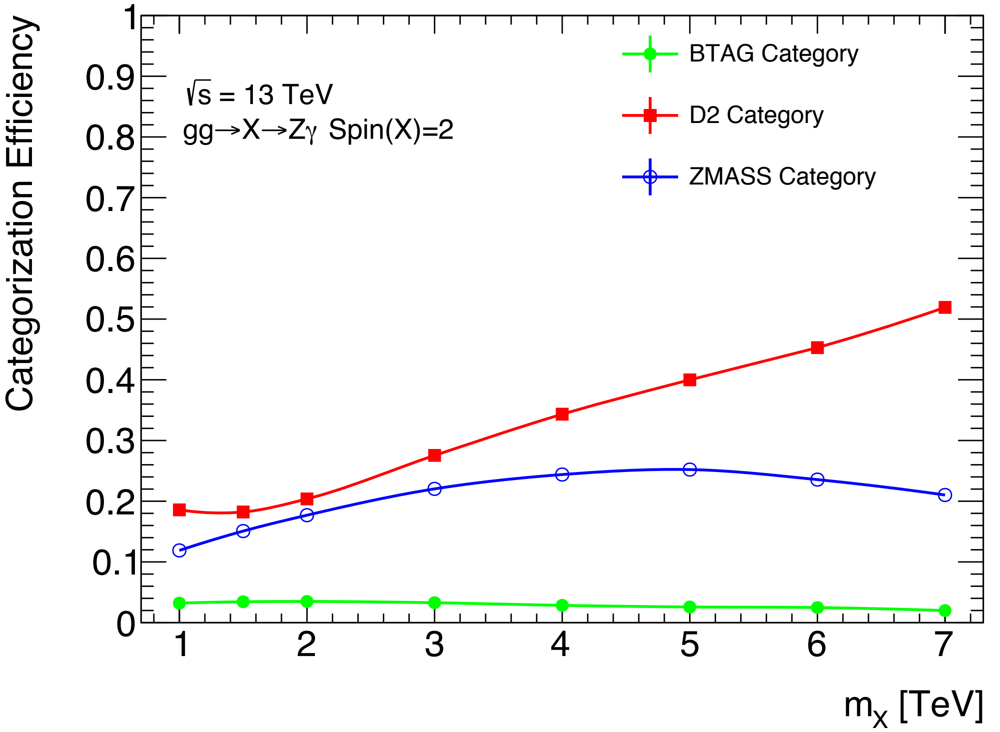

Background Categorization Efficiencies

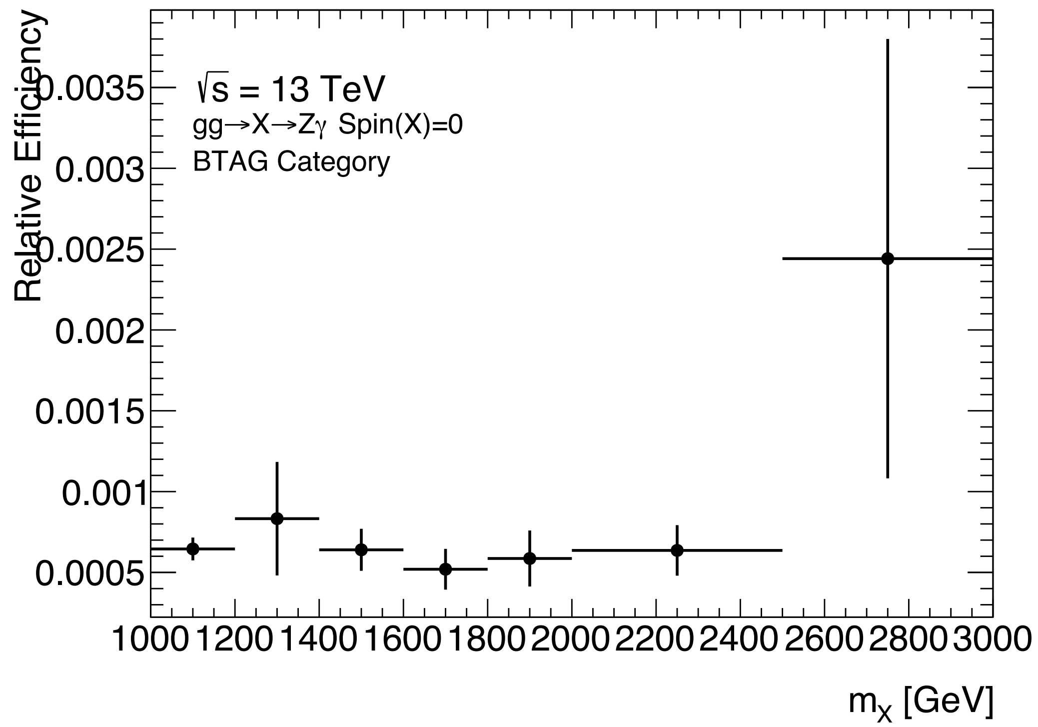

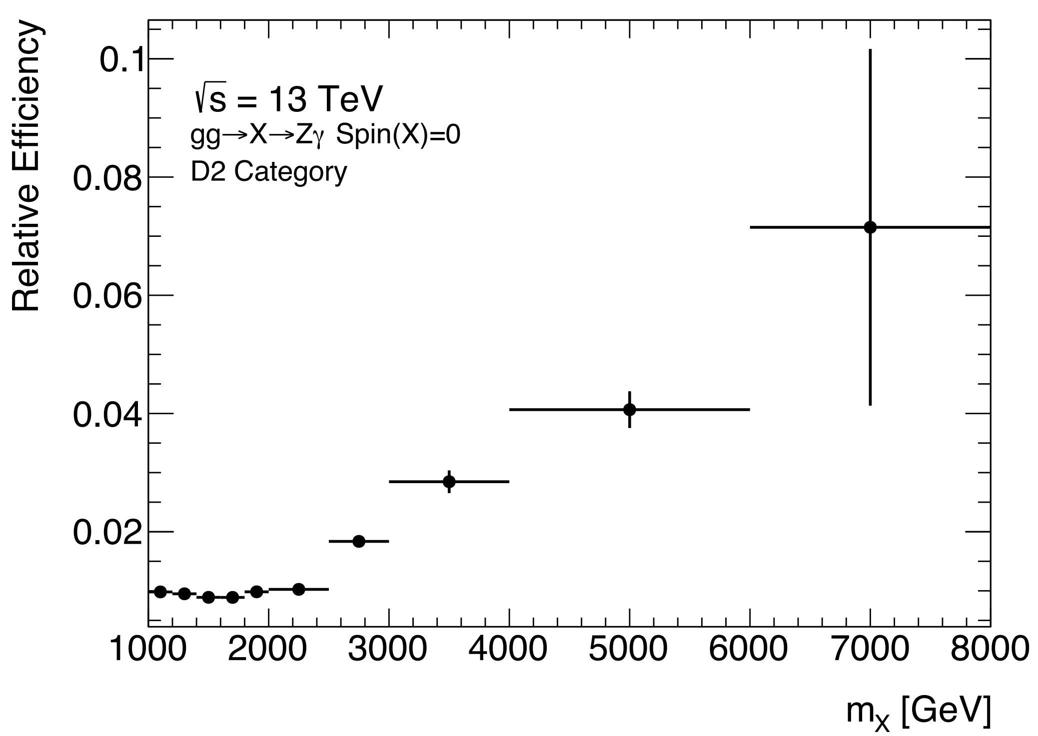

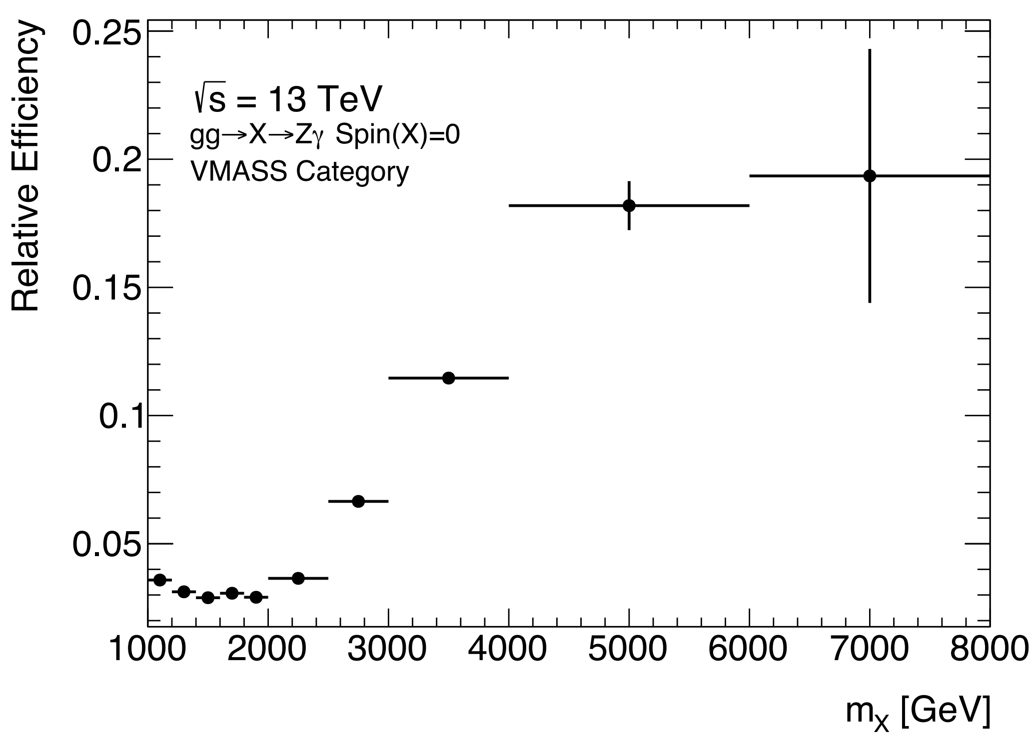

Background Categorization Efficiencies

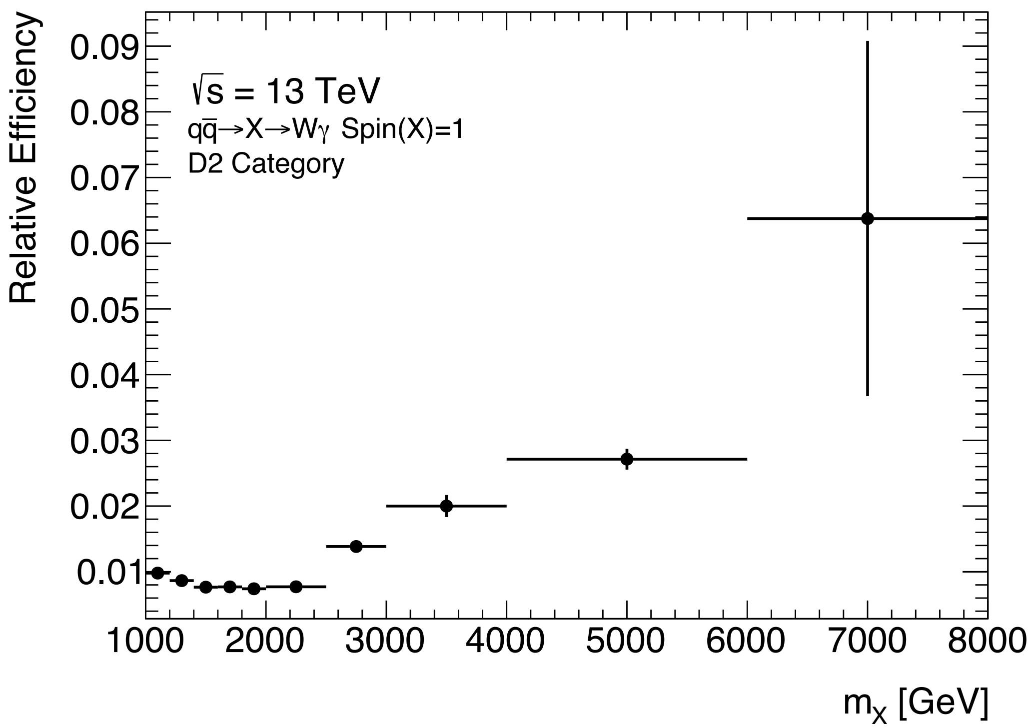

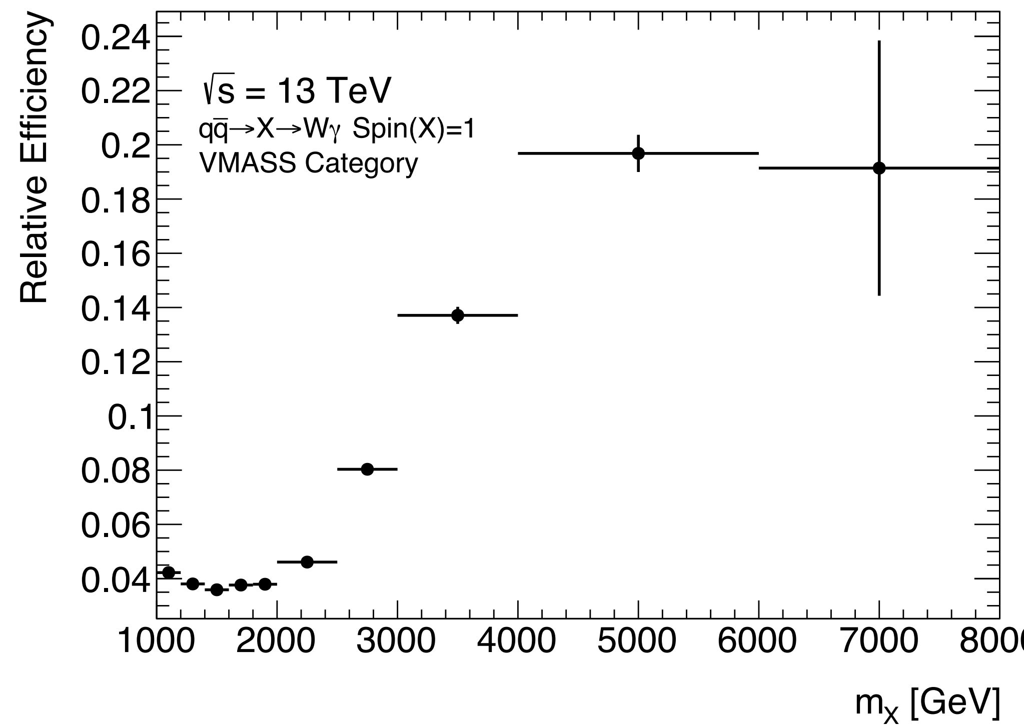

Signal Comparison

- The kinematics for each signal channels determines the different performance shown in signal efficiency plots.
- The pT distribution dominates the efficiency behavior in low mass region, and the angular distribution dominates high mass region.

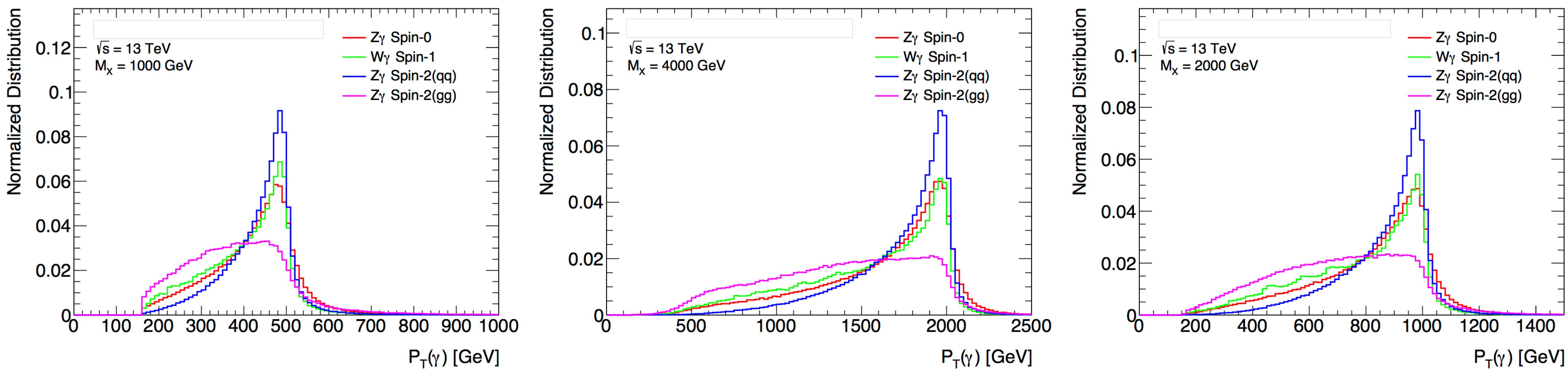

Signal Comparison

- The kinematics for each signal channels determines the different performance shown in signal efficiency plots.
- The pT distribution dominates the efficiency behavior in low mass region, and the angular distribution dominates high mass region.

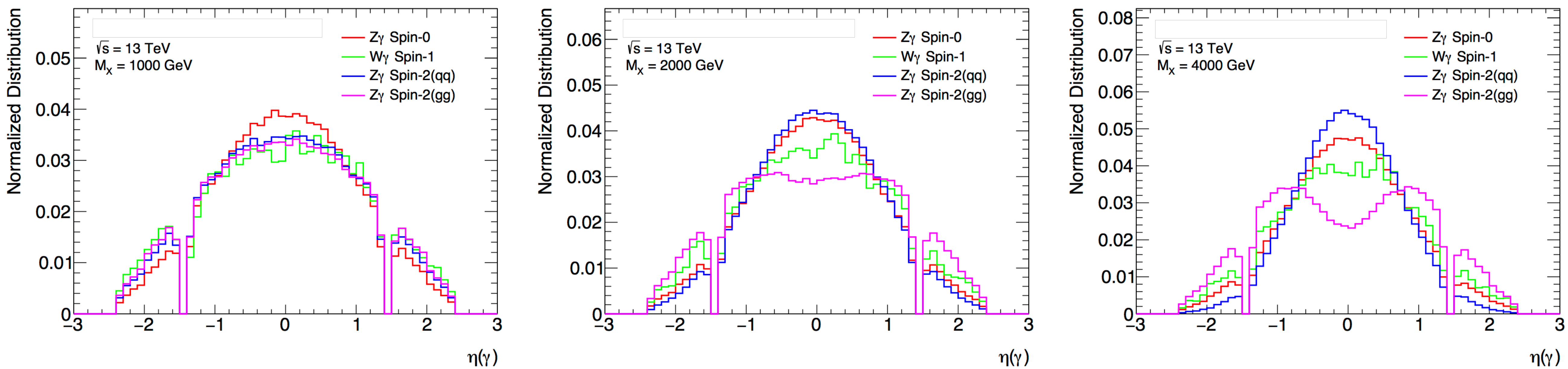

Signal Comparison

- The kinematics for each signal channels determines the different performance shown in signal efficiency plots.
- The pT distribution dominates the efficiency behavior in low mass region, and the angular distribution dominates high mass region.

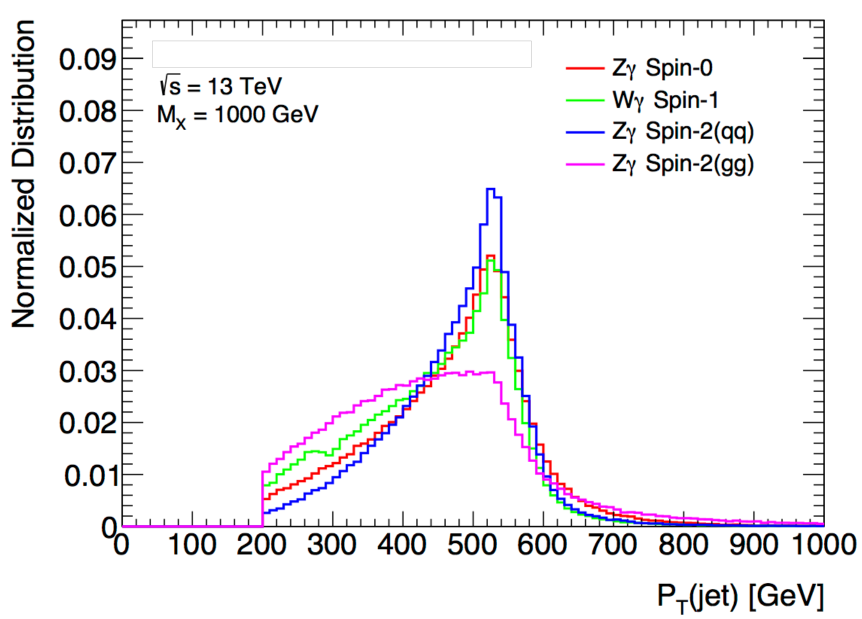

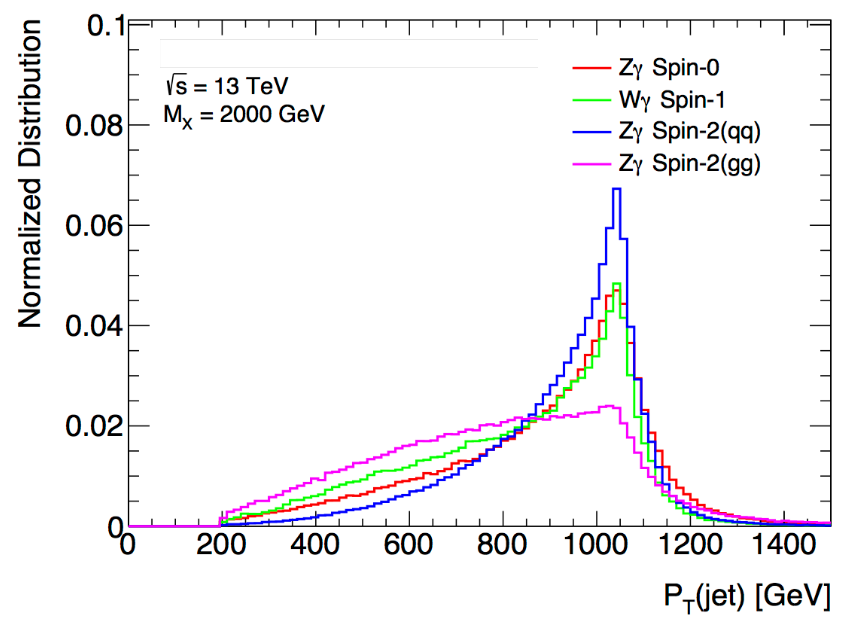

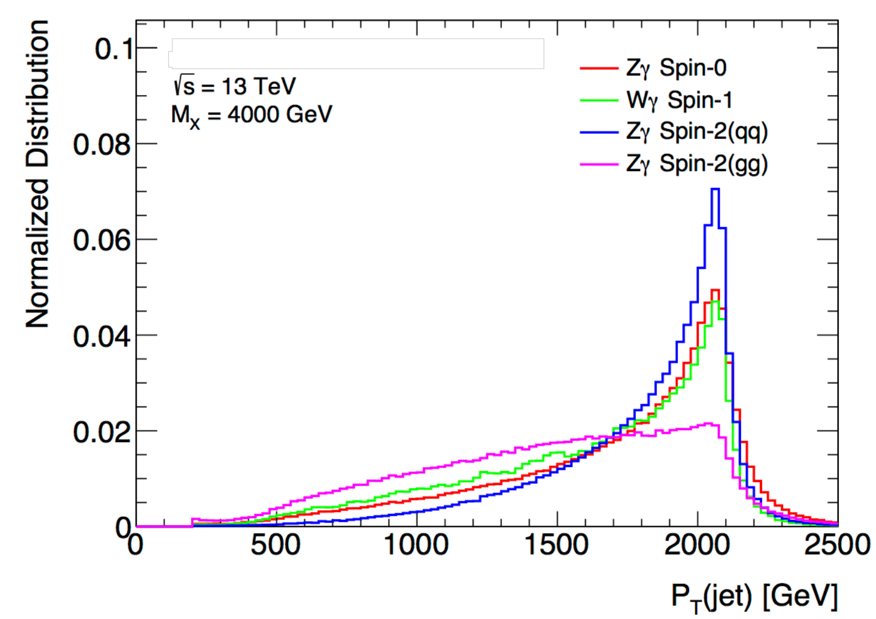

Data/MC comparison

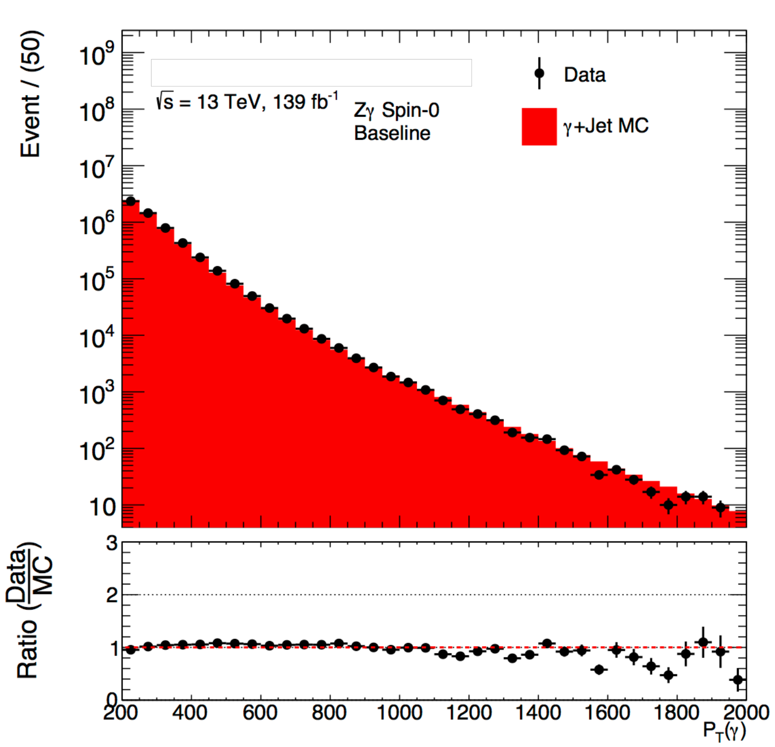

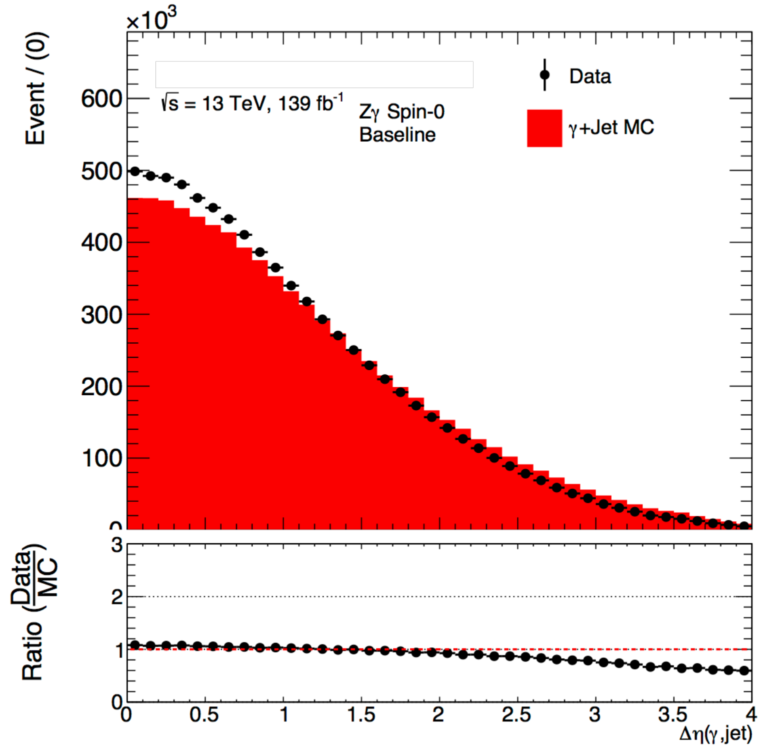

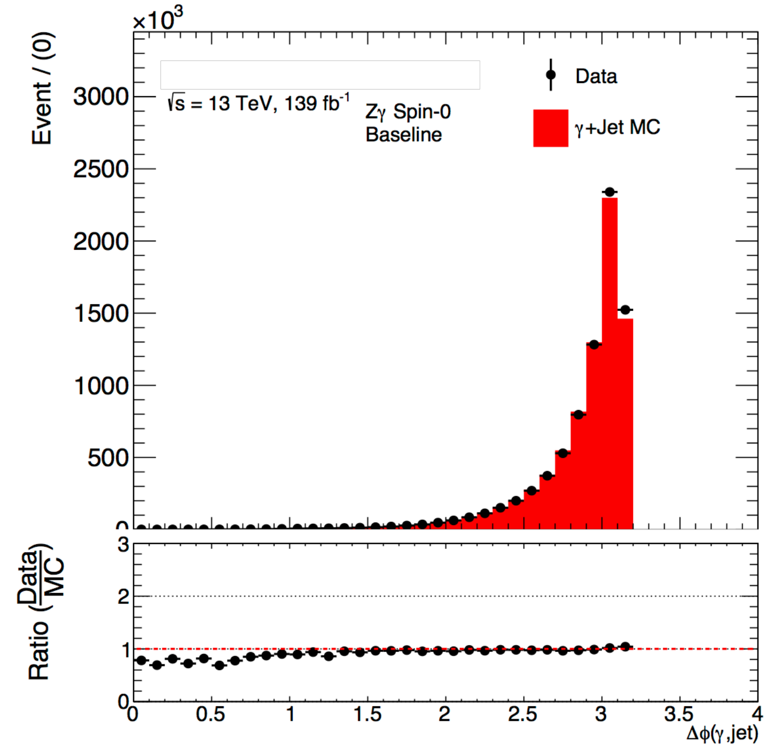

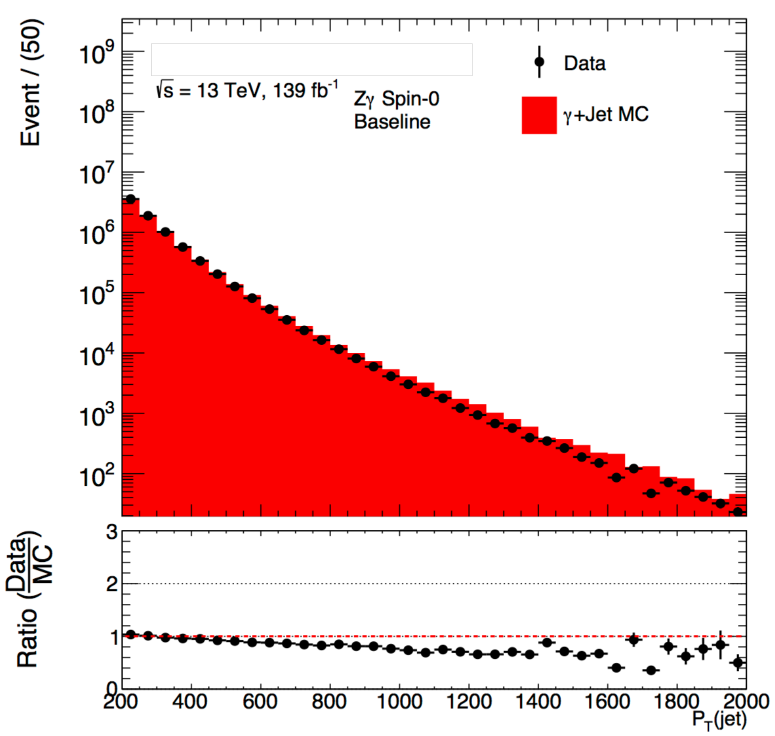

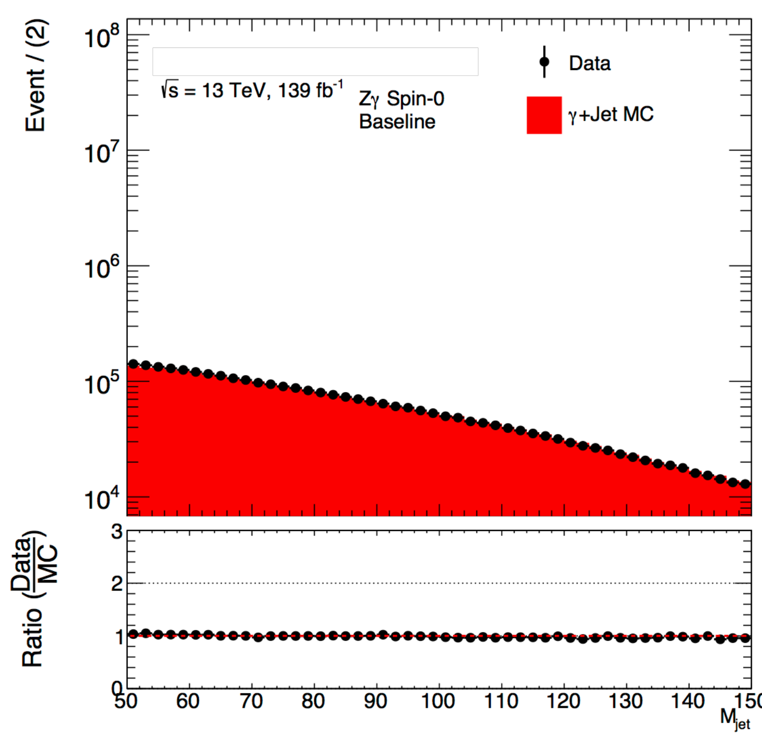

- No scale factors applied
- The ramp for jet pT is consistent with the sherpa NLO performance

(https://cds.cern.ch/record/2655001)

- The study on re-weighted samples are done, no impact on our analysis strategy

Re-weighted MC study

Ratio and Re-weighting function

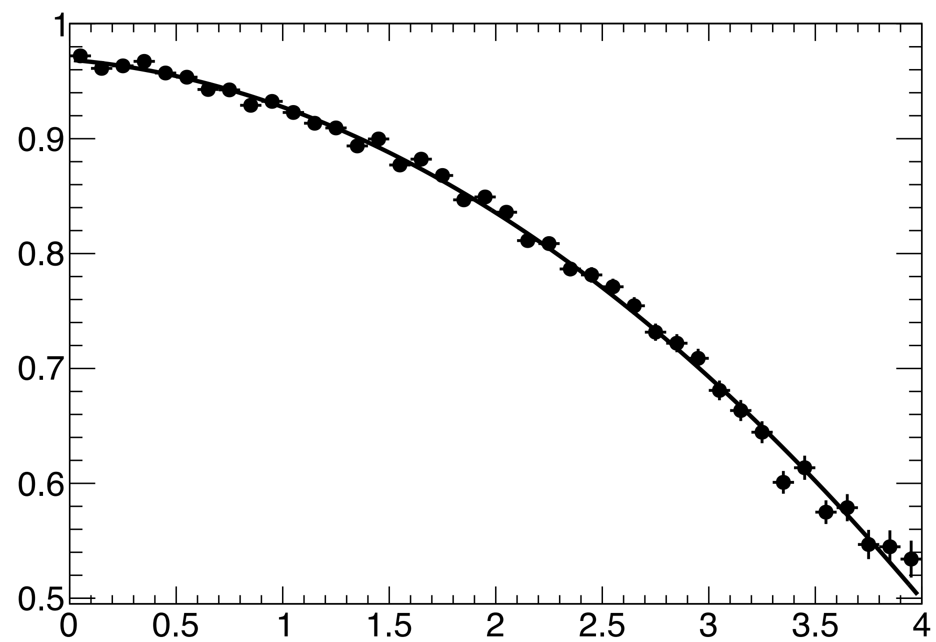

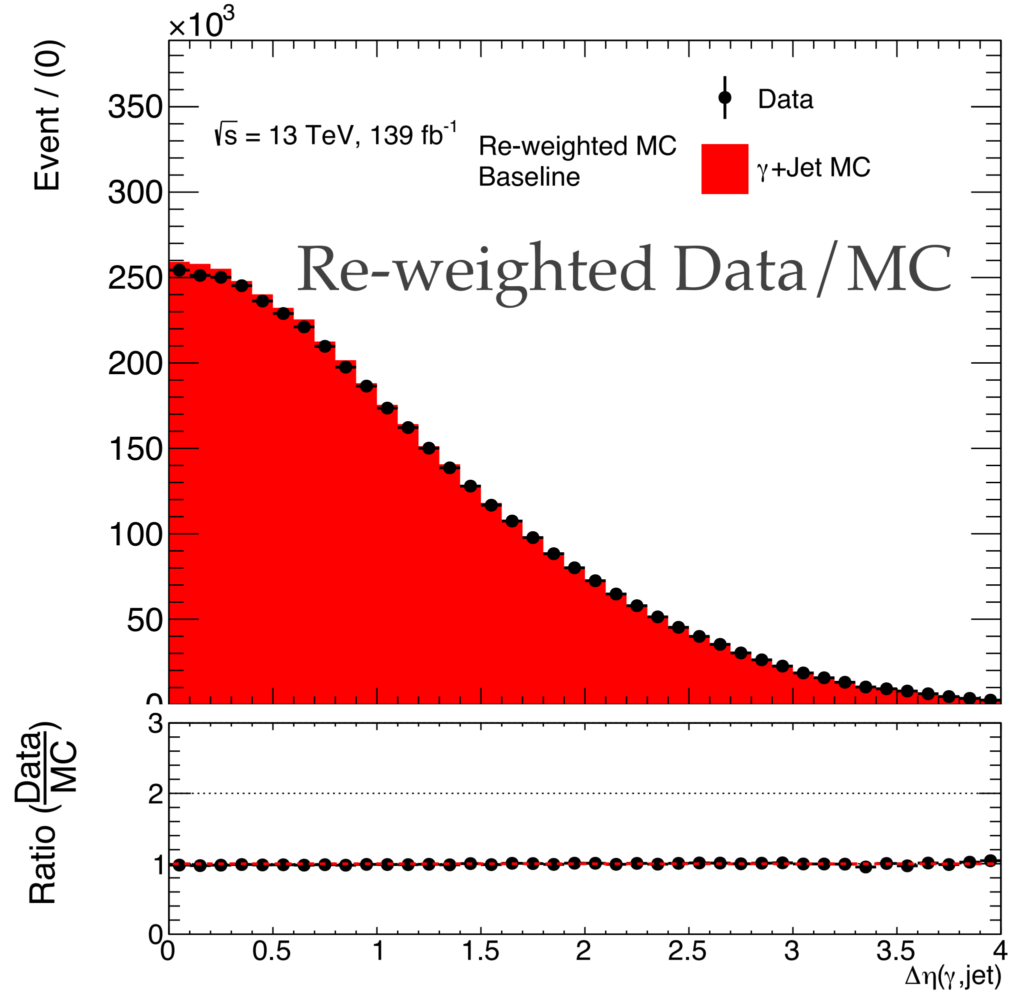

$Z\gamma$ Spin-0 D2 Category

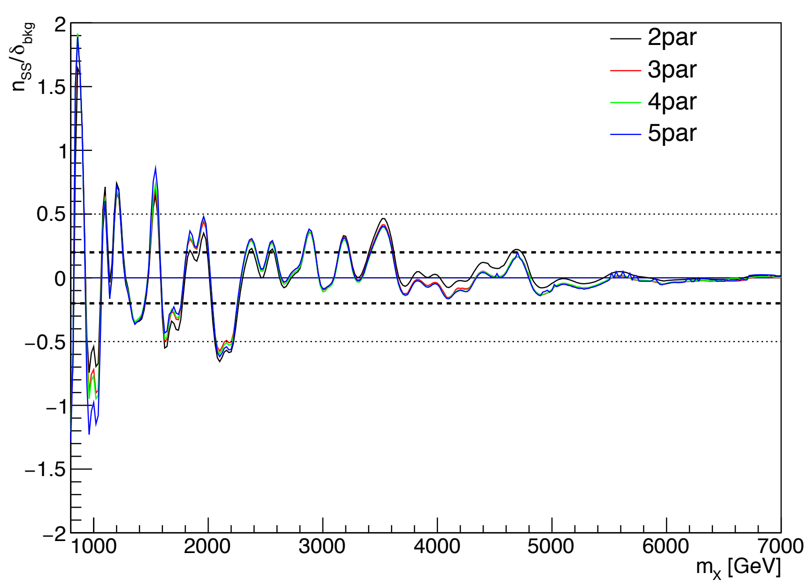

$Z\gamma$ Spin-0 Vmass Category

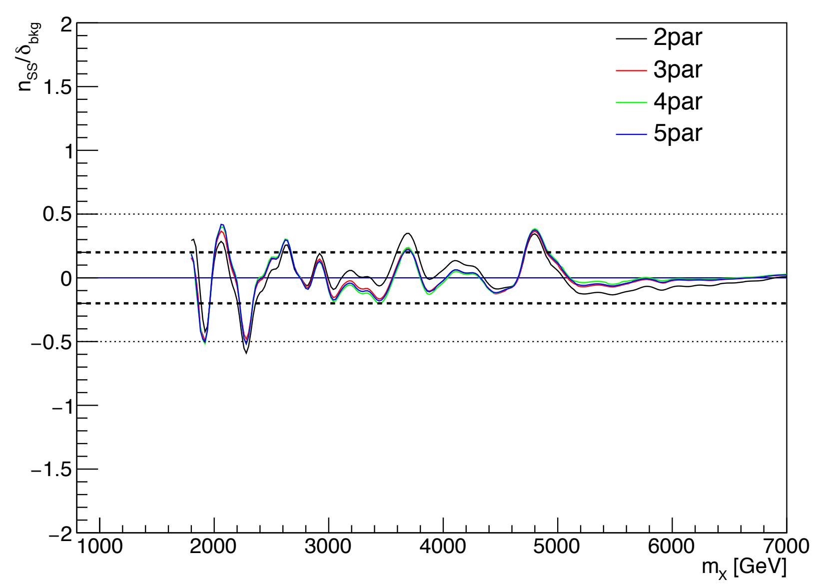

Fractional Spurious Signal Test

In order to identify the source of spikes in spurious signal test, the MC is evenly and randomly split into 2 or 3 subsets. Comparing the spurious signal test results for each of the subset, the correlation appears to be very weak. Therefore, the source of the spikes are probably from MC fluctuation limited by the size of the MC samples.